Elucidation of Hair Growth and Hair Pigmentation Promotion Effect of 3,4,5-Tri-*O*-Caffeoylquinic Acid

March 2020

Meriem BEJAOUI

Elucidation of Hair Growth and Hair Pigmentation Promotion Effect of 3,4,5-Tri-*O*-Caffeoylquinic Acid

A Dissertation Submitted to

the School of the Integrative and Global Majors,

the University of Tsukuba

in Partial Fulfillment of the Requirements

for the Degree of Doctor of Philosophy in Medical Science

(Doctoral Program in Life Science Innovation)

Meriem BEJAOUI

Abstract

Hair follicle (HF) undergoes a regular cycle composed of three phases: anagen, catagen, and telogen. During anagen phase or the growth phase, dermal papilla cells (DPs) located at the proximal end of the HF, regulates the induction of the hair cycle and the formation of the hair shaft. Moreover, during this phase, the bulbar melanocytes are active and produce the pigment melanin. The HF enters then a regression phase (catagen) followed by a resting phase (telogen) where the hairs are normally shed. Various signaling pathways regulate the hair growth cycle, such as the canonical Wnt/β-catenin signaling as it is involved in the regulation of the development, growth, and proliferation of the HF and the regulation of the melanocytes and the pigmentation. Wnt/β-catenin activation in the HF initiates the anagen phase initiation by inducing the proliferation and differentiation of matrix cells producing the pigmented hair shaft. An alteration in the pathways regulating the HF, can lead to a shorten length of anagen phase and an increase rate of hair loss (alopecia) and hair graying (canities).

As hair plays an important role in individual's general appearance, hair problems are a major concern in the modern society. Hair loss and hair graying are common disorders that appear both in men and women undependably of the age or the origin, yet the mechanism by which they occur is not well understood. The current available therapies rely on synthetic chemicals ingredients and have showed many severe side effects and temporary results. The Food and Drug Administration (FDA) have approved two treatment against hair loss: Minoxidil and Finasteride but unwanted sides effect were observed including: impotence, dizziness, unwanted grown hair, weakness, headache, skin rash, and others. Developing a safe drug with a lasting effect has become a necessity to treat hair disorders and to have an alternative therapy for promoting hair growth and pigmentation.

In this context, caffeoylquinic acid (CQA) is a phenylpropanoid compound exhibiting several beneficial properties including anti-oxidant, anti-allergic, neuroprotective, and melanogenesis-regulating effects. TCQA or 3,4,5-tri-*O*-caffeoylquinic acid is a derivative of CQA and chlorogenic acid (CGA) family that has a stable albumin affinity and is composed of multi-esters formed between quinic acid and one-to-four residues of trans-caffeic acids. TCQA has been found to induce a powerful inhibitory activities against aldose reductase, hypertension, hyperglycemia, and Alzheimer's disease without unwanted secondary effects. Moreover, TCQA

induces neurogenesis, improves learning and memory in aged mice, and promotes the differentiation of human neural stem cells, however its effect on hair growth and hair pigmentation promotion has not yet been assessed. In the present study, the effect of TCQA on the induction of hair pigmentation and growth through exploring the possible common pathways such as Wnt/β-catenin was investigated

In this purpose, the dorsal back of eight-weeks-old C3H male mice was shaved and TCQA was applied topically for a month. Results showed that TCQA stimulated the induction and the acceleration of the anagen phase of the hair growth cycle compared to the untreated mice. TCQA significantly enhanced the hair growth by approximately 120% by the end of treatment. In contrast, for the control group, only 37% hair regrowth area was observed. In addition, the hair plucked from the treated area of TCQA-treated mice displayed a darker color compared with the control and melanin assay showed that the melanin content increased up to 175% after TCQA application. To uncover the mechanism behind the effect of TCQA on hair cycle, microarray analysis was conducted. An upregulation in hair growth- and pigmentation-associated genes was observed. Genes relevant in β-catenin binding, pigmentation, neural cells differentiation and migration, transcription regulation, and Wnt signaling were upregulated. On the other hand, genes involved in Wnt repression, melanin degradation, and β-catenin degradation complex were downregulated. Immunohistochemistry results from skin collected from the treated area, revealed an accumulation of β-catenin expression in the epidermis and the hair bulb where the DPs and the active melanocytes are located. These results demonstrated also an activation of Tyrosinase (TYR) involved in melanin synthesis, in the hair bulb, showing that the melanocyte are active and producing the pigment melanin. A staining of CD34 an anagen marker in the skin, showed the stimulation of this protein in TCQA-treated skin compared with the control. These immunohistochemistry results revealed that the HF from TCQA-treated mice are in the anagen phase of the hair cycle, which means that the hair matrix cells are differentiating to form the hair shaft and the melanocytes are active and produce the melanin.

Furthermore, TCQA was used on human and mouse cell lines to further validate its effect on hair growth and melanogenesis. Human hair follicle dermal papilla cells (HFDPC) was cultured in the presence of the sample and the proliferation along with the ATP content were significantly enhanced upon the treatment. In addition, the protein and the gene expression of β-catenin was

upregulated in TCQA-treated cells, even after inhibition with XAV939. This results prove further the effect of TCQA on the stimulation of hair growth via the activation of β-catenin in dermal papilla cells.

Human melanocytes (HEM), melanin-producing cells and B16 murine melanoma cells (B16F10), were used to further validate the effect of TCQA on pigmentation. Melanin content along with the gene and protein expression of the melanogenesis enzymes TYR, TYRP1 (tyrosinase-related protein 1), and DCT (dopachrome tautomerase) were upregulated upon treatment. This effect is attributed to the activation of microphthalmia-associated transcription factor (MITF) the transcription factor of the melanogenesis enzymes caused by the enhancement of the expression of β-catenin known to activate Mitf.

Taken together, the finding of this thesis showed that TCQA triggered the activation of Wnt/β-catenin pathway leading to the transition from telogen to anagen phase, anagen phase initiation and elongation, hair matrix differentiation, and hair shaft development and pigmentation.

Furthermore, the observed stimulation of hair growth cycle was supported by the downregulation of telogen- and aging-associated genes, Wnt signal inhibitors, and melanin degradation-associated genes which contributed to further enhance the effect of β-catenin and Wnt proteins activation. TCQA successfully activated the proliferation of dermal papilla cells often considered the key regulator of hair growth cycle and the melanocytes, melanin-producing cells.

In this context, the potential effect of TCQA on the activation of melanocytes through a communication with dermal papilla cells via Wnt/β-catenin will be looked at. Clinical studies would be however necessary to introduce TCQA as a safer drug to initiate the hair growth cycle and to enhance melanogenesis.

Table of Contents

List of Figures

List of Tables

Abbreviations

ALP: alkaline phosphatase

ATP: adenosine triphosphate

β-catenin: catenin (cadherin associated protein), beta 1

BMP: bone morrow protein

B16F10: B16 murine melanoma cells

CDH11: cadherin 11

CGA: chlorogenic acid

CQA: caffeoylquinic acid

DAVID: database for annotation, visualization, and integrated discovery

DCT: dopachrome tautomerase

DKK-1: Dickkopf 1

DS: dermal sheath

DP: dermal papilla

EM: epidermal melanocytes

FDA: Food and Drug Administration

FGF: fibroblast growth factor

FM: follicular melanocyte

FZD: frizzled

GAPDH: glyceraldehyde 3-phosphate dehydrogenase

HEM: human epidermal melanocytes

HF: hair follicle

HFDPC: human hair follicle dermal papilla cells

IRS: inner root sheath

Kitl: kit ligand

MAPK: mitogen-activated protein kinase

Mc1r: melanocortin 1 receptor

MITF: microphthalmia-associated transcription factor

MTT: 3-(4,5-dimethyl-thiazol-2-y1) 2,5-diphenyl tetrazolium bromide

NFATC1: Nuclear factor of activated T cells, cytoplasmic, calcineurin dependent 1

ORS: outer root sheath

OCT: optimum cutting temperature

Pax3: paired box 3

PBS: phosphate-buffered saline

PVDF: polyvinylidene difluoride membrane

RBPj: recombining binding protein suppressor of hairless

RT: room temperature

SDS-PAGE: sodium dodecyl sulphate-polyacrylamide gel electrophoresis

SHH: Sonic hedgehog

SOX10: SRY (sex determining region Y)-box 10

TAC: Transcriptome Analysis Console

TCQA: 3,4,5-tri-*O*-caffeoylquinic acid

TGF-β: Transforming growth factor β

TYR: tyrosinase

TYRP1: tyrosinase-related protein 1

List of publications

Bejaoui, M., Villareal, M. O., and Isoda, H. (2019). β-catenin-mediated hair growth induction effect of 3,4,5-tri-*O*-caffeoylquinic acid. *Aging (Albany. NY).* 11, 4216–4237. doi:10.18632/aging.102048

Chapter I:

General Introduction

1. The hair follicle

1.1. Biology

The Hair follicle (HF) is considered to be an integral part of mammalian skin where along with the epidermis maintain the body's protective barrier against its external environment [1]. Roughly five million HFs are found in the human body and they are formed during fetal and perinatal skin development, and their morphogenesis is controlled by a complex interaction governed by mesenchymal (dermal)-epithelial (epidermal) signals [2]. During the 8^{th} and 12^{th} weeks of the embryonic stage, in response to mesenchymal signaling (First dermal signal), the HF development and formation starts and the epithelial cells grow downwards into the dermis and the initial placode is formed. By 12–14 weeks gestation, an epithelial signal from the placode causes the mesenchymal cells to condensate and form aggregates below the epidermis. These aggregates will send a second dermal signal to the epithelial placode cells to proliferate and then invade the dermis surrounding the dermal aggregates or condensates. Therefore these aggregates, form the dermal portion containing, the dermal papilla (DP) and the dermal sheath (DS) and this stage of development is known by hair peg stage [3,4]. In stage 5 (13–16 weeks gestation), the upper portions of the HF divide into two distinct bulges: the upper bulge located near the skin surface and the sebaceous gland, and the lower bulge considered as a reservoir of stem cells. During this stage as well, a more enhanced differentiation of the epidermal cells is observed and results in the formation of the inner root sheath (IRS) and the hair shaft of the mature follicle [5,6]. The HF contains as well melanin producing cells the melanocytes which are originally derived from the neural crest cells, and the precursors the melanoblasts migrated to be localized in the HF and the epidermis [7]. In the HF, melanogenically active melanocytes are located in the hair bulb, adjacent to the DP and the keratinocytes whereas amelanotic melanocytes or melanocytes stem cells (MSCs) are found at the outer root sheath (ORS) and in the bulge region [8].

1.2. Cycle

The HF is a dynamic mini-organ that undergoes continuous cycling throughout adult life during which various cell populations of neural crest, ectodermal or mesodermal origin, which are located in different part of the HF and are distinct in their function and gene and protein expression characteristics, are renewed [9]. The cycle is typically defined into three phases: growth (anagen), apoptosis-driven regression (catagen), and relative quiescence (telogen)(**Figure 1.1**).

1.2.1. Anagen phase

During this growth phase, the DP send signals to the bulge where the stem cells are residing and in response to these signals, the cells will migrate to the lower part of the HF to the hair bulb exactly. There, the stem cells proliferate to form the matrix cells that are differentiating into the uprising hair shaft [10]. This regenerative phase is classified into different sub-stages that goes from anagen I to anagen VI, and during the final sub-stage, histologically, the HF are long, straight, and angled [11]. During this phase, the melanocytes located at the bulb area of the HF, are activated and synthesize the pigment melanin that are transferred in the melanosomes to the hair progenitors cells (hair matrix) that will give arise to the hair shafts in the mature HF **(Figure 1.2)** [12,13]. The extent of anagen is determined by the rate of differentiation of the progenitors cells or the matrix cells, and is responsible of the regulation of the hair shaft length [14].

1.2.2. Catagen phase

Catagen also called the regression phase, is the dynamic transition between anagen and telogen where the activity of the progenitors and the HF slows down and eventually cease [15]. In this phase, the lower cycling portion of the HF regress entirely and the epithelial cells in the bulb including the melanocytes, the ORS, and the outermost epithelial layer goes through apoptosis [16]. The hair shaft differentiation stops eventually and its bottom will form a rounded structure called hair club that is attached to the permanent non cycling upper portion of the HF during the next phase. As for DP fate, it will connect to the formed hair club [17].

1.2.3. Telogen phase

Following catagen, the HF is resting and no activity is detected including the pigment synthesis by the melanocytes and this phase is called the resting phase or telogen [18]. For the next hair cycle initiation, multipotent epidermal stem cells residing in lowest permanent portion of the HF (the bulge) are activated to become the transit-amplifying cells that are fated to form the new HF, whereas the old club hair sheds (exogen) [19].

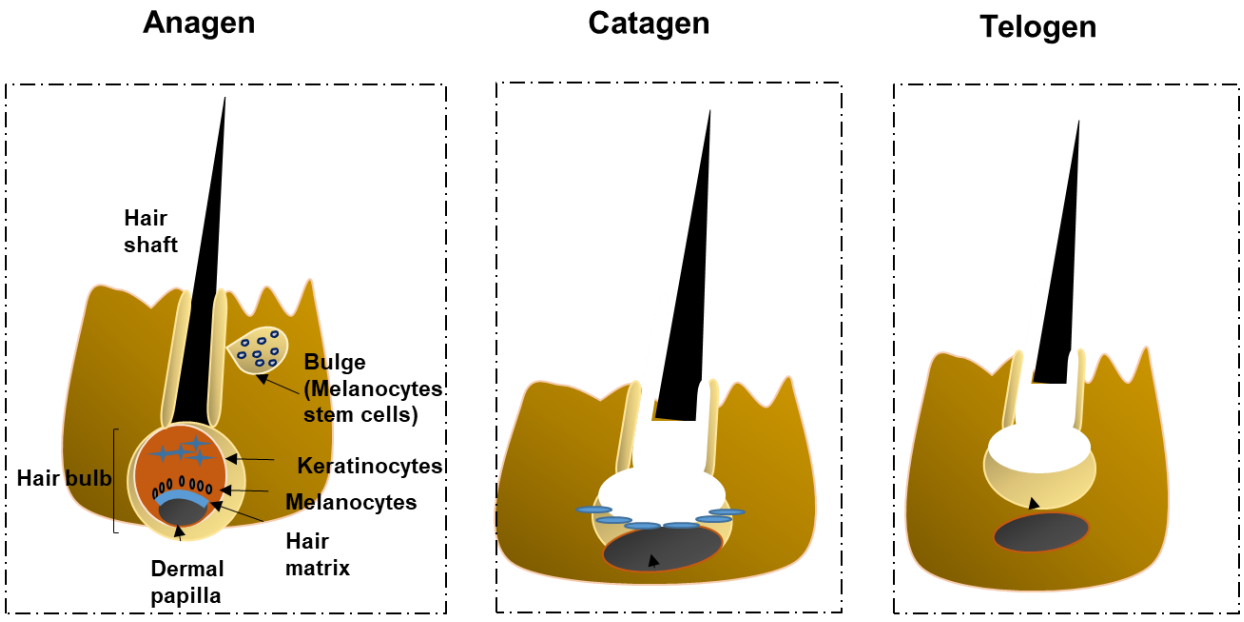

Figure 1.1. Hair growth cycle

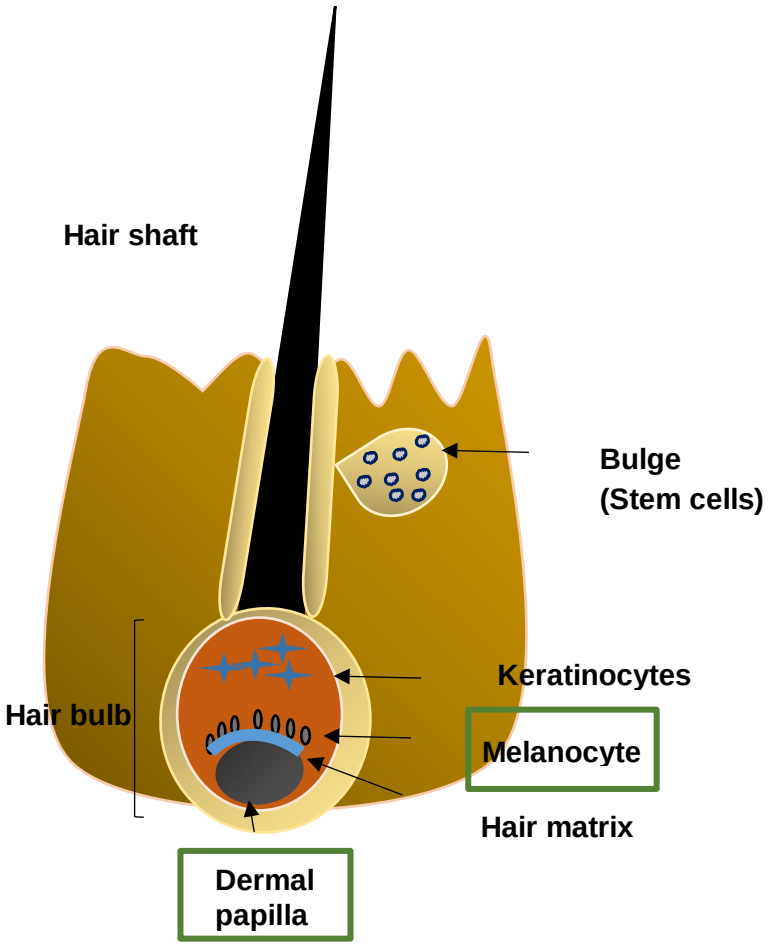

Figure 1.2. Hair follicle structure during anagen phase

1.3. Signaling pathways regulating the HF

HF development, maintenance, and cycle involve a reciprocal signaling interactions between the epithelium and the dermis. Previous studies have identified Wnt, fibroblast growth factors (FGF), sonic hedgehog (Shh), bone morrow protein (BMP), and Notch signaling, and several transcription factors as regulators of the hair cycle (Figure 1.3)

1.3.1. The Wnt/ β-catenin signaling

The canonical Wnt/β-catenin signaling is activated first by the binding of Wnt ligand to the receptors of frizzled (FZD) and LRP5/6. The formed complex will induce the translocation of β-catenin to the nucleus. Once it is activated, β-catenin regulates the expression and the activity of target genes significant in the regulation of hair growth and pigmentation cycle. It has been reported that β-catenin regulates Wnt, FGF1, and FGF2 involved in the differentiation of matrix cells to form the hair shaft. Additionally, it is involved in the positive regulation of microphthalmia-associated transcription factor (Mitf) known as pigmentation master regulator [20,21].

This pathway is considered by numerous studies as one of the most important signaling pathway responsible of the initiation of the growth phase of the hair cycle as it was found that the progenitor cells accumulate nuclear β-catenin [22]. During the quiescence phase, bulge stem cells reside in a Wnt-restricted environment. The transition from telogen to anagen is initiated when nuclear β-catenin and Lef1/β-catenin reporter are expressed at the bulge area, near the recently emerging HF [23,24]. Studies were done using transgenic mice overexpressing β-catenin, and results showed that these mice are characterized by an increase in the follicle density and an early entry to the regenerative phase of hair growth (anagen phase) [25].

Moreover, the abrogation of β-catenin results in an entire alopecia, an inhibition of hair cell proliferation, an absence of HF morphogenesis, and a loss of stem cell niche [26]. Additionally, an ectopic expression of Dickkopf 1 (Dkk-1) a Wnt inhibitor results in the failure of HF development. These results are considered as a strong scientific proofs of the essential role of Wnt/β-catenin signaling in the regulation of hair growth and pigmentation cycle and the maintenance of epithelial stem cells niche shaft [27,28].

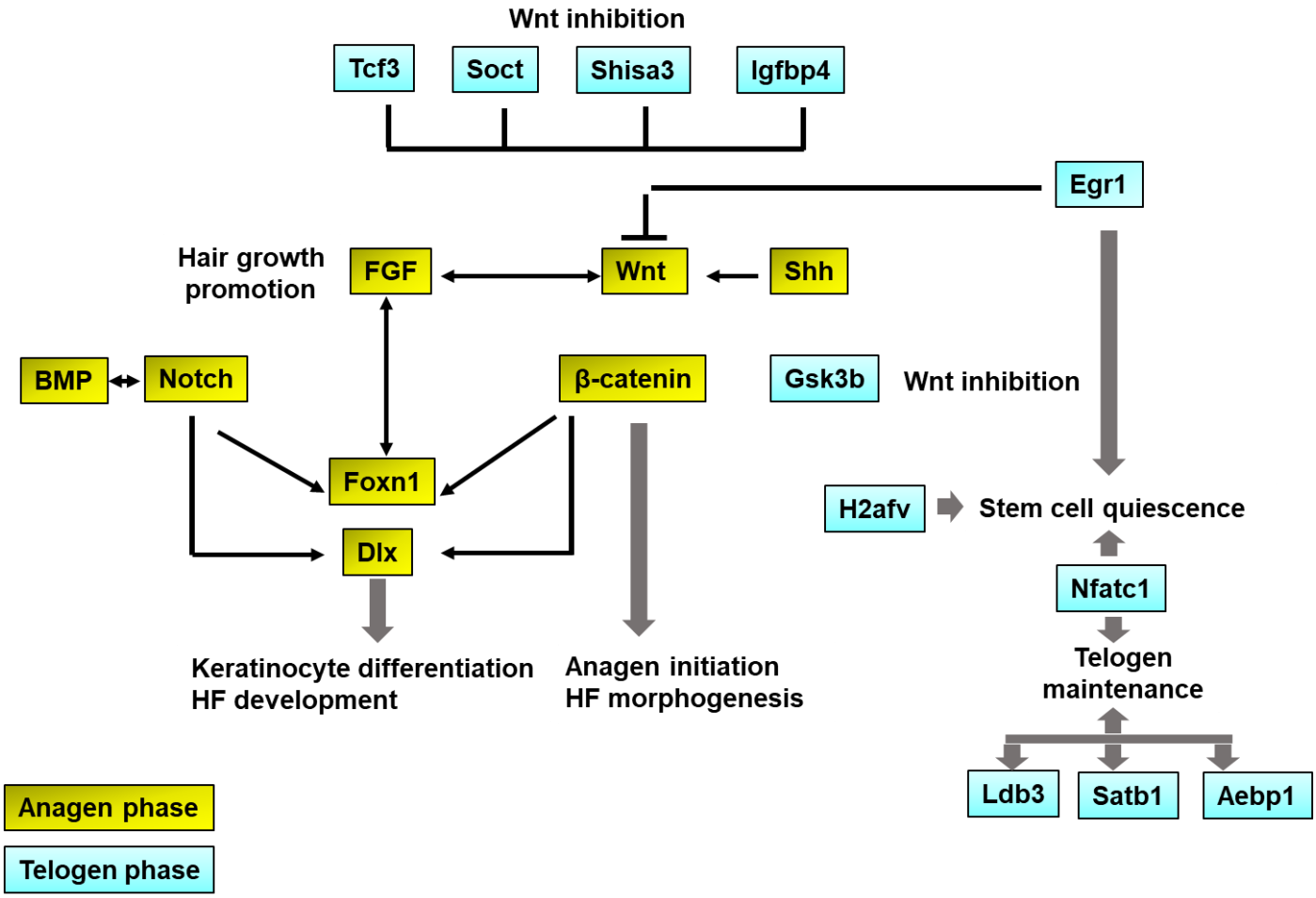

Figure 1.3: Pathways governing the hair follicle.

1.3.2. The Sonic hedgehog (Shh) pathway

The Shh pathway plays a major role in the HF morphogenesis and cycle. As mentioned above, β-catenin regulates the induction of the anagen phase, this process is followed by the activation of bulge stem cells and the proliferation of progenitors cells located at ORS and this proliferation is under the influence of Shh [29]. Furthermore, the inhibition of Shh pathway during embryonic and adults development results, respectively, in the arrest of HF morphogenesis and the anagen phase [30,31] .

1.3.3. The Notch pathway

The role of Notch signaling in the differentiation of follicular stem cells in the bulge, and in the maintenance of HF structure, has been established by various studies. Actually, several Notch signaling receptors including recombining binding protein suppressor of hairless (RBPj) are located in the bulb region of the HF to regulate the differentiation of matrix cells [32].

1.3.4. The Fibroblast growth factor (FGF) signaling pathway

During HF morphogenesis at embryonic stage, the placode formation is followed by dermal fibroblasts condensation mediated by FGF signaling mainly FGF 20 via a crosstalk with Wnt/β-catenin [33]. FGF1 and FGF2 affect the growth, development, and differentiation of HF by promoting DP cell proliferation leading to an increase in the size of HF in mice. These FGF signaling molecules are involved as well in keratinocytes differentiation, hair growth cycle, and wound healing [34,35].

1.3.5. The Bone morrow protein (BMP) signaling pathway

BMPs signaling molecules are a part of the TGF-β superfamily, and they play a major role in the development, proliferation, differentiation, and apoptosis of the skin via an interaction with various signaling pathway including Wnt/β-catenin, Shh, TGF-β, FGF, and Notch [36,37]. BMP signaling is likely to be involved in the activation of hair matrix cell, and therefore the implication in HF morphogenesis, postnatal regeneration, and the control of the hair growth cycle [38]. In adult follicle stem cells, BMP6 expression level is upregulated, implying that BMP molecules are expressed in the bulge. On the other hand, this signaling pathway mediates the differentiation of keratinocytes cells to produce the ORS and the lower part of the HF [39].

1.3.6. Pigmentation-related pathways

The process of production of the melanin responsible of the color of the hair shaft is called melanogenesis. This process occurs in the melanosomes of the melanocytes, then the pigment is transferred to the adjacent keratinocytes. Melanogenesis and pigment transfer to the adjacent keratinocytes located at the bulb area, are under the regulation of various signaling transduction pathways intrinsic to the skin and HF, and determined as well by the availability of melanin precursors. Melanin is synthesized through a series of interactions starting with L-tyrosine and catalyzed by tyrosinase (TYR), tyrosinase-related protein 1 (TYRP1), and dopachrome tautomerase (DCT) [12,40]. The expression of these three enzymes often called the melanogenesis enzymes is regulated by the transcription factor microphthalmia-associated transcription factor (Mitf) playing an important role in the development and survival of the melanocytes. Melanin synthesis is under the influence of various signaling systems and transcription factors including the tyrosine kinase receptor KIT, its ligand SCF, MC1R, cAMP, and Wnt/β-catenin [41,42]. Additionally, Mitf is regulated by PAX3, CREB, SOX9, and SOX10. Furthermore, mitogen-activated protein kinase (MAPK), glycogen synthase kinase-3β (GSK3β), and p38 phosphorylate MITF, leading to the modulation of its transcriptional activity and the reduction of the melanin biosynthesis [43–45].

2. Hair problems

2.1. Hair loss

The role of the mentioned pathways is essential in maintaining the balance between the different phases of the hair cycle so an alteration in these pathways can lead to a shorten length of anagen phase, an increase rate of hair loss and thus an impression of baldness [28,46,47]. The severity and nature of baldness vary depending on the gender, and can be influenced by several factors including: age, genetic, nutrition, hormonal imbalance, environmental factors, stress, and others [48]. It has been reported that there is different types of hair loss or alopecia including, involutional alopecia which occurs with aging and during which the HFs are into the telogen phase and the hair shaft is short and thin. Androgenic alopecia affect both men and women independently of the age and it's characterized by a gradual disappearance of hair from the crown and frontal scalp [49]. Another type is alopecia areata that often starts suddenly and causes patchy hair loss in both young adults and children [50].

Moreover, telogen effluvium is a type of alopecia characterized by a temporary hair thinning that happens due to a fast transition from anagen to telogen phase, and eventually a longer telogen phase. In contrast, alopecia can be permanent as well, like scarring alopecia causing skin and scalp disorders and inflammation [51].

2.2. Hair graying

Hair graying is often associated with aging and despite not being a severe disease, it may be a cause of low self-esteem. Additionally, a premature hair graying can be a sign of systemic disease like osteopenia or coronary artery [52,53]. The causes of hair graying are not well understood, but it can be inherited in an autosomal-dominant manner or associated with autoimmune disorders including vitiligo [54,55]. Drugs and nutritional deficiencies like vitamins can be a cause of premature hair graying [56].

Furthermore, the involvement of MSC and bulbar melanocytes in hair graying is established although it is not well understood, but it is likely the most striking cause. Studies have showed that graying is caused by the depletion of HF bulbar melanocytes and therefore the cease of melanin synthesis in the hair shaft [57]. This depletion can be induced by an accumulation of reactive oxygen species (ROS), oxidative stress, ultraviolet light, inflammation, and environmental factors [58,59]. Moreover the dysregulation of, tyrosinase activity in bulbar melanocytes, melanosomes transfer, and the interaction between melanocytes and keratinocytes of hair bulbs, affect the melanin synthesis in the HF [60]. On the other hand, the defective self-maintenance and self-renewal of MSCs, and their failure to migrate and differentiate into bulbar melanocytes is reported to be a cause of hair graying. This defectiveness is caused by a low expression of growth factor-β (TGF-β) and collagen XVII (Col17A1) [61–63].

2.3. Current therapies

The current available therapy for hair loss and graying rely on synthetic chemicals ingredients and have showed many severe side effects and temporary results. The Food and Drug Administration (FDA) have approved two treatment against hair loss: Minoxidil and Finasteride. Minoxidil is used to treat individuals with androgenetic alopecia and it stimulates DP cells through β-catenin activation [64]. As for finasteride, it is also used for human in case of androgenetic alopecia [65]. However unwanted sides effect were observed including: impotence, dizziness,

unwanted grown hair, weakness, headache, skin rash, and others [66–68]. On the other hand, there is no approved drug against hair graying yet.

3. Caffeoylquinic acid derivatives

Recent studies aim to develop a drug without undesirable side effects and with a long lasting action in order to have an alternative therapy for promoting hair growth and hair pigmentation. Caffeoylquinic acid (CQA) is a polyphenolic compound with several beneficial properties including anti-oxidant, anti-histaminic, neuroprotective, and pigmentation-regulating effects [69–72].

3.1. 3,4,5-tri-O-caffeoylquinic acid

TCQA or 3,4,5-tri-*O*-caffeoylquinic acid with an IUPAC name (3R,5R)-3,4,5-tris[[(E)-3-(3,4-dihydroxyphenyl)prop-2-enoyl]oxy]-1-hydroxycyclohexane-1-carboxylic acid, is a CQA derivative composed of multi-esters formed between quinic acid and one-to-four residues of trans-caffeic acids, and known to have a stable albumin affinity as it can highly bind to human serum albumin (**Figure 1.4**). TCQA has been found to highly inhibit aldose reductase, hypertension, hyperglycemia, and Alzheimer's disease, and to increase ATP production [73]. In addition, TCQA was observed to promote neurogenesis by inducing the differentiation of neural stem cells, and also to improve learning and memory in old mice [74].

4. Objectives of the thesis

The major objective of this study is to determine the effect of TCQA on the promotion of hair growth and the enhancement of hair pigmentation. This thesis contains five chapters. Chapter I is the general introduction, it gives an explanation about the background of the study.

In chapter II, TCQA was tested in eight-weeks-old male C3H mice in order to check its effect on hair growth and pigmentation *in vivo* and to reveal the molecular mechanism behind the observed effect. The effect of TCQA on pathways involved in both pigmentation and growth mainly Wnt/ β-catenin pathway was investigated.

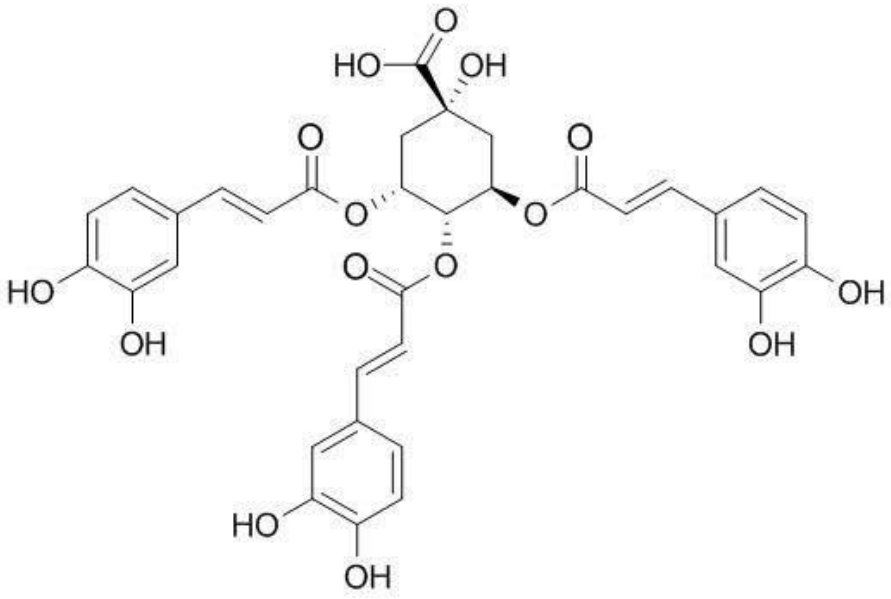

Figure 1.4. Chemical structure of 3,4,5 tri-*O*-caffeoylquinic acid (TCQA)

The objective of chapter III is to check the effect of TCQA on hair growth using human hair follicle human dermal papilla cells (HFDPCs). The proliferation and the ATP content assay of these cells were conducted to investigate the effect of TCQA on the activation of DP cells. In addition, the expression of β-catenin was assessed in the presence of TCQA and an inhibitor of Wnt/β-catenin pathway.

In chapter IV, human epidermal melanocytes (HEM) and B16 murine melanoma cells (B16F10) were used to check the effect of TCQA on melanogenesis *in vitro*. For that, the melanin content, the expression of the melanogenesis enzymes and their transcription factor were investigated upon TCQA treatment in both cell lines. Additionally, β-catenin expression was checked in the presence of TCQA and an inhibitor.

All finding were discussed collectively in chapter V proposing TCQA as a novel candidate for the promotion of hair growth and pigmentation. Further evidence with clinical study involving human subject will be however required to establish TCQA as an approved drug against hair loss and hair graying.

Chapter II: Evaluation of the effect of 3,4,5-tri-*O*-caffeoylquinic acid (TCQA) on hair growth and pigmentation *in vivo*

1. Introduction

The hair follicle (HF) is a miniorgan with a complex biological system that undergoes repeated cycle of regulated proliferation, apoptosis, differentiation, and regeneration over its lifetime [29]. Knowing and understanding the regulation of the regeneration process of any organ in general is of fundamental importance in the age of stem cell biology and regenerative medicine and HF is considered to be a great model for this objective [75].

Mammal's hair coat, goes as well through cycles of regeneration giving arise to a constant supply of new hairs throughout the lifetime of the animal. The phases of the hair cycle in mice are similar to human involving three phases: anagen, catagen, and telogen [76]. During the regeneration phase, keratinocytes like cells known as matrix cells located in the hair bulb near dermal papilla cells (DPs) goes into a proliferation and differentiation process giving arise to different cell populations forming the hair shaft [77]. During this phase, follicular melanocytes (at the bulb region) synthesize the pigment melanin that will be transferred in the melanosomes to the adjacent keratinocytes also known as hair progenitors or matrix cells that differentiate into the hair shafts [12,13]. Then the HF enters the catagen phase where the hair matrix activity ceases, the lower third part of the HF goes through apoptosis including the melanocytes, and the hair is attached to a keratin matrix above the DP [18]. Catagen phase is followed by telogen or the quiescent period, during which the follicle is resting [78].

In mouse model, the HF cycle is completed by the first 3 1/2 weeks after birth and then followed by the second hair cycle. At this young age, the HFs on the dorsal skin are regenerated in a nearly synchronized manner. The first anagen phase of the HF of the dorsal skin occurs from postnatal days 1 to day 12, then from day 17 is the catagen phase that will last approximately three days. Finally from day 21 is the telogen phase for 1 or 2 days [79].

Previous studies demonstrated the major role playing by the Wnt/β-catenin signaling pathway in the development, growth, and proliferation of the HF, the pigmentation of the hair shaft, and the regulation of the activity of melanocytes stem cells (MSCs) [80,81]. The activation of β-catenin is initiated by the formation of a complex that contains Wnt ligand, frizzled (FZD), and LRP5/6. This complex binds to β-catenin that will be translocating into the nucleus to activate target genes. These canonical genes are significant in the growth and pigmentation of the HF [20,82,83] [43–45]. Briefly, Wnt/β-catenin activation in the HF induces the anagen induction by

activating genes and pathways involved in the proliferation and differentiation of the progenitors cells that form the pigmented hair shaft [84].

On the other hand, the non-activation of β-catenin affects mouse hair growth cycle and it has been found that β-catenin is highly expressed in the DP in order to promote postnatal hair growth and to regulate the anagen phase [28,46,47]. Activating β-catenin expression is therefore considered significant in the initiation of the anagen phase and the promotion of hair growth/pigmentation cycle. :

The objective of this chapter is to determine the effect of TCQA on the enhancement of hair growth and pigmentation *in vivo* and to elucidate the molecular mechanism behind it.

2. Materials and methods

2.1. TCQA preparation

For animal test, synthesized 97% pure TCQA kindly provided from Dr. Kozo Sato from Synthetic Organic Chemistry Laboratories, the FUJIFILM Corporation (Kanagawa, Japan) was used. TCQA was dissolved in 70% ethanol and then diluted in milli-Q water before the application on mice.

2.2. Animal experiment

This following experiment was conducted to evaluate the effect of TCQA on the promotion of hair growth/pigmentation in mice models. For this purpose, eight-weeks-old male C3H mice (black laboratory mice) purchased from Charles River Laboratories, Japan Inc. (Kanagawa, Japan) were kept in separate cages at Gene Research Center of the University of Tsukuba, and allowed to acclimatize to the new conditions for one week, under controlled settings of temperature (21-23°C) and light (light: dark 12:12) with access to food and water. Then, two groups of C3H mice were generated randomly (n=5), TCQA-treated group and control group treated with milli-Q water (vehicle).

As mentioned in the introduction part, hair growth and pigmentation occurs at the same time during anagen phase, and at eight-weeks-old, the hair follicle (HF) of C3H mice are at the telogen phase, so in order to initiate the transition from the quiescence phase to the growth phase, the two groups of mice were subjected first to an anesthesia with isoflurane (Wako Pure Chemical Industries, Tokyo, Japan) and then the dorsal part was gently shaved using hair clipper. Each mouse then received a topical application of 1 wt% TCQA (1 g TCQA in 100 ml milli-Q water) or water daily for four weeks in which the mice were observed and photographed. The mice were then scarified by cervical spine dislocation, and then the treated skin were collected part. Before conservation at −80 °C, the skin were cut into four pieces and washed with PBS and then immersed in liquid nitrogen. Additionally, the hair from the shaved and treated area (with TCQA or vehicle) were plucked and kept in -80°C as well. The ImageJ processing program (National Institutes of Health, Bethesda, USA) was used to measure the intensity of the hair color in the collected hair shaft and the hair regrowth in the treated area. All animal procedures performed were approved by the Animal Study Committee of the University of Tsukuba (No.17-060), and were handled

according to the guidelines for the Care and Use of Animals. This procedure is detailed in the following research article [85]

2.3. Melanin assay from the plucked hair shaft

After mice sacrifice, the hair shafts were plucked from the treated area located at the dorsal skin of C3H mice from TCQA-treated group and control group using small sterilized forceps. First, the plucked hair were visualized to detect any change in the color, using a contrast microscope (Leica Microsystems, Wetzlar, Germany) and the intensity of the color were measured using ImageJ processing program.

In order to measure the melanin content in the hair shaft, 1.5 mg of the plucked hair were weighed in sterilized tubes using a high-precision balance, and then 1 ml of 1M NaOH was added to cover the hair for 2-4 hours at 80-85°C under slight agitation. Every 30 min, the tubes were opened to release the gas, then mixed by inversion, followed by a centrifugation at 12,000 rpm for 5 min at room temperature (RT). The amount of melanin was determined after measuring the absorbance at 470 nm. The total melanin content was evaluated using the standard curve for synthetic melanin [86].

2.4. DNA microarray analysis

RNA used as a template were extracted from skin tissues treated either with water or TCQA of mice dorsal part using ISOGEN solution (Nippon Gene, Tokyo, Japan) following the manufacturer's instructions. Briefly, the generated microarray hybridization probes from the extracted RNA were amplified, fragmented, and biotin labeled as aRNA. Then, the aRNA was hybridized to the Affymetrix mouse 430 PM Array strips (Affymetrix, Santa Clara, USA) (Affymetrix) containing probes for 45141 mouse genes. The GeneChip (Mouse Genome 430 2.0 Array) was washed, stained, and scanned using Affymetrix GeneAtlas Imaging Station to obtain the mRNA expression of various genes from mouse genome. The gene ontology, biological process, and fold-change in gene expression (2-fold change, control vs TCQA), were then analyzed using Transcriptome Analysis Console (TAC) software (version 4.0.1) and database for annotation, visualization, and integrated discovery (DAVID) bioinformatics resources 6.8 [87,88]. The average signal log2 (control vs TCQA) was subjected to hierarchical clustering using Euclidean distance and average linkage algorithm of the TIGR Mev version 3.0.3 software (The Institute for Genomic Research, MD, USA).

2.5. Quantitative real-time PCR analysis

As mentioned above, the total RNA was extracted from mice treated skin, then quantified, and the cDNA was synthesized using SuperScript III reverse transcription kit (Invitrogen, CA, USA). The cycling protocol is as follows: 95 °C for 10 min, 40 cycles of 95 °C for 15 s, and 60 °C for 1 min. TaqMan Universal PCR mix and TaqMan probes specific to *Ctnnb1* (Mm 00483039_ m1), *Mitf* (Mm00434954_m1), *Tyr* (Mm00495817_m1), *Tyrp1* (Mm00453201_m1), and *Dct* (Mm01225584_m1), (Applied Biosystems, CA, USA) were used for real-time PCR reaction. *Gapdh* (Mm99999915_g1) (Applied Biosystems, CA, USA) was used as an endogenous control.

2.6. Western blot analysis

Proteins from tissues collected from treated area at mice dorsal part, were extracted using a homogenizer in solution of radio-immunoprecipitation assay (RIPA) buffer (SIGMA, Saint Louis, USA) and protease inhibitor following the manufacturer's instructions. Protein samples (15 µg) were quantified using 2-D Quant kit according to manufacturer's instructions (GE Healthcare, Chicago, USA) and then separated in 10% sodium dodecyl sulphate-polyacrylamide gel electrophoresis (SDS-PAGE). The transfer was done under agitation to the polyvinylidene difluoride membrane (PVDF) (Millipore, NJ, USA). The membrane were blocked for 1 h at RT, then a solution of 1:1000 of the primary antibody β-catenin 71-2700 (Thermo Fisher Scientific, Massachusetts, USA) was added. After overnight incubation at 4°C, the membrane were immersed in a solution of the second antibody goat anti-rabbit IRDye 800 CW. Then the expression was detected using LI-COR Odyssey Infrared Imaging System (LI-COR, NE, USA).

2.7. Immunohistochemistry analysis

After the sacrifice, the skin tissues collected from mice treated area with TCQA and milli-Q water, were divided into four parts, and then embedded in optimum cutting temperature (OCT) compound. Therefore, the sections were cut at a thickness of 10 µm using a cryostat, dried at RT, and fixed in 4% paraformaldehyde (SIGMA, Saint Louis, USA). Different washing solutions of PBS, 20 mM glycine/PBS (SIGMA, Saint Louis, USA), and 0.1% v/v Triton X-100 /PBS (SIGMA, Saint Louis, USA) were applied to the embedded, fixed skin sections prior to blocking with a blocking solution covering the whole surface of the slides, in a wet chamber for 1 h at RT. The blocking solution was then removed and the slides were incubated with primary antibodies

prepared in the same blocking solution for overnight at 4°C in the same wet chamber. In this study, the following antibodies were used (1:100 dilution): rabbit anti-Tyrosinase (Abcam, Rockford, USA), mouse anti-CD34 (Abcam, Rockford, USA), and rabbit anti- β-catenin (Abcam, Rockford, USA). Then a washing in 0.1% v/v Triton X-100 /PBS was conducted, and the slides were immersed in a solution of Alexa 594-conjugated anti-rabbit (Abcam, Rockford, USA) and Alexa fluor 488-conjugated anti-mouse (Abcam, Rockford, USA) prepared in the same blocking solution for 1 h at RT. After drying, the sections were stained with Hoechst and mounted in antifade solution (p-phenylenediamine, PBS, and glycerol) prior to visualization using a confocal microscope Leica, TCS, SP8 (Leica Microsystems, Wetzlar, Germany).

2.8. Statistical analysis

Results were expressed as mean ± standard deviation (SD). ANOVA (One-way between-subject ANOVA unpaired) was performed to assess the level of significance between treated groups. The gene in gene expression was considered significant when change in expression was at least 2-fold (control vs TCQA).

3. Results

3.1. TCQA promoted hair regrowth in C3H mice

Eight-weeks-old male C3H mice were used to investigate the effect of TCQA on the induction of hair growth/pigmentation cycle. During the treatment period, the mice were observed and photographed daily. At day 30, TCQA-treated group exhibited a full and markedly hair regrowth in the shaved treated area (**Figure 2.1**). The direction of the new growing hair was random and in different orientations in both groups. Results showed that this polyphenolic compound remarkably stimulated the growth of the hair shafts by approximately 40%, 80%, and 120% at day 14, 20, and 30, respectively, compared with the control (**Figure 2.2**). As for the control group (milli-Q water-treated group), only 37% of the shaved area had new hair (**Figure 2.2**). These results showed that TCQA accelerated the hair growth cycle giving arise to a fully developed hair shaft. Furthermore, following TCQA application no sign of inflammation or irritation was observed in mice epidermis (**Figure 2.3**). As mentioned in chapter I, section 1.2.1, the growth phase of the hair cycle or the anagen phase is composed of six sub-stages and according to the literature review the growth of the HF can be determined starting the third phase. In Figure 2.3 (arrows), the shape and the morphology of the HF from TCQA-treated group indicated that these HF are at advanced stage of the anagen phase. These results further show that TCQA induced the transition of the hair cycle from telogen to anagen phase accelerating hair growth in mice.

3.2. TCQA enhanced the melanin content in the hair shaft of C3H mice

To evaluate the effect of TCQA on hair pigmentation, the hair shafts from the treated area of eight-weeks-old male C3H were plucked at day 30 after treatment and visualized under the microscope. Results revealed that the hair shaft of TCQA-treated mice displayed a darker color compared with the control (**Figure 2.4a**). To prove further this point, the color intensity of the photographed hair was measured and results showed that the color of the hair shaft treated with TCQA is enhanced up to 3.26-fold compared with the control (**Figure 2.4b**). In addition, melanin assay from the plucked hair was conducted, and in Figure 2.5 we observed that the melanin content increased up to 175% after TCQA application. These results indicated that TCQA enhanced pigmentation of the hair shaft *in vivo*.

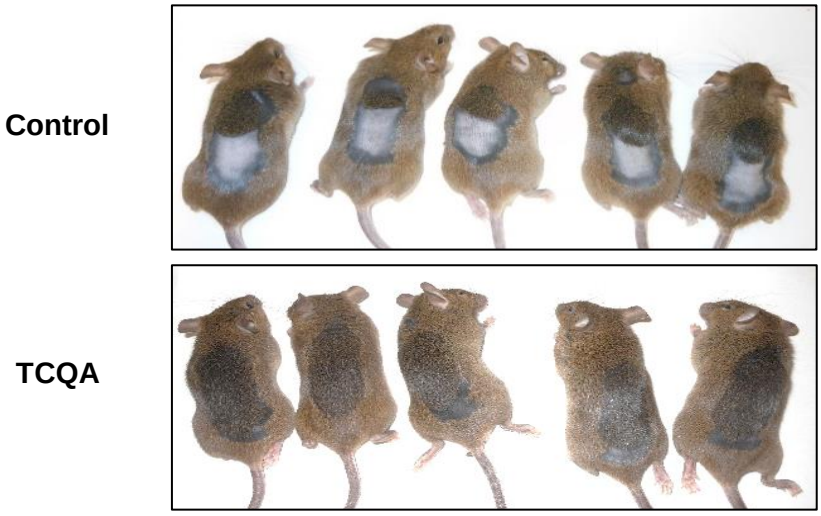

Figure 2.1. **A complete regeneration of a new hair coat in TCQA-treated group compared with the controls at day 30**. The dorsal part of eight-weeks-old male C3H was shaved and treated with topical application of 1% TCQA and the vehicle (MilliQ-water) for a month.

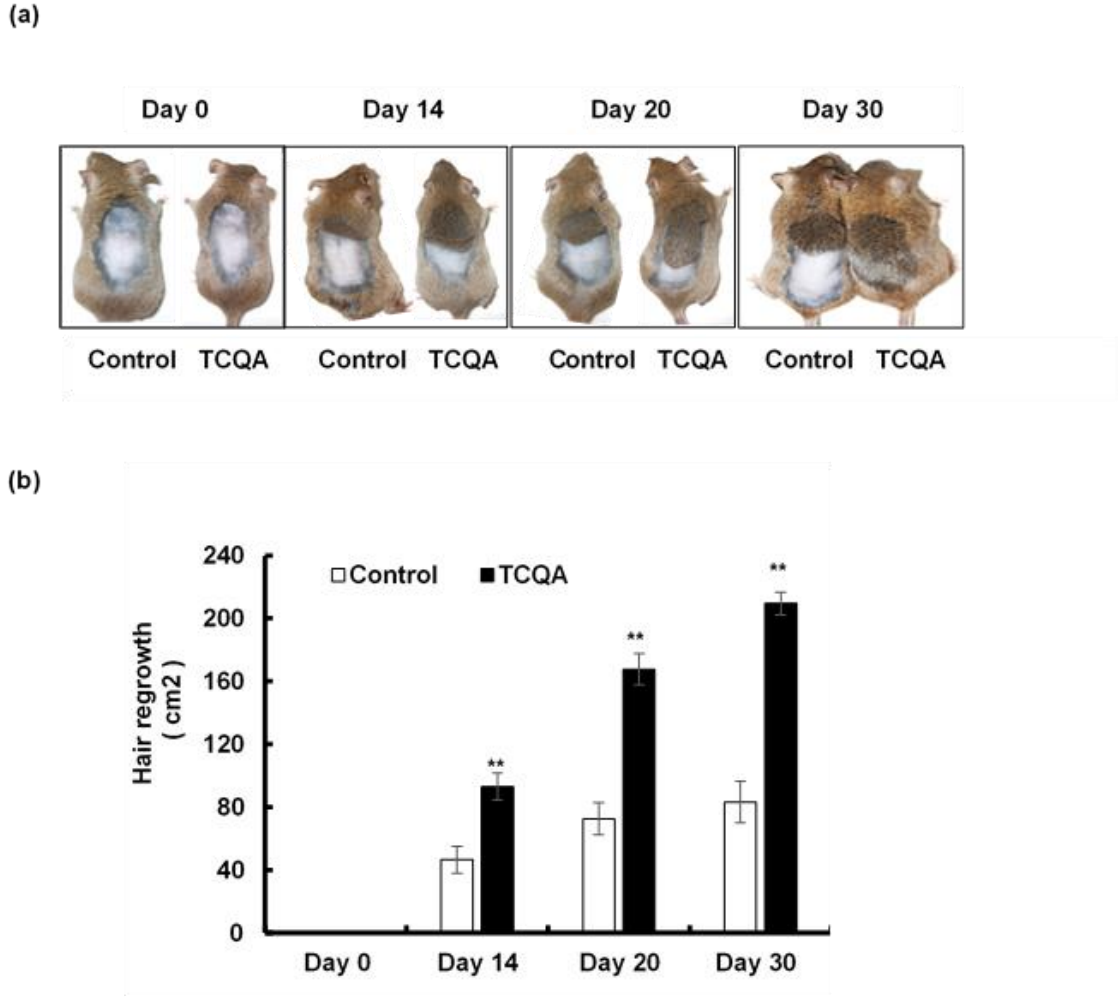

Figure 2.2. TCQA stimulated hair regrowth at the back of C3H mice. (a) Photos of the treated mice at day 0, 14, 20, and 30. (b) Measure of the new generated coat by ImageJ. *Statistically significant ($P \leq 0.05$) difference between control and TCQA-treated group. **Statistically significant ($P \leq 0.01$) difference between control and TCQA-treated mice.

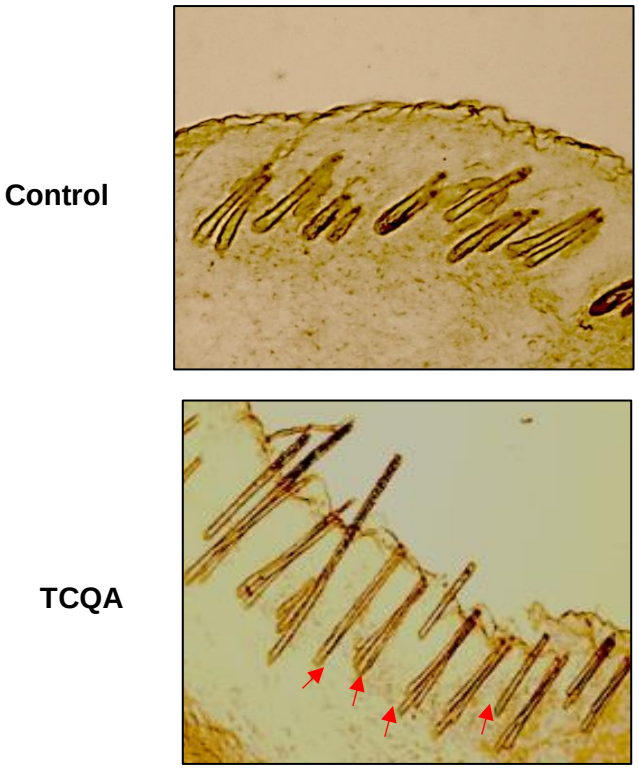

Figure 2.3. Skin sections observation. Skin from treated area from TCQA-treated group and control group were cut at thickness of 10 µm and visualized under the microscope. *Statistically significant ($P \leq 0.05$) difference between control and TCQA-treated group. **Statistically significant ($P \leq 0.01$) difference between control and TCQA-treated mice.

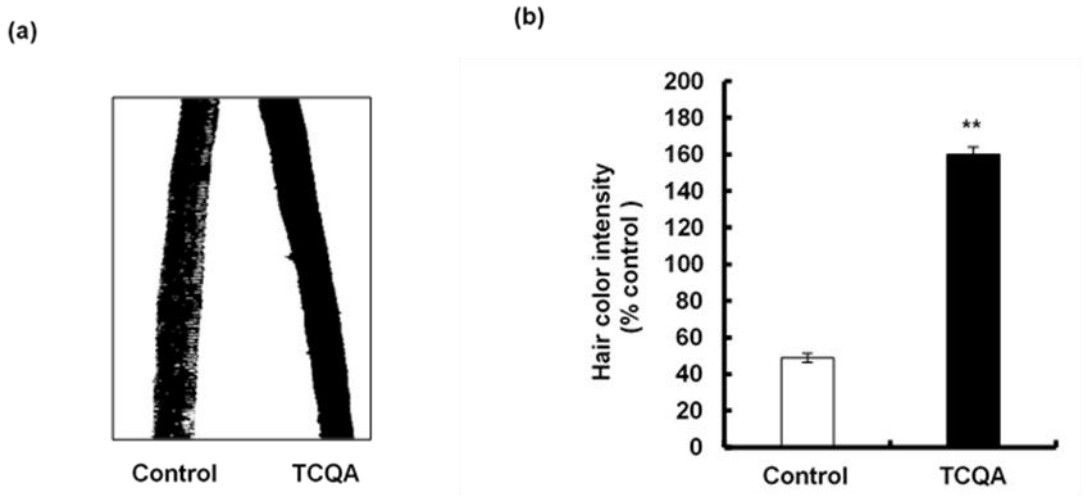

Figure 2.4. TCQA enhanced hair shaft pigmentation. (a) Hair plucked from the mice treated area and photographed under the microscope by the end of the treatment period. (b) Hair color quantification measured by Image J.*Statistically significant ($P \leq 0.05$) difference between vehicle-treated mice and TCQA-treated mice. ** Statistically significant *(*$P \leq 0.01$) difference between vehicle-treated mice and TCQA-treated mice**.**

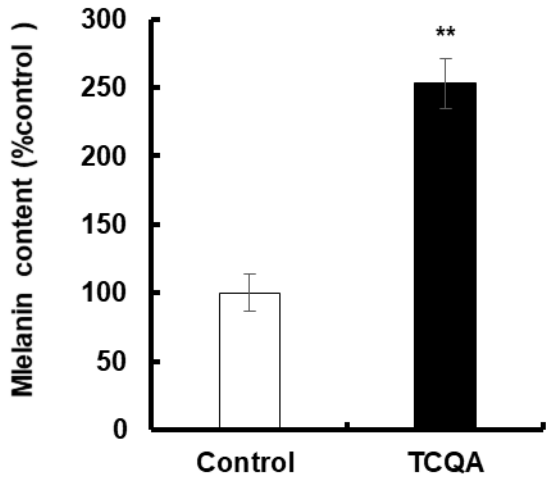

Figure 2.5. Total melanin content was determined after the end of the treatment period from the plucked hair.* statistically significant ($P \leq 0.05$) difference between vehicle-treated mice and TCQA-treated mice. ** Statistically significant ($P \leq 0.01$) difference between vehicle-treated mice and TCQA-treated mice.

3.3. Gene expression changes in C3H mice skin caused by TCQA

To uncover the mechanism behind the stimulation of hair growth and the enhancement of pigmentation by TCQA, global gene expression analysis was assessed from the treated skin. The expression of 1235 genes was modulated between the two group (control vs TCQA), and to compare the expression of these genes a volcano plot was generated. The volcano plot showed that TCQA affected positively (2-fold change) the expression of 435 genes presented in red color and downregulated 800 genes (-2-fold change) illustrated in green color, as for the rest of the genes presented in gray, their expression was not modulated (**Figure 2.6**).

As expected, both hair growth- and pigmentation-associated genes were upregulated. For the hair growth stimulation part, an enhancement in the gene expression of Wnt/β-catenin-associated genes including, *Wls, Wnt2b, Wnt4,* and *Ctnnb1*, was detected (**Table 2.1**). TCQA stimulated as well Notch, FGF, and Rac/Ras pathway-related genes. Genes significant for keratinocytes proliferation, oxidation-reduction process, ATP binding, and cell cycle were enhanced by TCQA (**Table 2.1 and 2.2**). The downregulated genes mostly were linked with the resting phase, inhibition of Wnt signaling, β-catenin degradation, and aging (**Table 2.3**).

On the other hand, for the pigmentation part, β-catenin expression was stimulated and this is the most likely cause for *Mitf* (the master regulator of the melanogenesis) upregulation up to 2.17-fold compared with the control, as β-catenin is a transcription factor stimulating Mitf activation. This upregulation was not only restricted to *Mitf* but also the gene expression of the melanogenesis enzymes *Tyr, Tyrp1,* and *Dct* was also enhanced (**Table 2.4**). A further confirmation of the effect of TCQA on the upregulation of the gene expression of the melanogenic enzymes, their transcription factor, and β-catenin was carried out by Quantitative real-time PCR analysis. Results revealed an enhancement of the gene expression of *Ctnnb1, Mitf, Tyr, Tyrp1,* and *Dct* in mice skin, proving that TCQA stimulated hair shaft pigmentation via the activation of β-catenin that triggered the transcription of Mitf, followed by the transcription of melanogenic enzymes catalyzing the reaction of melanin synthesis (**Figure 2.7**). Additionally, in microarray analysis we observed that TCQA enhanced the expression of various transcription factor regulating the melanogenesis including *Pax3, Stat3, Sox10,* and *Creb*.

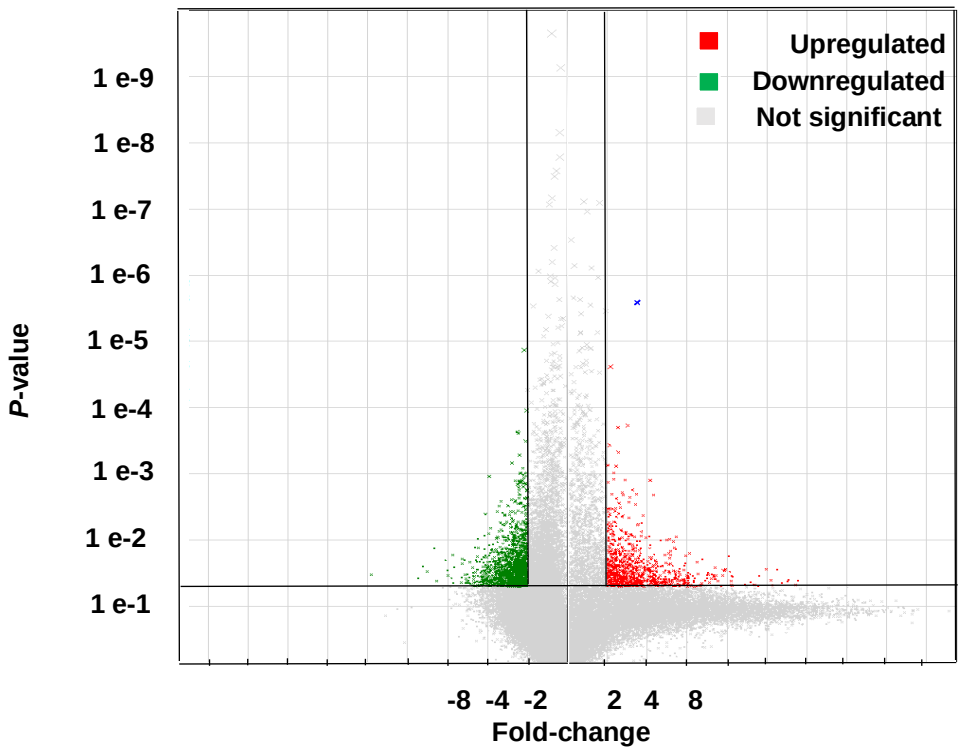

Figure 2.6. The volcano plot represent the regulated genes between the control and TCQA. The red color represent the upregulated genes, the green color the downregulated genes, and the grey color the unregulated genes. The expression of the genes above or below, left or right, the lines differed more than 2-fold change between the control and TCQA group.

Table 2.1. Top upregulated anagen-associated genes in TCQA-treated mice (vs control)

Gene symbol	Gene name	Biological function	Fold-change	*P* value **
Wls	Wntless	Wnt secretion	3.39	0.026
Fgf1	Fibroblast growth factor 1	Hair morphogenesis	3.22	0.026
Ctnnb1	Catenin (cadherin associated protein), beta 1	Cell differentiation; hair follicle morphogenesis; hair cycle process; positive regulation of fibroblast growth factor	3.2	0.043
Wnt4	Wingless-related MMTV integration site 4	Hair morphogenesis	2.87	0.047
Tspan10	Tetraspanin 10	Notch signaling promotion	2.86	0.011
RBPj	Recombination signal binding protein for immunoglobulin kappa J region-like	Hair fate determination of hair follicular stem cells	2.72	0.003
AlpL	Alkaline phosphatase	Dermal papilla marker	2.33	0.007
Dlx	Distal-less homeobox	Regulator of hair follicle differentiation and cycling	2.31	0.034
Rps3	Ribosomal protein S3	Positive regulation of NF-kB required for anagen maintenance	2.17	0.000017
Wnt2b	Wingless related MMTV integration site 2b	Hair morphogenesis	2.16	0.0002
Foxn1	Forkhead box N1	Keratinocyte differentiation; hair follicle development	2.06	0.00015
Krt14	Keratin 14	Formation of epithelial hair buds; hair cycle	2.04	0.002
Corin	Corin serine peptidase	Dermal papilla marker upregulated during anagen	2.03	0.006
Fgf2	Fibroblast growth factor 2	Hair follicle growth	2.02	0.006

* Gene functions were obtained from Mouse Genome Informatics (MGI). **ANOVA was performed to assess the level of significance between groups. The gene expression was considered significant when fold change was ≥ 2-fold (control vs TCQA).

Table 2.2. Top upregulated genes associated with the observed hair growth in TCQA-treated mice (vs control).

Gene symbol	Gene name	Biological function	Fold-change	*P* value **
Smchd1	SMC hinge domain containing 1	ATP binding	6.83	0.021
Dock2	Dedicator of cyto-kinesis 2	Positive regulation of Rac protein signal transduction	2.78	0.00014
Rassf1	Ras association domain family member 1	Ras protein signal transduction ; cell cycle	2.69	0.007
Sapcd2	Suppressor APC domain containing 2	Cell proliferation; cell cycle	2.66	0.005
Txnrd1	Thioredoxin reductase 1	Oxidation-reduction process; protection against oxidative stress	2.63	0.001
Tada3	Transcriptional adaptor 3	Stabilization and activation of the p53	2.58	0.011
Fmo4	Flavin containing monooxygenase 4	Oxidation-reduction process	2.49	0.0003
Cyp11a1	Cytochrome family 11a, polypeptide 1	Oxidation-reduction process	2.42	0.003
Kif1b	Kinesin family member 1B	ATP binding	2.3	0.004
Rasgrp2	RAS, guanyl releasing protein 2	Ras activation	2.28	0.0004
Agbl4	ATP/GTP binding protein-like 4	ATP binding	2.2	0.0001
Dgki	Diacylglycerol kinase, iota	Ras protein signal transduction regulation	2.17	1.26E-07
Plk2	Polo-like kinase 2	Ras protein signal transduction	2.17	0.027
Map3k12	Mitogen-activated protein kinase kinase kinase 12	ATP binding, cell-cycle progression	2.11	0.004

Gene functions were obtained from Mouse Genome Informatics (MGI)

**ANOVA was performed to assess the level of significance between groups. The gene expression was considered significant when fold change was ≥ 2-fold (control vs TCQA).

Table 2.3. Top downregulated genes in TCQA-treated mice (vs control).

Gene symbol	Gene name	Biological function	Fold-change	*P* value **
Ldb3	LIM domain binding 3	Regulator of transcription during telogen	-8.65	0.040
Cryab	Crystallin, alpha B	Negative regulator of apoptosis	-6.89	0.035
Ak1	Adenylate kinase 1	Cell cycle arrest	-6.24	0.027
Dst	Dystonin	Cell cycle arrest	-5.34	0.027
Gsk3b	Glycogen synthase kinase 3 beta	Phosphorylation of β-catenin	-5.08	0.002
Tcf3	Transcription factor 3	Wnt/β-Catenin repression	-4.72	0.042
Soct	Sclerostin	Wnt/β-Catenin inhibition	-4.53	0.013
Aebp1	AE binding protein 1	Regulator of telogen hair follicle	-3.8	0.015
Satb1	Special AT-rich sequence binding protein 1	Regulator of transcription during telogen	-3.36	0.026
H2afv	H2A histone family	Stem cell quiescence	-3.31	0.040
Egr1	Early growth response 1	Negative regulation of Wnt/β-Catenin; upregulated with aging	-2.59	0.045
Igfbp4	Insulin-like growth factor binding protein 3	Negative regulation of Wnt/β-Catenin	-2.55	0.031
lL-6	Interleukin 6	Inflammation response	-2.44	0.026
Shisa3	Shisa family member 3	Negative regulator of Wnt/β-Catenin	-2.39	0.002
Abra	Actin-binding Rho activating protein	Regulator of transcription during telogen	-2.22	0.046
Nfatc1	Nuclear factor of activated T cells, cytoplasmic, calcineurin dependent 1	Stem cells quiescence	-2.09	0.011

*Gene functions were obtained from Mouse Genome Informatics (MGI). **ANOVA was performed to assess the level of significance between groups. The gene expression was considered significant when fold change was ≥ 2-fold (control vs TCQA).

Table 2.4. Top upregulated pigmentation-associated genes in TCQA-treated mice (vs control).

Gene symbol	Gene name	Biological function	Fold-change	*P* value **
Cdh11	Cadherin 11	Influence the melanin biosynthesis via Wnt pathway	5.37	0.005
Pax3	Paired box 3	DCT regulation; neural crest migration; MITF activation	3.38	0.026
Ctnnb1	Catenin (cadherin associated protein), beta 1	Melanocytes stem cells differentiation; MITF activation; pigmentation	3.33	0.043
Fzd2	Frizzled class receptor 2	Canonical Wnt signaling pathway activation	2.89	0.035
Creb	cAMP responsive element binding protein	Transcription of MITF	2.67	0.031
Stat3	Signal transducer activator of transcription 3	PAX3 activation; melanocyte viability	2.34	0.004
Tyr	Tyrosinase	Melanin biosynthetic process; melanocytes proliferation	2.34	0.002
Dct	Dopachrome tautomerase	Melanin biosynthetic process; melanocytes development	2.28	
Tyrp1	Tyrosinase-related protein 1	Melanin biosynthetic process; Melanosome membrane	2.23	0.085
Agmo	Alkylglycerol monooxygenase	Reduction of ROS emission	2.22	0.021
Mitf	Microphthalmia-associated transcription factor	Pigmentation; positive regulation of transcription; melanocyte differentiation	2.17	0.007
Mc1r	Melanocortin 1 receptor	Melanin biosynthetic process; pigmentation	2.06	0.002
Sox10	SRY (sex determining region Y)-box 10	Melanocyte differentiation in the hair follicle; pigmentation	2.06	0.003
Kitl	kit ligand	Neural crest cell migration; melanocytes proliferation	2.03	0.015

*Gene functions were obtained from Mouse Genome Informatics (MGI).

**ANOVA was performed to assess the level of significance between groups. The gene expression was considered significant when fold change was ≥ 2-fold (control vs TCQA).

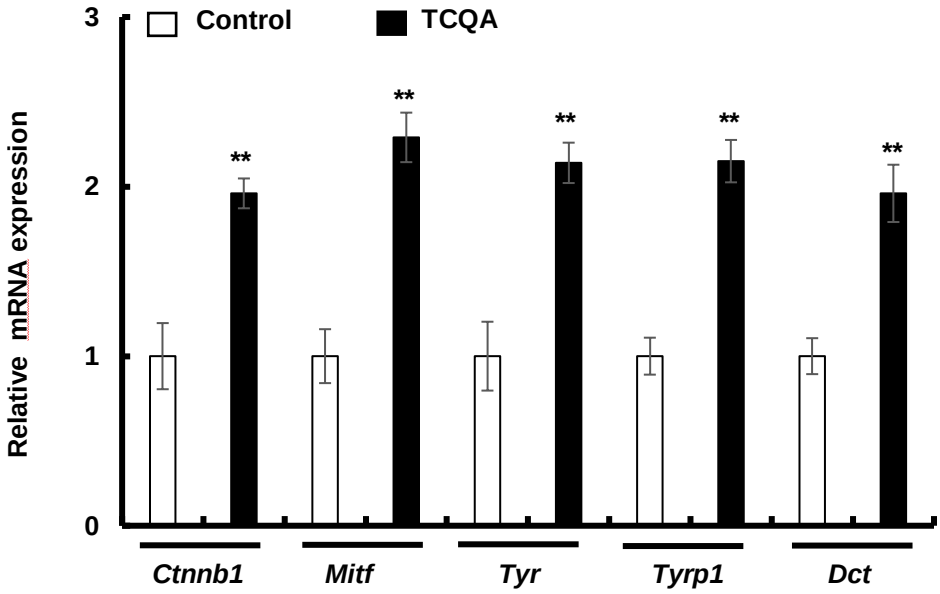

Figure 2.7. *Ctnnb1, Mitf, Tyr, Tyrp1*, and *Dct* relative mRNA expression after treatment with TCQA. The mRNA level was quantified using TaqMan real-time PCR from RNA extracted from the treated area (TCQA or milli-Q water) from the mice dorsal back. .* Statistically significant ($P \leq 0.05$) difference between vehicle-treated mice and TCQA-treated mice. ** Statistically significant ($P \leq 0.01$) difference between vehicle-treated mice and TCQA-treated mice.

Table 2.5 displays the downregulated genes by TCQA, these genes are associated with melanin degradation, melanogenesis inhibition (*Jun*, *Hdac2*, *Rps6*, and *Akt*), MAKP and mTOR pathway involved in the inhibition of melanin biosynthesis, and autophagy and apoptosis.

These results indicated that TCQA stimulated the induction and elongation of the anagen phase of the hair cycle leading to an increase of the growth rate of the HF and the pigmentation of the hair shaft.

3.4. TCQA affected the protein expression of β-catenin in mice treated skin

The hair regrowth phenotype induced by TCQA, indicated that the HFs at the treated area are characterized by an accelerated anagen phase, and microarray results revealed an upregulation in Wnt/ β-catenin-associated genes mainly *Ctnnb1* known to regulates the initiation and elongation of the anagen phase, so for this purpose the effect of TCQA on β-catenin protein expression was looked at in mice treated skin. Immunohistochemistry results revealed that upon TCQA treatment β-catenin is highly expressed in the HF precisely in the root sheath and in the bulb area where DP cells and the melanocytes are located (**Figure 2.8**). However, for the untreated control, it was mostly expressed near the upper area of the dermis and in the epidermis (**Figure 2.8**). In addition, to quantify the results of immunohistochemistry, the protein expression of β-catenin was determined by western blot and results showed as well an enhancement in its expression in TCQA-treated mice skin (**Figure 2.9**)**.** The current findings demonstrated that TCQA targeted β-catenin activation inducing the fast transition from telogen to anagen and the increase of the hair growth rate.

3.5. TCQA upregulated the protein expression of Tyrosinase (Tyr) and CD34 in mice treated skin

The protein expression of tyrosinase (Tyr) and CD34 was checked in the skin of C3H mice from the two treated groups. Tyr is considered as a marker of active melanocytes (bulbar melanocytes) that are capable of producing the pigment melanin during the anagen phase of the hair cycle. *Tyr* gene expression was upregulated in mice skin (**Table 2.4**). To further investigate the effect of TCQA on Tyr, its protein expression in mice treated skin was checked.

Table 2.5: **Top downregulated genes in TCQA-treated mice (vs control).**

Gene symbol	Gene name	Biological function	Fold-change	*P* value **
Jun	Jun proto-oncogene	JNK pathway; downregulation of melanogenesis	-4.62	0.049
Hdac2	Histone deacetylase 2	Negative regulation of canonical Wnt signaling	-4.49	0.044
Cox-2	Cyclooxygenase-2	Inducible nitric oxide synthase; Implication in melanoma	-4.13	0.016
ATG6	Autophagy related 6	Autophagy; melanin degradation	-3.96	0.023
Rps6	Ribosomal protein S6	TOR hyperactivation; melanin degradation	-3.44	0.025
Jkamp	JNK1/MAPK8-associated membrane protein	Activation by UV-radiation; MAPK activation	-2.96	0.023
Lamtor4	Late endosomal/lysosomal adaptor, MAPK and MTOR activator 4	Positive regulation of TOR signaling	-2.72	0.010
Mmp2	Matrix metallopeptidase 2	Involvement in skin damage	-2.72	0.044
Sirt1	Sirtuin 1	Negative regulation of NF-kB signaling	-2.63	0.046
Akt	Thymoma viral proto-oncogene 1	Inhibition of melanogenesis	-2.22	0.030
Wipi1	WD repeat domain, phosphoinositide interacting 1	Autophagy; modulating melanogenesis	-2.22	0.019
Lamtor5	Late endosomal/lysosomal adaptor, MAPK and MTOR activator 5	Activation of mTOR pathway promoting tumorigenesis; blocking melanin synthesis	-2.18	0.020
Mdm4	Transformed mouse 3T3 cell double minute 4	Negative regulation of apoptotic process	-2.08	0.043
Bcl-2	B cell leukemia/lymphoma 2	Cell aging; proapoptotic and antiapoptotic regulators of apoptosis	-2.06	0.021

* Gene functions were obtained from Mouse Genome Informatics (MGI).

**ANOVA was performed to assess the level of significance between groups.The gene expression was considered significant when fold change was ≥ 2-fold (control vs TCQA).

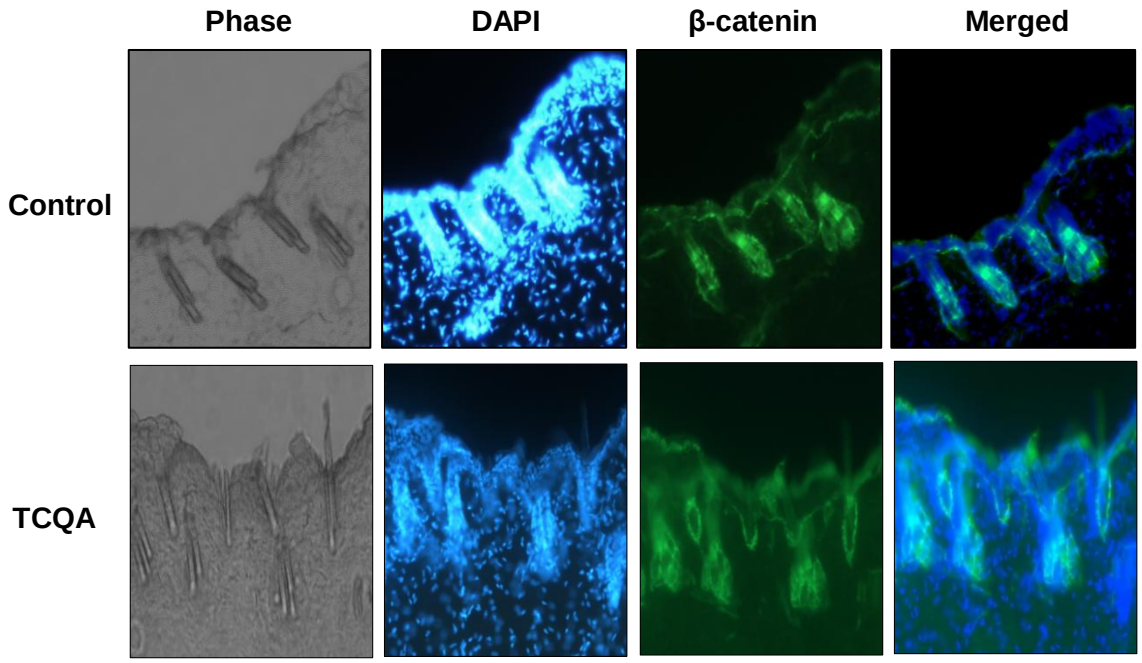

Figure 2.8. **TCQA enhanced β-catenin expression in the hair follicle.** Immunohistochemistry was performed to measure β-catenin expression in skin collected from the treated area from mice dorsal part at 30 days after treatment. The figure is divided into four panels, the first panel is the phase, the second is DAPI to stain the nucleus, the third is for β-catenin staining, and the last panel is a merge between β-catenin and the nucleus.

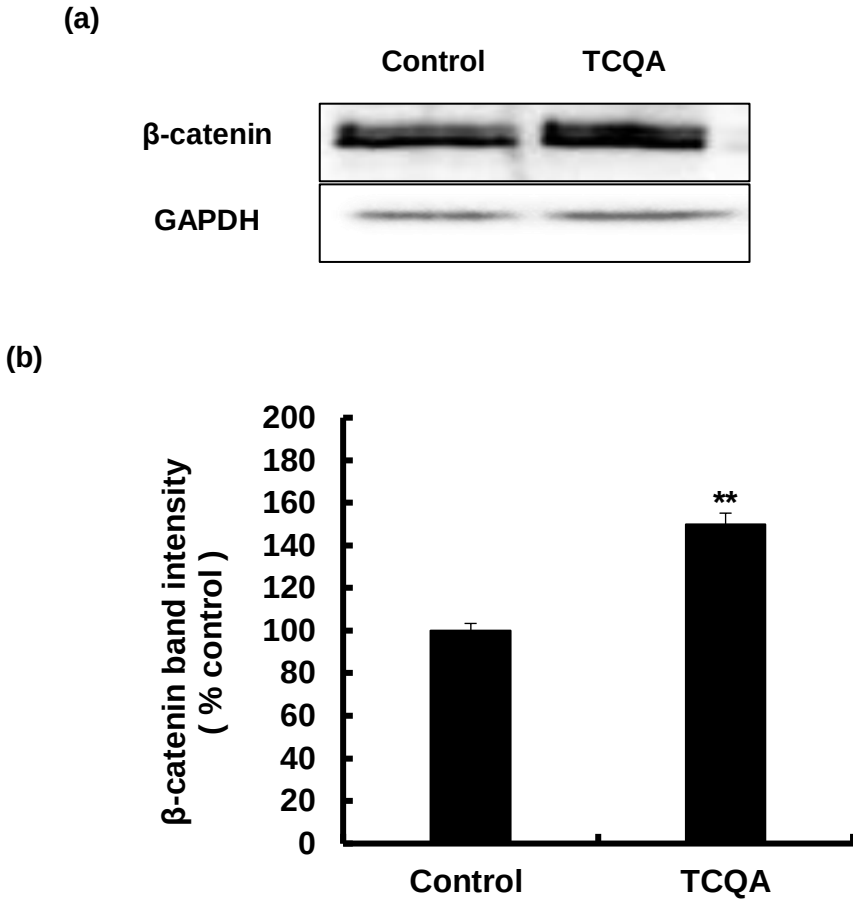

Figure 2.9. β-catenin protein expression was determined at the end of the treatment period. (a) The protein was extracted from the treated area from the mice dorsal part, and western blot was carried away. (b) Band intensities was done assessed using LI-COR system. Results represent the mean ± SD of three independent experiments. *Statistically significant ($P \leq 0.05$) difference between control and TCQA-treated mice. **Statistically significant ($P \leq 0.01$) difference between control and TCQA-treated mice

Results revealed that Tyr expression was observed to be enhanced in the epidermis and in the bulb area of the HF suggesting the activation of the melanocytes and production of melanin in mice treated hair shaft (**Figure 2.10**). On the other hand, the expression of CD34 expressed in the epithelial cells of the HF and known to be upregulated during anagen phase was determined as well. CD34 expression was enhanced in the outer root sheath and the bulge area of the HF (**Figure 2.10**).

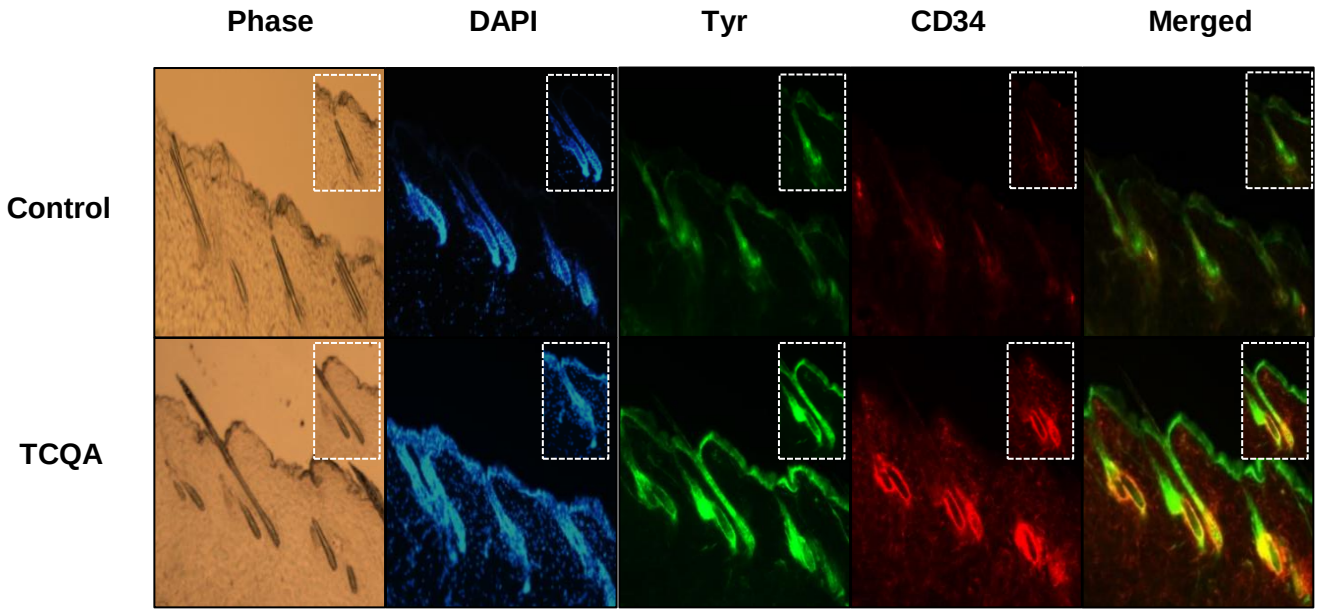

Figure 2.10. **Immunohistochemistry analysis of TYR and CD34 in the hair follicle and the epidermis of the treated skin.** The first panel is the phase, the second is DAPI to stain the nucleus, the third is for TYR staining, the fourth is for CD34 staining, and the last panel is a merge between TYR and CD34.* statistically significant *(*$P \leq 0.05$) difference between vehicle-treated mice and TCQA-treated mice. ** Statistically significant ($P \leq 0.01$) difference between vehicle-treated mice and TCQA-treated mice.

4. Discussion

The hair follicle (HF) activity is governed by various signaling transduction pathways that control the development, differentiation, pigmentation, and growth. Due to its cyclical nature, it is establish as model to investigate the mechanism behind each different phases: growth, regression, and resting [89].

Here in this chapter II, the role of a caffeoylquinic acid derivatives, 3,4,5-tri-*O*-caffeoylquinic acid (TCQA) on the promotion of hair growth/pigmentation cycle *in vivo* via the stimulation of Wnt//β-catenin pathway was investigated. Results showed that TCQA induced a complete hair regrowth in the shaved area of the back of eight-week-old C3H male mice (**Figure 2.1 and 2.2**). TCQA hair regrowth stimulating effect was very much alike to the hair growth promoting effect of minoxidil an approved drug against alopecia in this exact mice strain [90]. The HFs from TCQA-treated mice are characterized by an anagen phase structure and morphology compared to control mice (**Figure 2.3**). Actually, during the growth phase, the HF grows to form the hair bulb containing the dermal papilla (DP) and the hair shaft becomes rooted deep in the sebaceous gland and the dermis [91]. TCQA-treated mice HFs are then in advanced stage of anagen phase of the hair cycle confirming that TCQA promoted the transition from the telogen to anagen phase.

The life of the melanocytes located at the hair bulb or follicular melanocytes (FM) is totally linked with the hair cycle and the pigmentation only occurs during the anagen phase [63,92]. Results showed that TCQA induced the initiation of the anagen phase so the question if TCQA could stimulate as well the pigmentation of the hair shaft was raised. Results revealed that TCQA actually enhanced the color and the melanin content of the hair shaft after one month application (**Figure 2.4 and 2.5**).

A further investigation of the molecular mechanism behind TCQA hair growth and pigmentation promotion effect in C3H mice was carried out. Global gene expression analysis revealed that the expression of 1,235 genes was regulated after treatment with TCQA and results showed an upregulation of 435 and a downregulation of 800 genes (**Figure 2.6**). First of all, an increase in the expression of markers of the hair growth cycle and mainly of DP cells was observed including alkaline phosphatase (*Alpl)* and *Corin* (**Table 2.1**). *Alpl* is expressed in all phases of the hair cycle but its expression increases during the anagen phase in the DP, as for Corin is reported

to be upregulated in DP during the regeneration phase only [93]. These results further showed the effect of TCQA on the activation of the anagen phase of the hair cycle.

Interestingly, pathways involved in both hair growth and pigmentation were stimulated by TCQA in C3H mice treated skin (**Table 2.1 and 2.4**). Wnt/ β-catenin, Notch, and FGF pathway play a major role for the regulation of the HF cycle and the formation of hair shaft from the differentiated hair progenitors [94,95]. Microarray results revealed an upregulation in the expression of Notch signaling-associated gene including, *RBPj* and *Tspan10* involved both in the regulation of hair growth cycle and matrix cell differentiation [96–99]. The HFs of TCQA-treated mice were in advanced stage of the growth phase compared with the control, and this appears to be caused by an upregulation in Wnt/β-catenin-related genes and their target genes like *Foxn1,* known to initiate the regeneration of the HF and the differentiation of matrix cell [23,100,101]. An upregulation in FGF pathway-related genes *Fgf1* and *Fgf2* was observed in Table 2. These FGF molecules are involved in the promotion of the anagen phase of the HF of C57BL/6 mice which are initially at the telogen phase [94,102]. Additionally, there is a crosstalk between Wnt/β-catenin and FGF pathway as it has been reported that the abrogation of Wnt/β-catenin signaling decrease the expression of FGF signaling genes [103]. The major role playing by β-catenin for the initiation and elongation of the anagen phase is well establish and the absence induces a premature catagen phase [23,104,105]. Here, TCQA caused β-catenin to translocate into the nucleus of DP causing its activation and therefore inducing an early and longer anagen phase of the HF (**Figure 2.7, 2.8 and 2.9**).

On the other hand, pigmentation-associated genes were stimulated as well (**Table 2.4**). This effect can be attributed also to β-catenin activation. In fact, it has been revealed that Wnt/β-catenin pathway is involved in the development, survival, and differentiation of melanocyte during formation and maturation. Also, β-catenin regulates positively *Mitf* expression at the transcriptional level promoting the pigmentation [106–108]. Moreover, Wnt/β-catenin and Kit signaling sequentially regulate MSCs migration and differentiation [106]. In this study, β-catenin gene expression and its receptor *Fzd2,* as well as *Kit,* and *Mitf* gene expression were enhanced after TCQA treatment (**Table 2.4 and Figure 2.8**).

MITF is the transcription factor of the three melanogenesis enzymes and is known to play a crucial role in the regulation of melanocyte development, function, and survival, and mice

carrying null alleles of *Mitf* gene showed a loss of melanocytes derived from the neural crest cells [109–111]. Mitf transcription is regulated by a number of signaling systems and transcription factors includingMCR1 and SCF-KIT pathway that are involved in melanocyte pigmentation and development [42,112,113]. TCQA enhanced the gene expression of these transcription factors as illustrated in Table 2.4. Although MITF is considered to be a major regulator of melanogenesis, it has been reported that alone it cannot activate completely Tyr gene expression [114,115]. Recently, the role of STAT3 in stimulating the transcription of Tyr is established [116]. Additionally, STAT3 transactivated PAX3 which plays an important role in neural crest cells and melanocyte development, and Mitf transcription through a communication with FGF2 [117,118]. In this study, the gene expression of *Stat3, Pax3,* and *Fgf2* was upregulated in TCQA-treated mice skin confirming further the activation of Mitf (**Table 2.1 and 2.4**).

The activation of Mitf may explain the enhancement of the gene expression of the melanogenic enzymes *Tyr, Tyrp1*, and *Dct* upon treatment with TCQA in mice collected skin (**Table 2.4 and Figure 2.7**). Mouse follicular pigmentation is under a genetic complex and the biosynthesis of melanin or melanogenesis is a results of series of transformations and reactions engaging l-tyrosine and mediated by TYR, TYRP1, and DCT [119,120]. Additionally, these enzymes are considered as a markers of melanocytes and often used in histological analysis allowing an accurate classification of the type and the stage of melanocytes, and the location in the HF [121]. In this study, histological analysis were performed to label the FM using Tyr expression and results showed that TCQA upregulated Tyr expression in the epidermis and along the HF especially in the bulb region and this indicated the activation of FM and the production of melanin during the anagen phase of the hair cycle (**Figure 2.10**). Moreover, a staining with CD34 was done and its expression was enhanced in the bulge area where the MSC are located (**Figure 2.10**). CD34 expression was checked because it is expressed only during anagen phase, and is considered to be a maker of MSC that have the ability to differentiate into active melanocytes [122,123].

TCQA effect on hair cycle is due to the upregulation of Wnt/β-catenin pathway and its target genes. This effect was further supported by a downregulation of genes repressing Wnt/β-catenin pathway including, *Gsk3b, Tcf3, Igfbp4,* and *Shisa3* (**Table 2.3**). Gsk3b forms a complex with Axin and induces the phosphorylation of β-catenin and this will cause its degradation and non-activation leading to an early entry to the catagen phase [124]. Tcf3 and Igfbp4 repressed the

canonical Wnt signaling during neocortical formation [22,125]. Telogen associated-genes were also negatively modulated by TCQA like *Aebp1* and *Nfatc1* involved, respectively in the regulation of MAPK pathway and stem cell quiescence [126] [127–129]. A repression of age-associated genes such as *Egr1* and *Fos* was observed as well in TCQA-treated mice skin (**Table 2.3**). TCQA affected he expression of genes in involved in the inhibition of melanogenesis, reactive oxygen species (ROS) autophagy, mTOR and AKT pathway (**Table 2.5**). Melanogenesis is a process that is affected by the autophagy as it participate in melanosome degradation, and an impaired melanosome function allows rampant UVR penetration and melanin degradation and AKT/mTOR pathways are one of the well-studied pathways involved in autophagy [130,131]. In addition, during melanin synthesis ROS are produced via the oxidation of L-tyrosine and this leads to the depletion of MSCs pool, melanocytes damage, and skin and hair shaft ageing [63,132,133].

Taken together, in this chapter II, TCQA triggered the activation of Wnt/β-catenin pathway leading to the initiation of the anagen phase of the hair cycle and therefore to the enhancement of hair growth and pigmentation in C3H mice hair shaft. In order to establish TCQA as a drug against hair loss and graying a validation of the observed effect was carried out in *in vitro*. TCQA was tested then in human hair follicle human dermal papilla (HFDPC) to check its effect on hair growth in chapter III, then in human melanocytes (HEM) and B16 murine melanoma cells (B16F10) to determine its effect on pigmentation in chapter IV.

Chapter III: Determination of the effect of 3,4,5-tri-*O*-caffeoylquinic acid (TCQA) on hair growth in human hair follicle dermal papilla cells (HFDPCs)

1. Introduction

The hair follicle (HF) is formed via a coordinated interaction between the epidermal (epithelial) and the dermal (mesenchymal). The dermal/mesenchymal compartment plays the role of inducers and the epithelial compartment of responders. The mesenchymal is formed by a pool of fibroblastic cells that are composed of the dermal papilla cells (DP), and the dermal sheath (DS) the reservoir to replenish the DP cells [134]. The DP cells are located at the bulb region surrounded by keratinocytes like cells called matrix cells [135].

The role of DP in the induction and maintenance of the hair growth cycle is crucial [14,136–138]. During the growth phase or the anagen phase, the DP regulates the movement of HF stem cells from their niche to the bulb area, where they differentiate to form the matrix cells that will be proliferating to give arise to the hair shaft [6,93]. During the catagen and telogen phase, the lower portion of the HF stop proliferating and eventually dies through apoptosis as the DP cells stop sending signals [18].

The Wnt/β-catenin signaling pathway plays an important role in the transition from telogen to anagen as well as the duration and elongation of the anagen phase [78]. Moreover, this pathway plays a major role in the development, growth, and proliferation of the HF and the regulation of the activity of embryonic and adult stem cell populations [80,81]. Upon β-catenin activation after its translocation to the nucleus, it regulates target genes responsible of the HF maintenance and it interact as well with other pathways including FGF,SHH, and BMP involved in keratinocytes differentiation and hair growth cycle regulation [20,82,83].

The inhibition of β-catenin expression affects mouse hair growth cycle and induces an early entry to the catagen phase, and on the other hand its overexpression in DP promotes postnatal hair growth due to a longer anagen phase [19–21]. Activating β-catenin expression is therefore considered significant in the initiation of the anagen phase and the promotion of hair growth cycle.

In this chapter, TCQA was tested in human hair follicle dermal papilla cells (HFDPCs) to confirm the hair growth promotion effect observed *in vivo* (chapter II).

2. Materials and methods

2.1. Sample preparation

Synthesized 3,4,5-tri-*O*-caffeoylquinic acid (TCQA) with 97% purity was provided by Dr. Kozo Sato from Synthetic Organic Chemistry Laboratories, the FUJIFILM Corporation (Kanagawa, Japan). Prior using to the cells, TCQA was dissolved in 70% ethanol and then diluted in cell culture medium.

2.2. Cells and cell culture

Human hair follicle dermal papilla cells (HFDPCs) were purchased from Cell Application Inc. (Tokyo, Japan). The cells were cultured in papilla cell growth medium (Toyobo, Osaka, Japan) supplemented with growth factors: fetal calf serum, insulin transferrin triiodothyronine, bovine pituitary extract, and cyproterone solution (Toyobo, Osaka, Japan) and were maintained in under sterile conditions at 37 °C (5% CO_2). The cells were cultured in 75-cm^2 flask (BD Falcon, England, UK) and the viability was determined prior to each experiment and at every passage.

2.3. MTT assay

To measure the cell proliferation after treatment with TCQA, MTT assay or the 3-(4,5-dimethyl-thiazol-2-y1) 2,5-diphenyl tetrazolium bromide (Dojindo, Kumamoto, Japan) was performed. Firstly, HFDPCs were seeded in 96-well plate at 3×10^5 cells/100 µl well at 37 °C. The cells were allowed to attach for 24 h, then the growth medium was changed and a treatment with different concentrations of TCQA was added. After 48 and 72 h treatment, 10 µl of 5 mg/ml MTT reagent was added to the cells for 6-8 h followed by an addition of 10% sodium dodecyl sulfate (SDS) for overnight. Microplate reader (Powerscan HT, NJ, USA) was used to measure the Absorbance (570 nm). The viability of the cells was quantified as the percentage (%) of living cells relative to the untreated cells. The cells were observed daily to check if there will be any differences in the morphology using a contrast microscope (Leica Microsystems, Wetzlar, Germany).

2.4. ATP assay

Adenosine triphosphate (ATP) assay was performed using a luminescence luciferase assay kit (Toyo Ink, Tokyo, Japan). After 24 h seeding in 96-well plate at 3×10^5 cells/ 100 µl well, the cells were treated with TCQA (0 and 10 µM) and with 0.1 µM minoxidil used as a positive control (Tokyo Chemical Industry, Tokyo, Japan) for 24 and 48 h. Prior to adding 100 µl of ATP reagent,

the plate was cooled down for 15 min at RT. Then the reagent and the treated cells were homogenized and the plate was incubated for 1 min in the dark, and 150 µl of the mixed suspension was transferred to a new white 96-well plate followed by a 10 min incubation at RT. HFDPCs ATP content was measured by luminescence and calculated as the percentage (%) of TCQA treated-cells relative to the untreated cells.

2.5. RNA extraction

HFDPCs were seeded at a density of 5×10^5 cells per 100-mm petri dish for 24 h. The cells were then treated with 0 and 10 µM TCQA and 0.1 µM minoxidil. Additionally, the cells were seeded into three different petri dish for 24 h, the first one was treated with 10 µM XAV939 a β-catenin inhibitor (SIGMA, Saint Louis, USA). The second one with 10 µM XAV939, then the medium was removed and replaced with a new one containing 10 µM TCQA (XAV939/TCQA), and in the final dish, HFDPCs were co-treated with 10 µM XAV939 and TCQA (XAV939+TCQA). The experiment was performed after 6 and 12 h treatment. Following the treatment, the growth medium was removed, and the cells were washed twice with cold PBS before the total RNA was extracted using ISOGEN kit (Nippon Gene, Tokyo, Japan) following the manufacturer's instructions. The extracted RNA was quantified using a NanoDrop 2000 spectrophotometer (NanoDrop Technologies, Massachusetts, USA).

2.6. Quantitative real-time PCR analysis

As mentioned above, the total RNA was extracted from HFDPCs, then quantified, and the cDNA was synthesized using SuperScript III reverse transcription kit (Invitrogen, CA, USA). The cycling protocol is as follows: 95 °C for 10 min, 40 cycles of 95 °C for 15 s, and 60 °C for 1 min. TaqMan Universal PCR mix and TaqMan probes specific to *CTNNB1* (Hs99999168_m1), and *ALPL* (Hs01029144) (Applied Biosystems, CA, USA) were used for real-time PCR reaction. *GAPDH* (Hs 02786624_ g1) (Applied Biosystems, CA, USA) was used as an endogenous control. All reactions were run in triplicates. The $2-\Delta\Delta Ct$ method was applied to calculate the relative mRNA expression levels using Gapdh and GAPDH as a housekeeping endogenous control.

2.7. *Protein extraction*

HFDPCs were seeded at density of 5×10^5 cells per 100-mm petri dish. After seeding, the cells were treated with 0 and 10 µM TCQA and 0.1 µM minoxidil for 12 and 24 h. Total protein

was extracted using radio-immunoprecipitation assay (RIPA) buffer (SIGMA, Saint Louis, USA) and protease inhibitor following the manufacturer's instructions. The quantification of the proteins (10-15 µg) was assessed using 2-D Quant kit according to manufacturer's instructions (GE Healthcare, Chicago, USA).

2.8. Western blot analysis

The extracted proteins were separated in 10% sodium dodecyl sulphate-polyacrylamide gel electrophoresis (SDS-PAGE). The transfer was done under agitation to the polyvinylidene difluoride membrane (PVDF) (Millipore, NJ, USA). The membrane was blocked for 1 h at RT, then a solution of 1:1000 of the primary antibody β-catenin 71-2700 (Thermo Fisher Scientific, Massachusetts, USA) was added. After overnight incubation at 4°C, the membrane was immersed in a solution of the second antibody goat anti-rabbit IRDye 800 CW. Then the expression was detected using LI-COR Odyssey Infrared Imaging System (LI-COR, NE, USA).

2.9. Immunocytochemistry

HFDPCs were seeded at a density of 3×10^4/well in lab-tek slides chambers (SIGMA, Saint Louis, USA), and then allowed to attached for overnight at 37 °C. The cells were treated with 0, and 10 µM TCQA and 0.1 µM Minox for 24 h followed by a washing with 0.1% v/v Triton X-100 /PBS. The cells were then fixed and immersed in the blocking solution for 1 h incubation at RT, then the first antibody rabbit anti-β-catenin (Abcam, Rockford, USA) was added for overnight at 4 °C. Therefore, the cells were immersed in a solution of 1:10000 dilution of Alexa 594-conjugated anti-rabbit (Abcam, Rockford, USA) and mounted with DAPI. The slides containing the cells were visualized under a confocal microscope Leica, TCS, SP8 (Leica Microsystems, Wetzlar, Germany).

2.10. Statistical analysis

Results were expressed as mean ± standard deviation (SD). Statistical analysis was performed using Student's t-test when comparing two value sets (control vs TCQA). *P* value of ≤ 0.05 was considered significant. ANOVA (one way between-subject ANOVA unpaired) was performed to assess the level of significance between Minox and TCQA-treated cells; A *P* value of ≤ 0.05 was considered significant.

3. Results

3.1. TCQA enhanced the proliferation and the ATP content of HFDPCs

MTT assay was conducted to check the effect of TCQA on the cell proliferation of DP cells. The cell viability assay was assessed after 48 and 72 h treatment with different concentrations of the compound. Results showed that TCQA was not cytotoxic to the cells at all concentrations and in fact, the proliferation of the cells was stimulated up to 160% with 10 µM TCQA after 48 h treatment in comparison with the untreated cells (**Figure 3.1**). The ATP content was checked as well, because the ATP increases in DP cells during anagen phase. 10 µM TCQA increased the ATP content of HFDPCs by around 60% after 48 h treatment (**Figure 3.2**). This result confirm to what have been found in gene expression analysis (illustrated in chapter II, Table 2.2) that TCQA positively modulate ATP binding genes.

3.2. Alkaline phosphatase (ALP) expression was enhanced by TCQA in HFDPCs

Alkaline phosphatase (ALP) marks DP cells during the HF cycle and it is expression increases during the anagen phase. Microarray results (presented in chapter II, Table 2.1) showed an upregulation in *ALPL* gene expression upon TCQA application, so its expression in HFDPCs was further checked. Here, we observed an upregulation in *ALPL* expression after 6 and 12 h treatment with TCQA (**Figure 3.3**). This results showed that the sample stimulated the proliferation of HFDPCs supporting the cell proliferation assay mentioned above.

3.3. *TCQA upregulated β-catenin expression in HFDPCs*

β-catenin is highly expressed in DP cells especially during the onset of the anagen phase and the absence results to an early entry to catagen phase [103]. For this purpose, the effect of TCQA on β-catenin protein and gene expression levels in DP cells was checked. In Figure 3.4, an increase in its protein expression after 12 and 24 h with 10 µM TCQA was observed. Immunostaining results showed that 10 µM TCQA caused the translocation and the accumulation of β-catenin into the nucleus and this prove further the activation of this protein after 24 h treatment (**Figure 3.5**). Moreover, TCQA enhanced the *CTNNB1* expression after 6 and 12 h (**Figure 3.6**).

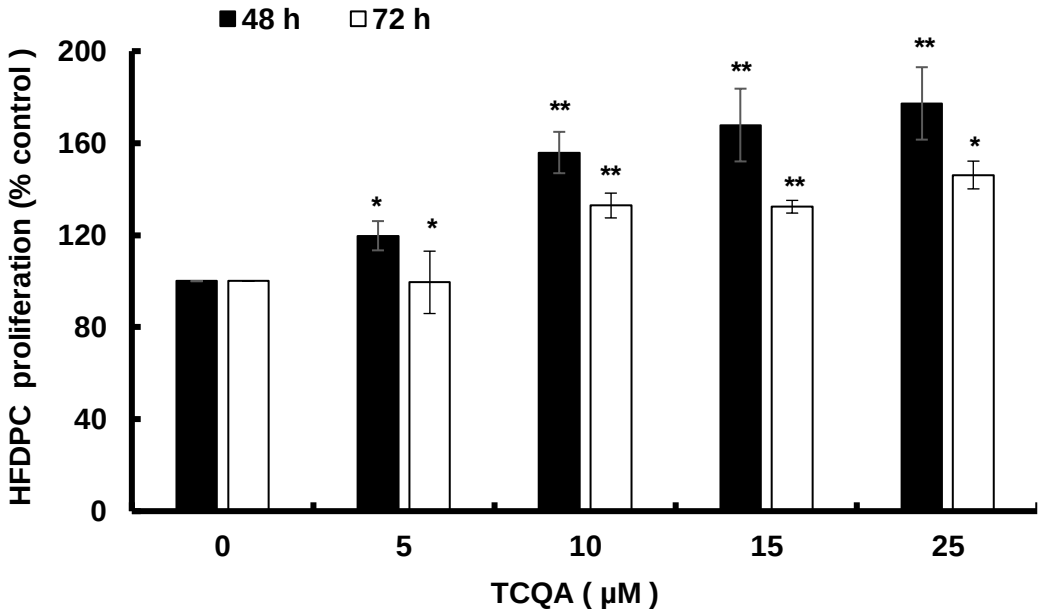

Figure 3.1. **TCQA stimulated HFDPCs cell proliferation after 48 and 72 h treatment**. Results represent the mean ± SD of three independent experiments. *Statistically significant ($P \leq 0.05$) difference between control and treated cells. **Statistically significant ($P \leq 0.01$) difference between control and treated cells.

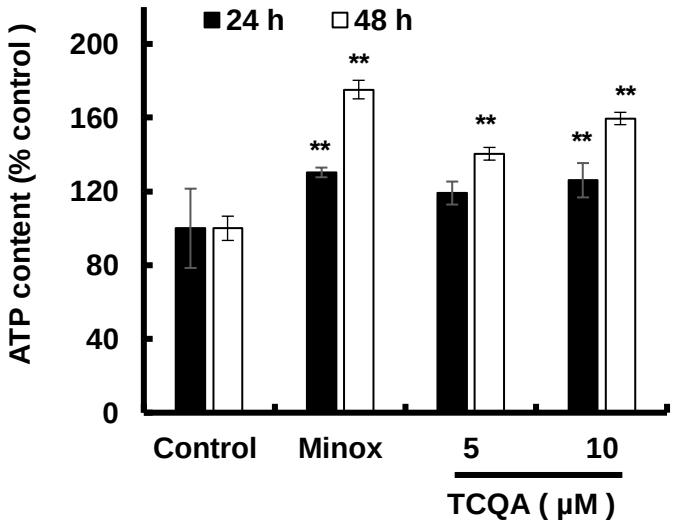

Figure 3.2. **ATP content determination after treatment with 5 and 10 µM of TCQA and 0.1 µM of Minox (minoxidil).** Results represent the mean ± SD of three independent experiments. *Statistically significant ($P \leq 0.05$) difference between control and treated cells. **Statistically significant ($P \leq 0.01$) difference between control and treated cells.

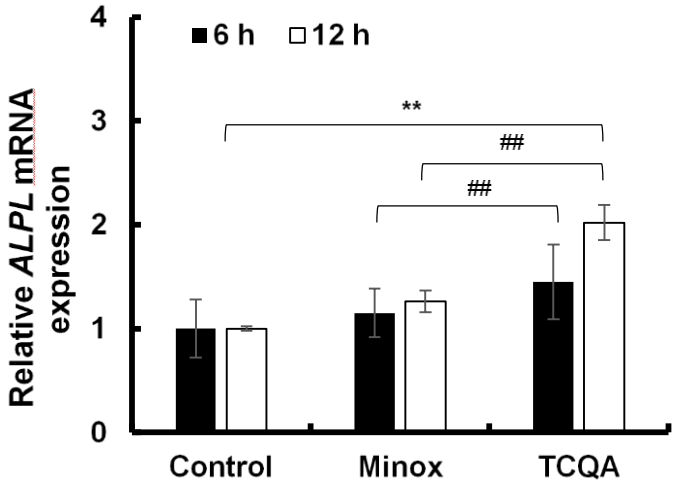

Figure 3.3. **Gene expression of *ALPL* (Alkaline Phosphatase) after 6 and 12 h treatment with 0, 10 µM TCQA, and 0.1 Minox (minoxidil).** The mRNA level was quantified using TaqMan real-time PCR after treatment. Results represent the mean ± SD of three independent experiments. *Statistically significant ($P \leq 0.05$) difference between control and treated cells. **Statistically significant ($P \leq 0.01$) difference between control and treated cells. ##Statistically significant ($P \leq 0.01$) difference between Minox-treated cells and TCQA-treated cells.

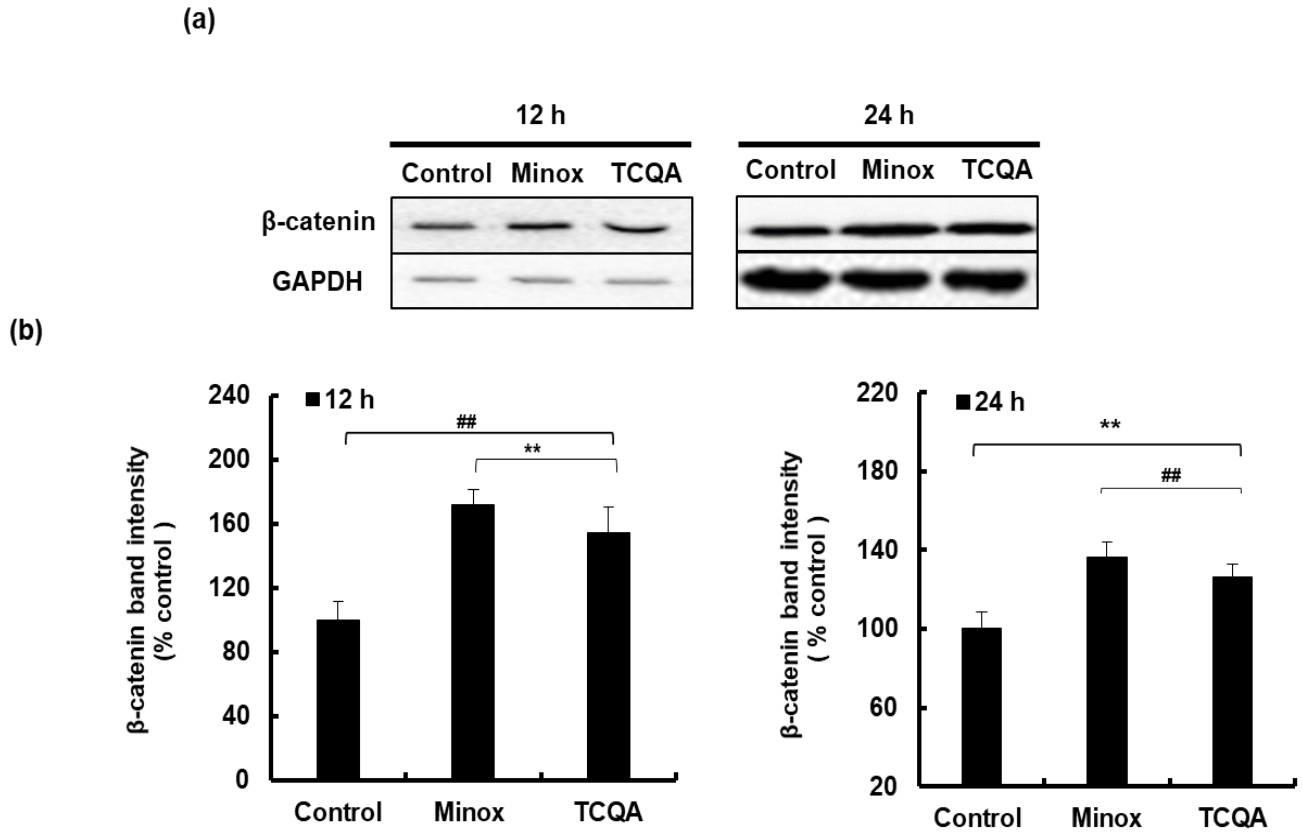

Figure 3.4. TCQA stimulated β-catenin expression in HFDPCs. (a) β-catenin protein expression after 12 and 24 h treatment with 0, 10 μM TCQA and 0.1 μM Minox (minoxidil). (b) Band intensities was done using LI-COR system after 12 and 24 h treatment. Results represent the mean ± SD of three independent experiments. *Statistically significant ($P \leq 0.05$) difference between control and treated cells. **Statistically significant ($P \leq 0.01$) difference between control and treated cells. ##Statistically significant ($P \leq 0.01$) difference between Minox-treated cells and TCQA-treated cells.

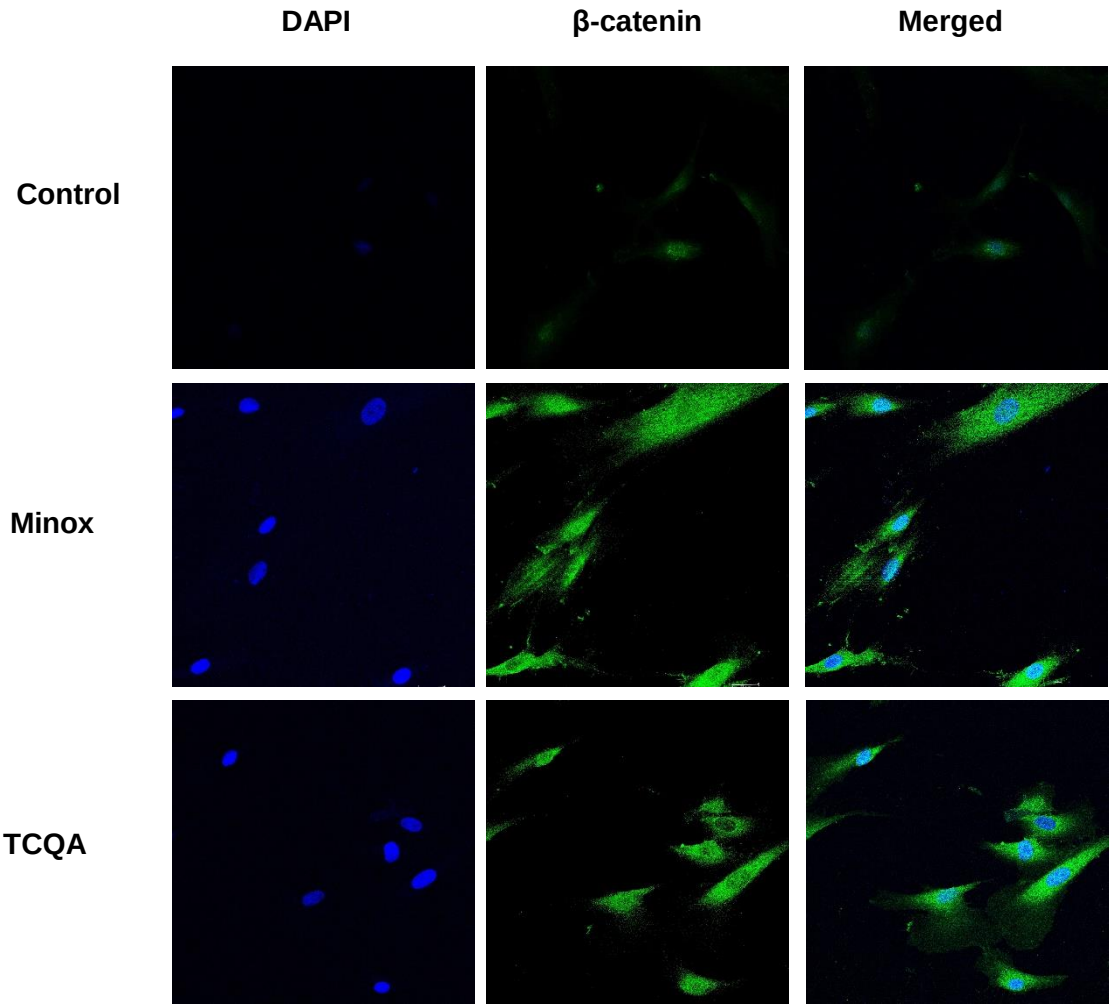

Figure 3.5. **Immunocytochemistry of β-catenin expression in HFDPC after 24 h treatment with 0, 10 µM TCQA and 0.1 µM Minox.** Scale bar = 25 µm; magnificence 40 X. The figure is divided into three panels, the first is DAPI to stain the nucleus, the second is for β-catenin staining, and the last panel is a merge between β-catenin and the nucleus.

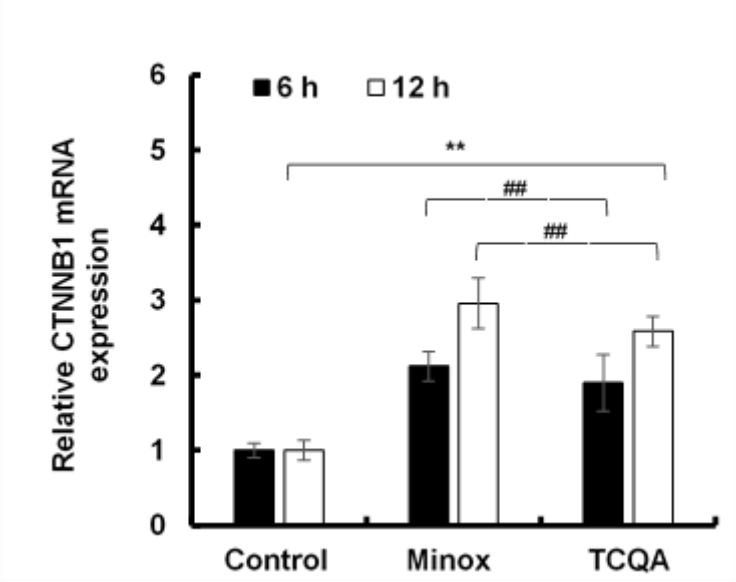

Figure 3.6. **Gene expression of *CTNNB1* (β-catenin) after treatment with 0 and 10 µM TCQA, and 0.1 µM Minox (minoxidil) for 6 and 12 h**. The mRNA level was quantified using TaqMan real-time PCR after treatment. Results represent the mean ± SD of three independent experiments. *Statistically significant ($P \leq 0.05$) difference between control and treated cells. **Statistically significant ($P \leq 0.01$) difference between control and treated cells. ##Statistically significant ($P \leq 0.01$) difference between Minox-treated cells and TCQA-treated cells.

3.4. TCQA upregulated β-catenin gene expression after inhibition with XAV939 in HFDPCs

XAV939 is a known inhibitor of β-catenin, actually it binds to tankyrase and this will lead to a higher expression of AXIN that induces the phosphorylation and the degradation of β-catenin [139]. To select the non-cytotoxic concentration of the inhibitor, an MTT assay was performed for 48 h and 10 µM XAV939 was used for further experiment (**Figure 3.7**).

After that, the cells were divided into three groups as explained in the materials and methods section of this third chapter. HFDPCs treated with only 10 µM XAV939 for 6 and 12 h had a decreased expression of *CTNNB1* compared with the control showing the inhibitory effect of the compound (**Figure 3.8**)**.** The second group of cells were treated firstly with the inhibitor for 6 and 12 h (separately) and then the medium was replaced with 10 µM TCQA for 6 and 12 h (separately). Results showed that TCQA significantly upregulated *CTNNB1* expression compared with the cells treated only with XAV939. Finally, after a co-treatment with XAV939 and TCQA, the gene expression of β-catenin was maintained higher than after treatment with the inhibitor only (**Figure 3.8**)**.** These results revealed that TCQA lifted the inhibition of β-catenin and showed that this studied compound targeted specifically β-catenin in DP causing the promotion of hair growth cycle.

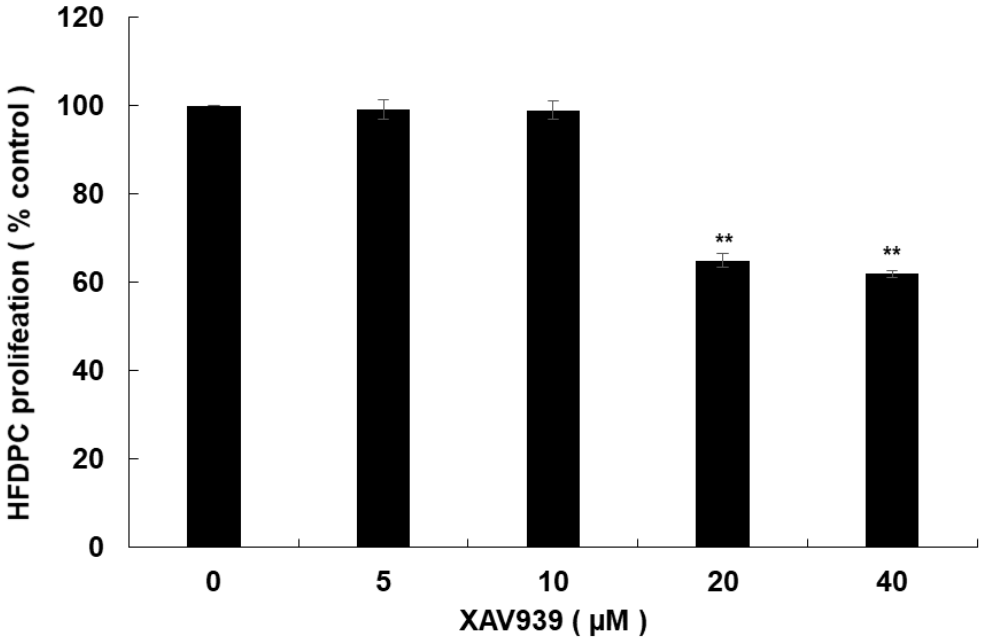

Figure 3.7. **Cell proliferation of HFDPC was assessed after 48 h treatment with various concentrations of XAV939 (β-catenin inhibitor)**. Results represent the mean ± SD of three independent experiments. *Statistically significant ($P \leq 0.05$) difference between control and treated cells. **Statistically significant ($P \leq 0.01$) difference between control and treated cells

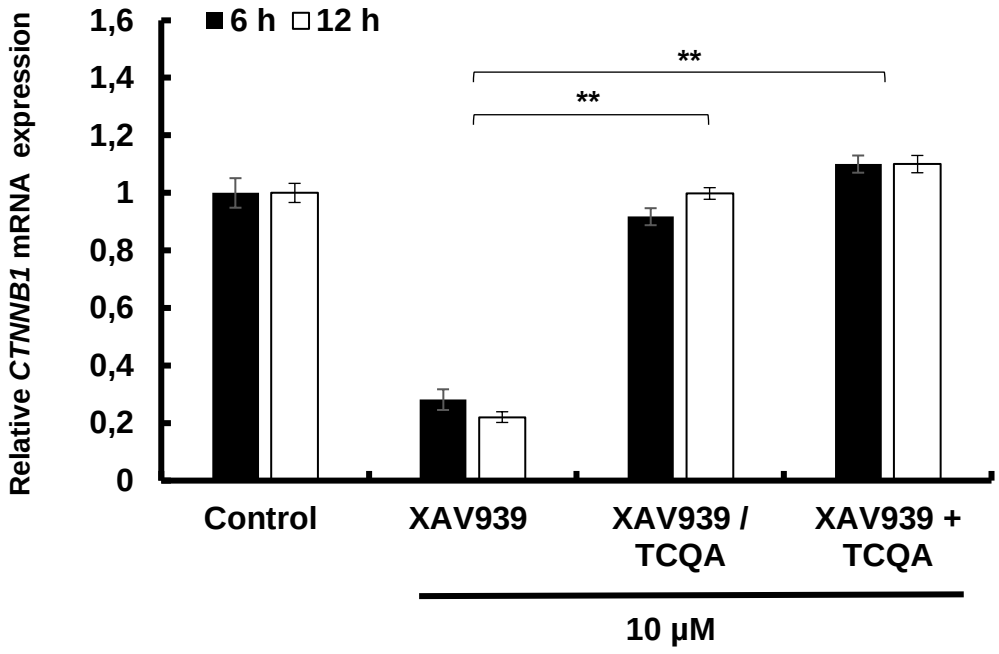

Figure 3.8. **TCQA enhanced *CTNNB1* expression even after inhibition**. Gene expression expressions of *CTNNB1* (β-catenin) after treatment with 10 µM XAV939 (inhibitor) for 6 and 12 h, with 10 µM XAV939 for 6 and 12 h then with 10 µM TCQA for 6 and 12 h (XAV939/TCQA), and finally with co-treatment of 10 µM XAV939 and 10 µM TCQA for 6 and 12 h (XAV939+TCQA). Results represent the mean ± SD of three independent experiments. *Statistically significant ($P \leq 0.05$) difference between control and treated cells. **Statistically significant ($P \leq 0.01$) difference between control and treated cells. ## Statistically significant ($P \leq 0.01$) difference between Minox-treated cells and TCQA-treated cells.

4. Discussion

The cyclical activity of the hair follicle (HF) is under the regulation of mesenchymal derived cells the dermal papilla (DP) that plays an essential role in maintaining the quiescence of the stem cells niche during telogen and their activation during anagen [129,138,140]. As mentioned earlier in this thesis in chapter II, TCQA enhanced hair growth in the shaved area of eight-weeks-old C3H male mice. A further investigation was carried out in human hair follicle dermal papilla cells (HFDPCs).

TCQA was applied to HFDPCs and results showed a stimulation of the cell proliferation and an increase of ATP content (**Figure 3.1 and 3.2**). During anagen phase, the number of cells in the DP increases as this can be explained by a replenishment from neighboring cells of the dermal sheath (DS) [25]. Also during anagen phase ,the ATP content increases promoting the expansion of the size of DP cells [141]. In addition, TCQA enhanced the gene expression of alkaline phosphatase (*ALPL*) (**Figure 3.3**). ALP is a marker of DP cells expressed during the three phases of the hair cycle and upregulated during anagen phase [93]. The results of microarray illustrated in chapter II, Table 2.1 supported these results as we observed an upregulation of ATP-related genes including *Smchd1* and DP markers including *Alpl*. Taken together, TCQA stimulated the proliferation, the ATP content, and makers of DP cells leading to the induction of the anagen phase of the hair cycle and therefore the stimulation of hair growth.

The Wnt/β-catenin signaling pathway plays important roles in HF morphogenesis and regeneration. Moreover, this pathway is involved in the activation of keratinocytes to induce HF regeneration and β-catenin signaling is highly expressed in hair bulb keratinocytes (matrix cells) and direct their differentiation into the hair shaft [24,142]. Studies revealed that Wnt/β-catenin regulates the interaction between the epithelial progenitor cells and the mesenchymal niche of the HF [105]. In the DP, β-catenin activity is considered a marker of the anagen phase, as it controls its initiation and duration via the regulation of canonical target genes, growth factors, and the interaction with various pathway including FGF, IGF, and BMP involved in hair shaft morphogenesis [105]. In the previous chapter, TCQA enhanced the hair growth via the activation of β-catenin and its target genes, so here after checking TCQA effect on β-catenin we observed an upregulation of its protein and gene expression in HFDPCs (**Figure 3.4 and 3.6).** The staining

results showed an enhancement of β-catenin expression in the nucleus confirming its activation in DP cells (**Figure 3.5**).

On the other hand, it has been reported that the absence of β-catenin in DP cells results in the dysregulation of hair growth cycle [28,46,47]. In this study, a further investigation of the effect of TCQA on β-catenin activation after inhibition was carried out. XAV939 is a small molecule that inhibit tankyrase proteins that promotes the activation of canonical Wnt pathway by reducing the activity of AXIN that induces β-catenin phosphorylation and degradation [143]. XAV939 induced the degradation of β-catenin in lung adenocarcinoma A549 cell [144]. However, the inhibitory effect of XAV939 on β-catenin in DP cells has not yet been assessed. In this study, this molecule decreased *CTNNB1* in HFDPCs but after TCQA treatment, β-catenin gene expression was lifted again (**Figure 3.8**). Therefore, i this study reportes for the first time that XAV939 inhibited β-catenin expression in human DP cells and that TCQA targets specifically this transcription factor.

In summary for this chapter III, TCQA enhanced the cell proliferation of DP cells, as well as the ATP content, and anagen phase marker such as ALP. Additionally, TCQA targeted the activation of β-catenin involved in the transition from telogen to anagen, anagen initiation and elongation, hair matrix differentiation, and hair shaft development. Therefore, TCQA enhanced successfully hair growth in C3H mice and in human dermal papilla cells via β-catenin activation.

Chapter IV: Evaluation of the effect of 3,4,5-tri-*O*-caffeoylquinic acid (TCQA) on the stimulation of pigmentation in human epidermal melanocytes (HEM) and B16F10 melanoma cell line (B16F10)

1. Introduction

In the adult hair follicle (HF), a coordinated and complex interaction between melanin producing cells the melanocytes, bulbar keratinocytes, and dermal papilla cells (DP) is responsible of hair shaft pigmentation [60,145]. The melanocytes, are originally derived from the neural crest cells. and their precursors the melanoblasts migrate and become localized in the HF where they are called follicular melanocytes (FM), and in the epidermis known as epidermal melanocytes (EM) [7]. FM and EM are considered as two distinct sub-population, but they share the same origin and the melanin producing function [146].

In the HF, melanogenically active melanocytes are located in the hair bulb, adjacent to the dermal papilla (DP) and the keratinocytes (matrix cells that give arise to the hair shaft) and amelanotic melanocytes or melanocytes stem cells (MSCs) are located at the outer root sheath and in the bulge, the region known to contain HF stem cells [8]. The life of FM is then totally linked with the hair growth cycle [63,92]. During the anagen phase, the FM are active and synthesize the pigment melanin that is transferred in a specialized organelles called melanosomes to the adjacent keratinocytes (hair progenitors cells) that differentiate to become a fully developed pigmented hair shaft [12,13]. The HF enters then a regression phase (catagen) and during which the activity of the FM is slowed down followed by a complete arrest during the next phase telogen as the lower third of the HF degenerates by apoptosis including the bulb region where the FM are located [63,147,148].

Melanogenesis is the production of the pigment melanin and is a complex process with different stages [149]. Melanin biosynthesis in the HF and the epidermis occurs through an oxidation process starting with L-tyrosine in the melanosomes that contain the enzymes tyrosinase (TYR), tyrosinase-related protein 1 (TYRP1), and dopachrome tautomerase (DCT) [12,40]. Two types of melanin exist, the dark-brown pigment called eumelanin and pheomelanin which is the red-yellow pigment [147]. The black pigment eumelanin is the most abundant type found in individuals with dark skin and hair and is more efficient in photoprotection against UV light which is one major function of melanin [150]. As for pheomelanin is found in people with red/blond hair and white skin, in whom skin tumors and cancer are more common [151].

The reaction of melanin biosynthesis is catalyzed by TYR, TYRP1, and DCT which are regulated by the transcription factor microphthalmia-associated transcription factor (Mitf). MITF

is known as the melanogenesis master regulator and plays an important role in the development and survival of the melanocytes. In the HF, the melanin is produced in the melanosomes and then transferred to bulb keratinocytes that later will be giving arise to the hair shaft [152]. The melanogenesis and the pigment transfer are under the regulation of various signal transduction pathways and determined by the availability of melanin precursors [60]. Various transcription factors are involved in the regulation of Mitf including the tyrosine kinase receptor KIT, its ligand SCF, and MC1R [41,42]. Mitf is regulated as well by PAX3, CREB, SOX9, SOX10, β-catenin and LEF1 and is also modified at post-transcriptional level by MAPK and Wnt/β-catenin/GSK3β pathway [43–45].

T Chapter IV aim is to check the effect of TCQA on the enhancement of pigmentation *in vitro* through the activation of β-catenin using pigment cells lines: human epidermal melanocytes (HEM) and B16 murine melanoma cells (B16F10).

2. Materials and methods

2.1. Sample preparation

Sample was prepared as explained in Chapter III, 2.Materials and methods, 2.1 Sample preparation.

2.2. Cells and cell culture

Human epidermal melanocytes (HEM) were purchased from Gibco Invitrogen cell culture. They are primary cells which can be cultured up to three passages before going into senescence. HEM were maintained in Medium 254 (Gibco, Massachusetts, USA) supplemented with human melanocyte growth supplement HMGS (Gibco, Massachusetts, USA).

B16 murine melanoma cells (B16F10) were purchased from the Riken Cell Bank in Tsukuba, Japan, and maintained under sterile conditions as a monolayer culture in Roswell Park memorial institute medium (RPMI) 1640 medium (Fisher scientific, UK) supplemented with 10% fetal bovine serum FBS (Gibco, Massachusetts, USA).

The cells were kept under sterile conditions at 37 °C in 75 cm^2 flask (BD Falcon, England, UK) in a humidified atmosphere of 5 % CO_2. Trypan blue exclusion was used to determine the cell viability.

2.3. Melanin and cell viability assay

The method used in this study to measure the melanin content was originally elaborated by Hasoi et al, but here we used it with some modifications [153]. Both cell lines were seeded at a density of 5×10^5 cells per 100-mm petri dish, and incubated for 24 h. The appropriate growth medium for each cell line was replaced with a fresh one containing different concentrations of TCQA and α-MSH (melanocyte-stimulating hormones (200 nM)) used as a positive control. After 48, 72, and 96 h, the growth medium was removed, and the cells were harvested by trypsinization (Gibco, Massachusetts, USA). The pelleted cells were solubilized by 0.1% Triton X-100 and precipitated in 10% trichloroacetate. The melanin was dissolved in 1 mL 8 N NaOH and incubated for 2 h at 80°C. The amount of melanin was determined after measuring the absorbance at 410 nm. The total melanin content was evaluated using the standard curve for synthetic melanin. The melanin content was expressed as melanin content/cell (% of control).The

number of viable cells for melanin assay was quantified using the ViaCount program of Guava PCA (GE Healthcare, Buckinghamshire, UK) following the manufacturer's instructions.

2.4. Protein extraction

The cells were seeded at density of 5×10^5 cells per 100-mm petri dish. HEM and B16F10 were allowed to attach for overnight, then the growth medium (Medium 254 or RPMI 1640 respectively for HEM and B16F10) was replaced with a new containing 0, 10 µM (for HEM) and 0, 25 µM (for B16F10) TCQA and 200 nM α-MSH (for both).

After 4, 8, 12, 24, and 48 h, total protein extraction was achieved as described in Chapter III, 2. Materials and methods section, 2.7 Protein extraction.

2.5. Western blot

The western blot was performed as described in Chapter III, 2.Materials and methods section, 2.8 Western blot analysis.

2.6. RNA extraction

The cells were seeded, allowed to attach overnight and then treated with 0, 10 and 0, 25 µM TCQA for HEM and B16F10, respectively, and with 200 nM α-MSH for both cell lines. After 1, 6, 12, 24, and 48 h treatment, the total RNA was extracted as described in Chapter III, 2.Materials and methods section, 2.5 RNA extraction.

2.7. Quantitative real-time PCR analysis

This experiment was performed as described in Chapter III, 2.Materials and methods section, 2.6 Quantitative real-time PCR analysis.

2.8. Immunocytochemistry

HEM were treated with 0 and 10 µM TCQA for 0, 6, and 12 h. Then, the immunostaining was performed as mentioned in Chapter III, 2.Materials and methods section, 2.9 Immunocytochemistry.

2.9. Statistical analysis

The significance was calculated as explained in Chapter III, 2.Materials and methods section, 2.10 Statistical analysis.

3. Results

3.1. TCQA enhanced the melanin content without affecting the viability of HEM and B16F10

TCQA enhanced the melanin content in mice hair shaft as discussed in chapter II. To further confirm its effect on melanogenesis, melanin assay was performed *in vitro* using human and mouse cell lines: HEM and B16F10. The cells were treated with various concentrations of TCQA for 48 , 72 , and 96 h. Results showed that 10 µM TCQA increased the melanin content in HEM by 30%, 50%, and 93% after 48, 72, and 96 h, respectively, compared with the control (**Figure 4.1**).

In B16F10 cells, the melanin content was increased as well by 70% and 62%, respectively, after 48 and 72 h with 25 µM TCQA (**Figure 4.2**). The enhancement of melanin content in both cell lines by TCQA was achieved without decreasing the cell viability. These results indicated that TCQA stimulated significantly the melanogenesis in pigment cell lines.

3.2. The expression of the melanogenesis enzymes was upregulated upon TCQA treatment in HEM and B16F10.

The expression of the melanogenic enzymes after TCQA treatment was carried out in HEM and B16F10. Results showed that the protein expression of TYR, TYRP1, and DCT was significantly enhanced in HEM after 48 h treatment with 10 µM TCQA (**Figure 4.3**). Same for the gene expression of *TYR*, *TYRP1*, and *DCT* that was upregulated after 24 and 48 h treatment in human melanocytes (**Figure 4.4**). Furthermore, these results correlated with the results obtained in B16F10, in which the gene and the protein expression of the three enzymes were significantly stimulated after 24 and 48 h treatment with 25 µM TCQA (**Figure 4.5 and 4.6**). These results suggest that TCQA enhanced the melanin synthesis by stimulating the protein and the gene expression of the melanogenesis enzymes.

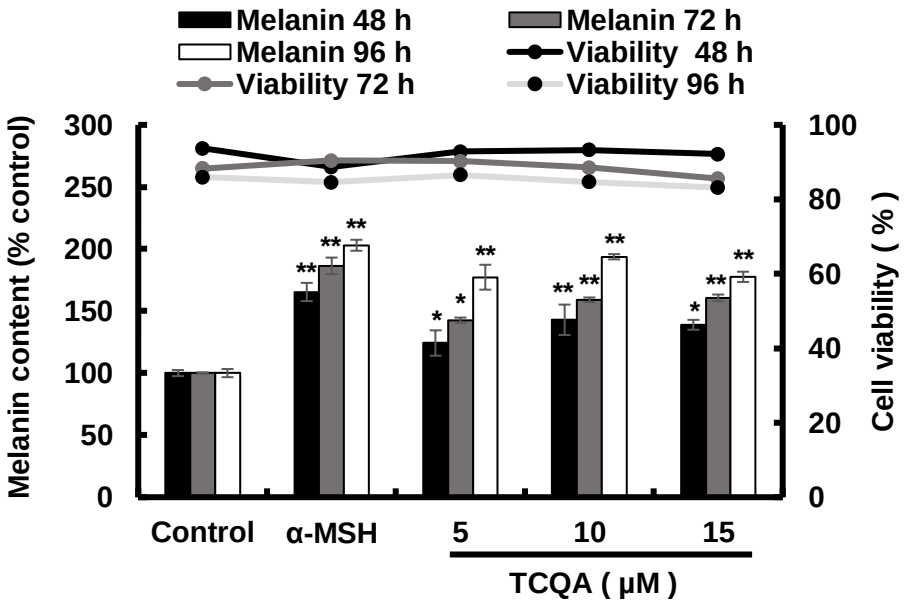

Figure 4.1. **TCQA stimulated the melanin content in HEM without decreasing the viability**. The cells were treated for 48, 72, and 96 h treatment with various concertation of TCQA and 200 nM α-MSH used as positive control without affecting the cell viability. Results represent the mean ± SD of three independent experiments. *Statistically significant ($P \leq 0.05$) difference between control and treated cells. **Statistically significant ($P \leq 0.01$) difference between control and treated cells.

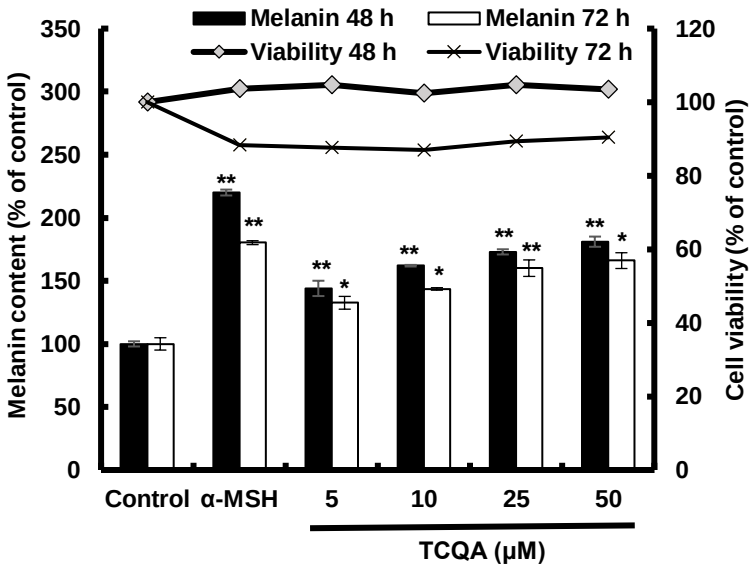

Figure 4.2. **TCQA stimulated the melanin content in B16F10 without decreasing the viability**. Cells were treated with various concertation of TCQA and 200 nM α-MSH used as positive control. Results represent the mean ± SD of three independent experiments. *Statistically significant ($P \leq 0.05$) difference between control and treated cells. **Statistically significant ($P \leq 0.01$) difference between control and treated cells.

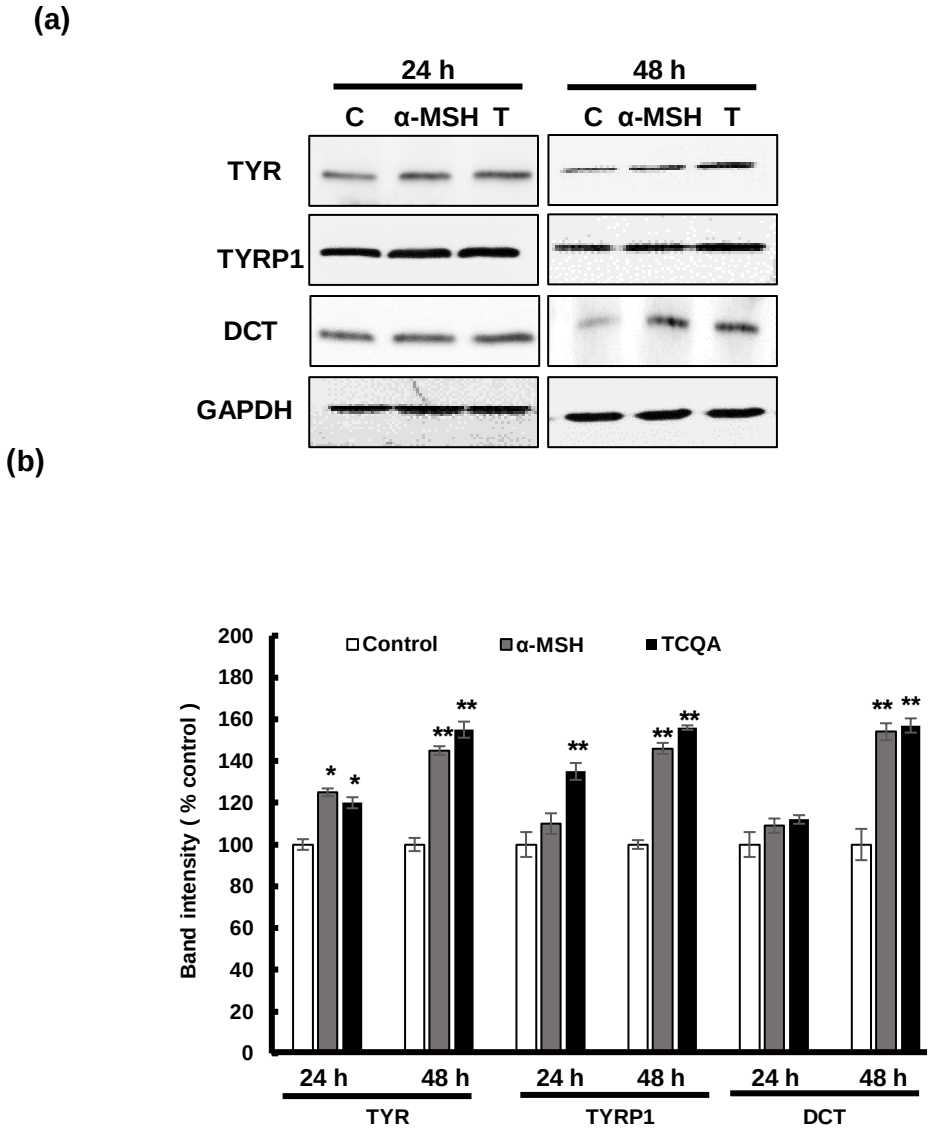

Figure 4.3. **TCQA upregulated the protein expression of the melanogenesis enzymes in HEM. (**a) Determination of the protein expression of the melanogenesis enzymes: TYR, TYRP1, and DCT after 24 and 48 h treatment with 0 and 10 µM TCQA and 200 nM α-MSH. (b) The band intensities was done comparing to GAPDH using LI-COR system. Results represent the mean ± SD of three independent experiments. *Statistically significant ($P \leq 0.05$) difference between control and treated cells. **Statistically significant ($P \leq 0.01$) difference between control and treated cells. C: control, T: TCQA.

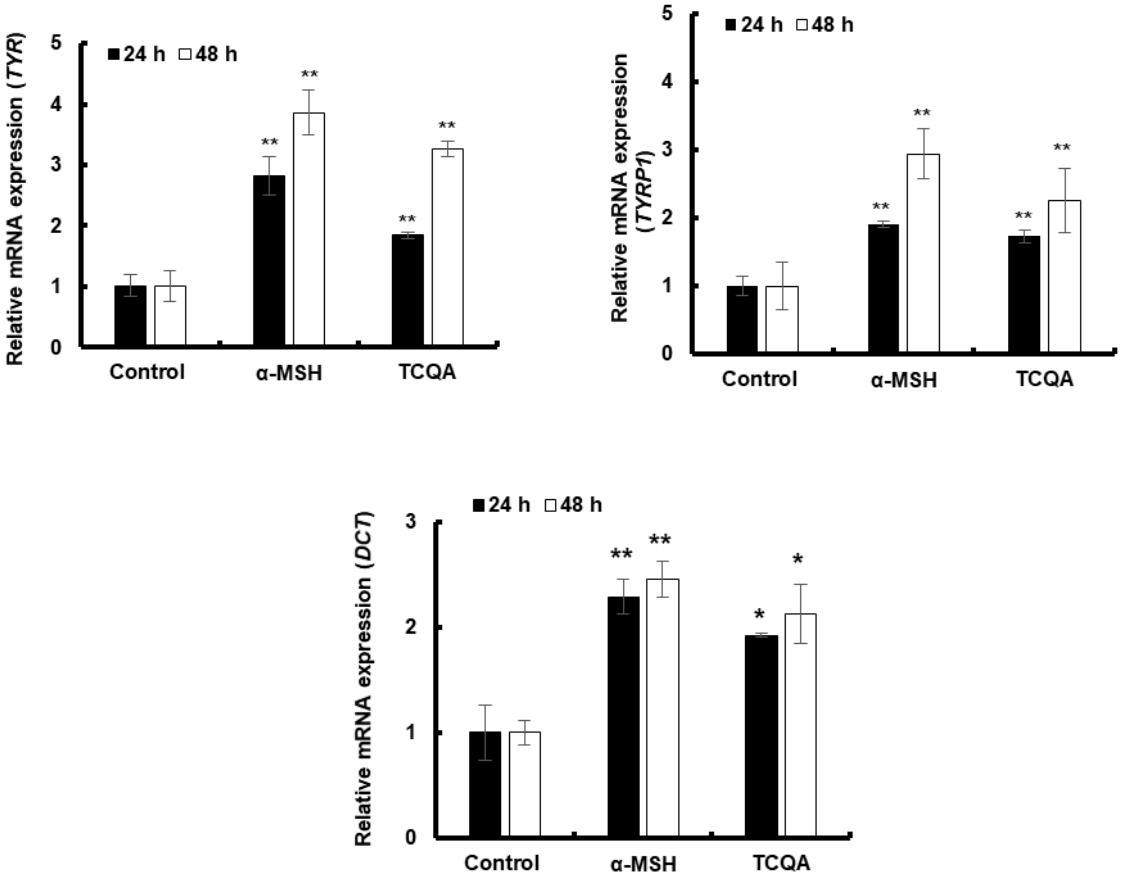

Figure 4.4. **Gene expression of *TYR, TYRP1,* and *DCT* after 24 and 48 h with 0 and 10 µM TCQA and 200 nM α-MSH in HEM**. The mRNA level was quantified using TaqMan real-time PCR. Results represent the mean ± SD of three independent experiments. *Statistically significant ($P \leq 0.05$) difference between control and treated cells. **Statistically significant ($P \leq 0.01$) difference between control and treated cells.

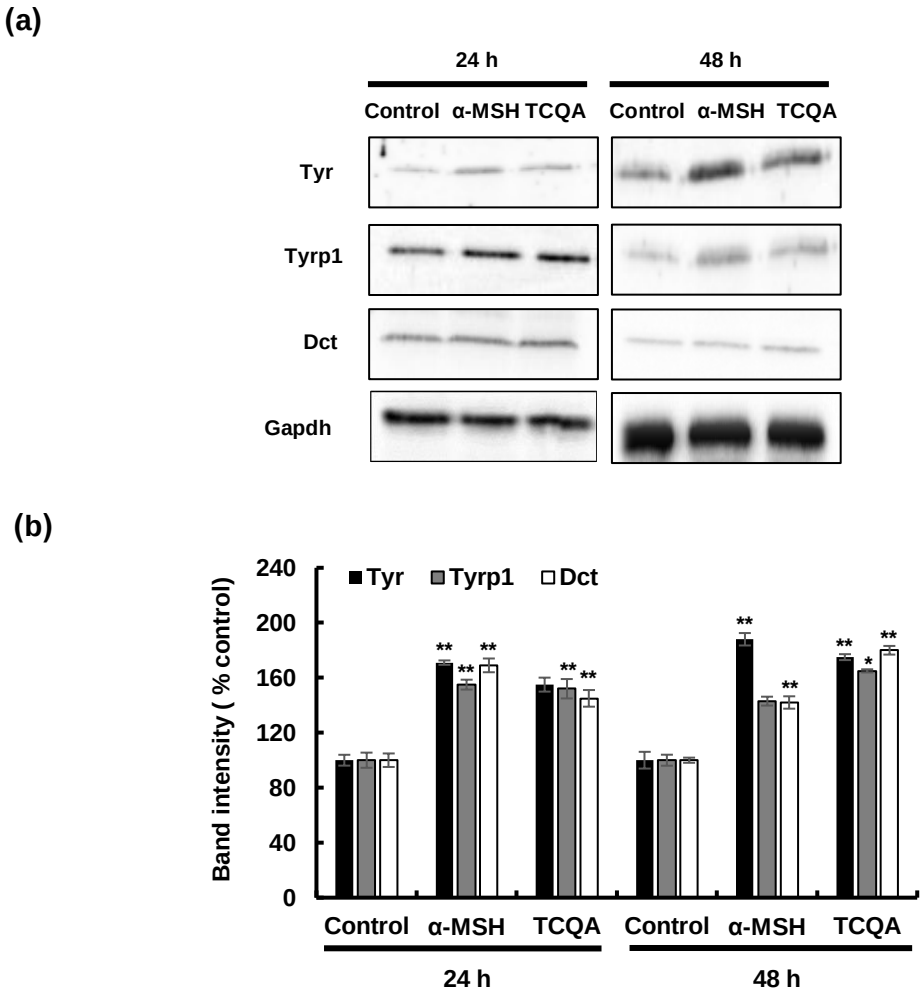

Figure 4.5. **TCQA enhanced the protein expression of the melanogenesis enzymes in B16F10.** **(**a) Determination of the protein expression of the melanogenesis enzymes: Tyr, Tyrp1, and Dct after 24 and 48 h treatment with 0 and 25 μM TCQA and 200 nM α-MSH in B16F10. (b) The band intensities was done comparing to GAPDH using LI-COR system. Results represent the mean ± SD of three independent experiments. *Statistically significant ($P \leq 0.05$) difference between control and treated cells. **Statistically significant ($P \leq 0.01$) difference between control and treated cells.

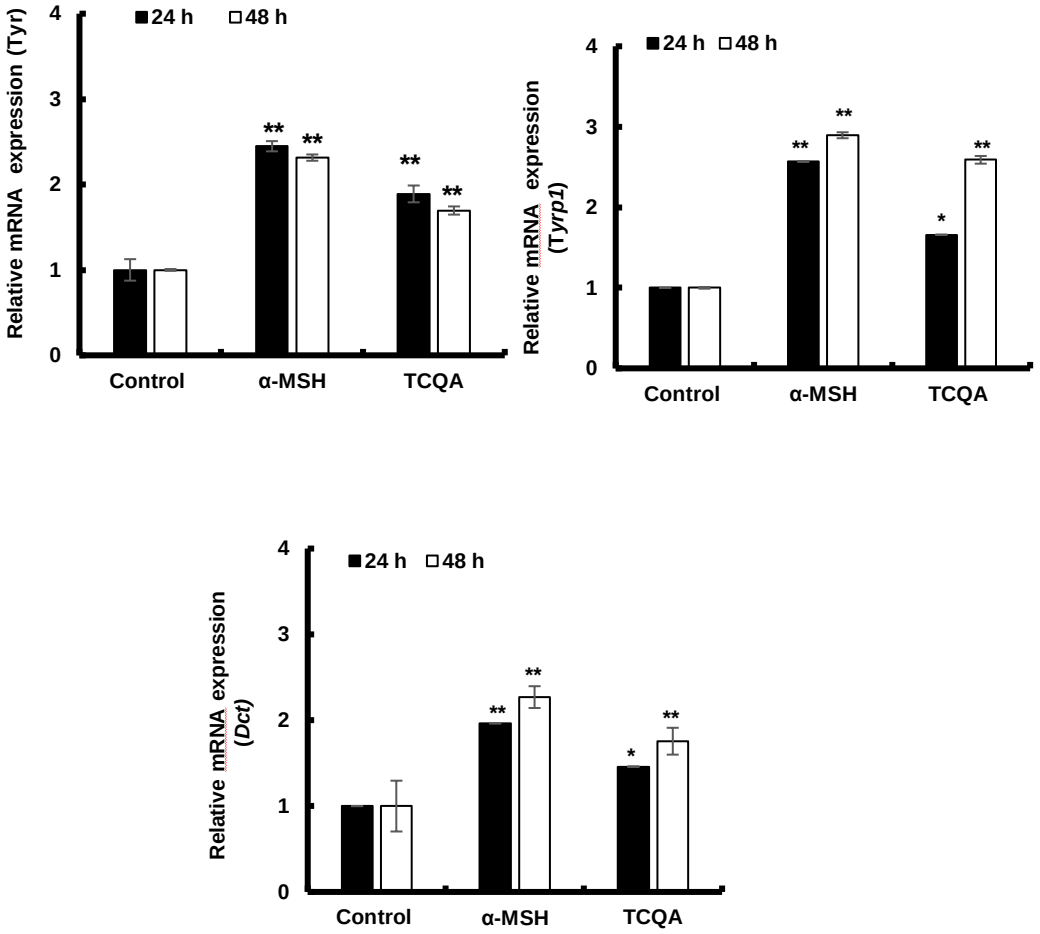

Figure 4.6. **Gene expression of *Tyr, Tyrp1*, and *Dct* after 24 and 48 h with 0 and 25 µM TCQA and 200 nM α-MSH in B16F10**. The mRNA level was quantified using TaqMan real-time PCR. Results represent the mean ± SD of three independent experiments. *Statistically significant ($P \leq 0.05$) difference between control and treated cells. **Statistically significant ($P \leq 0.01$) difference between control and treated cells.

3.3. MITF (microphthalmia-associated transcription factor) expression was upregulated after treatment with TCQA in pigment cell lines

MITF is the transcription factor of the melanogenesis enzymes and the pigmentation master regulator. *in vivo* experiment in chapter II, showed an upregulation in the gene expression of *Mitf* in mice skin treated with TCQA, the purpose was then to check its expression in the melanocytes and B16F10 cells. Figure 4.7 displays the results of MITF protein expression which was upregulated time-dependently after treatment with 10 µM TCQA in HEM. The gene expression was enhanced as well after 6 h treatment (**Figure 4.8**). In B16F10, 25 µM TCQA upregulated Mitf protein expression after 12 and 24 h, and the gene expression after 6, 12, and 24 h (**Figure 4.9 and 4.10**). These results showed that TCQA upregulated MITF expression in human and mouse pigment cells leading to the activation of the melanogenesis enzymes and therefore the enhancement of the melanin biosynthesis.

3.4. TCQA stimulated β-catenin expression in HEM and B16F10

β-catenin regulates Mitf expression and influences skin and hair shaft pigmentation. Results *in vivo* (in chapter II) showed an upregulation in β-catenin gene expression (*Ctnnb1*) upon TCQA treatment in mice skin and an accumulation of the protein expression in the hair bulb where the active melanocytes are located. So in this current hapter, the aim is to further investigate the effect of TCQA on the expression of β-catenin in pigment cells. Results showed that, the protein expression was enhanced time-dependently with 10 µM TCQA in HEM (**Figure 4. 11**). This results was supported by immunostaining analysis showing the translocation of β-catenin to the nucleus of HEM proving further its activation (**Figure 4.12**). The gene expression of β-catenin (*CTNNB1*) was enhanced as well up to 2.6-fold after 12 h treatment with 10 µM TCQA (**Figure 4.13**).XAV939 is a known inhibitor of β-catenin, actually it induces its phosphorylation and non-translocation to the nucleus [139]. HEM were treated with XAV939 only and results showed a decrease in *CTNNB1* expression. However this inhibition was lifted upon a co-treatment with TCQA (**Figure 4.14**)

Additionally, the protein and the gene expression of β-catenin was upregulated time-dependently in B16F10 (**Figure 4.15 and 4.16**). These results suggest that TCQA enhanced pigmentation through the upregulation of β-catenin ant its target Mitf leading to the activation of the melanogenic enzymes and the stimulation of melanin biosynthesis.

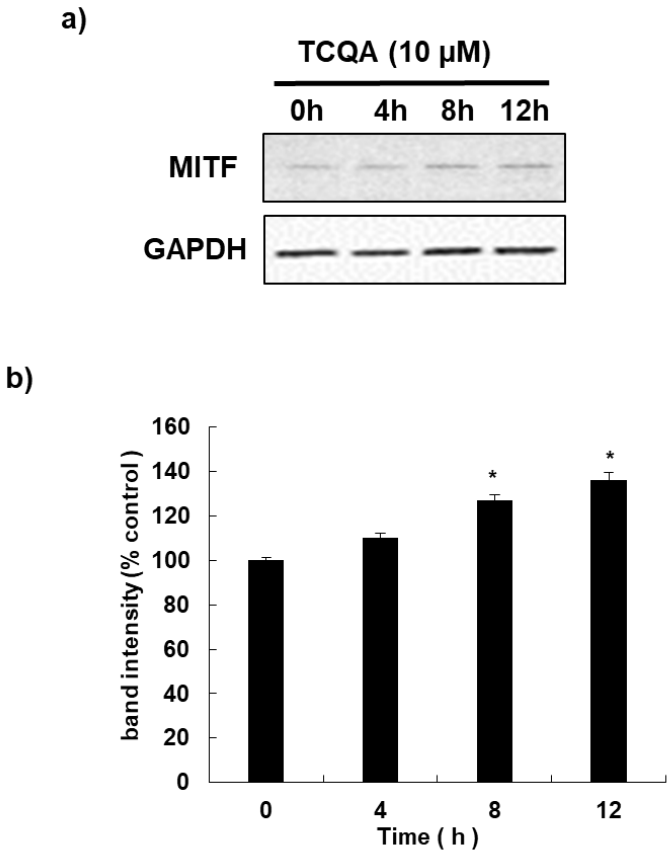

Figure 4.7. TCQA stimulated the protein expression of MITF time-dependently in HEM. (a) 10 μM TCQA stimulated MITF protein expression in HEM after 0, 4, 8, and 12 h treatment. (b) The band intensities was done comparing to GAPDH using LI-COR system. Results represent the mean ± SD of three independent experiments. *Statistically significant ($P \leq 0.05$) difference between control and treated cells. **Statistically significant ($P \leq 0.01$) difference between control and treated cells.

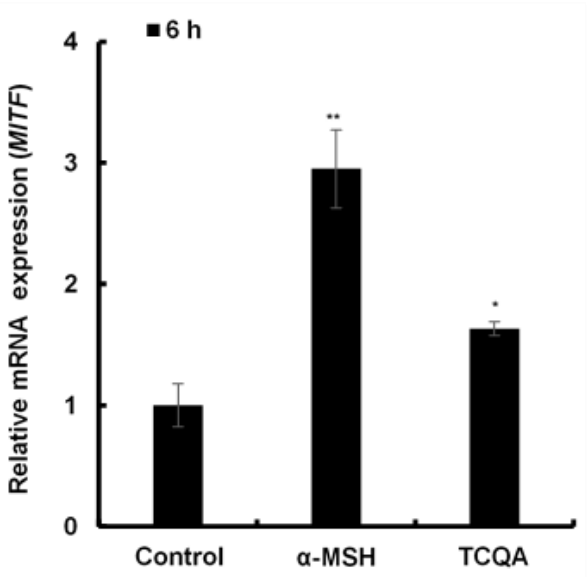

Figure 4.8. Gene expressions of *MITF* after 6 h treatment with 10 µM TCQA and 200 nM α-MSH in HEM. The mRNA level was quantified using TaqMan real-time PCR. Results represent the mean ± SD of three independent experiments. *Statistically significant ($P \leq 0.05$) difference between control and treated cells. **Statistically significant ($P \leq 0.01$) difference between control and treated cells.

(a)

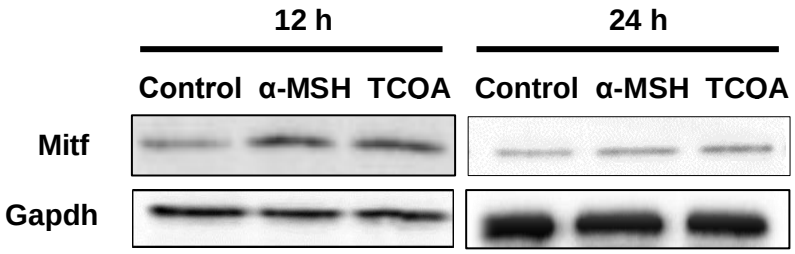

(b)

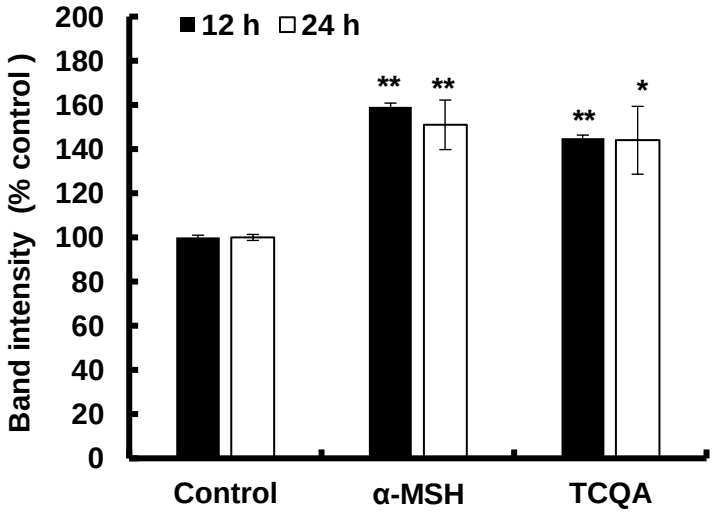

Figure 4.9. **MITF protein expression determination upon TCQA treatment in B16F10**

(a) 25 µM TCQA stimulated MITF protein expression after 12 and 24 h treatment. (b) The band intensities was done comparing to GAPDH using LI-COR system. Results represent the mean ± SD of three independent experiments. *Statistically significant ($P \leq 0.05$) difference between control and treated cells. **Statistically significant ($P \leq 0.01$) difference between control and treated cells.

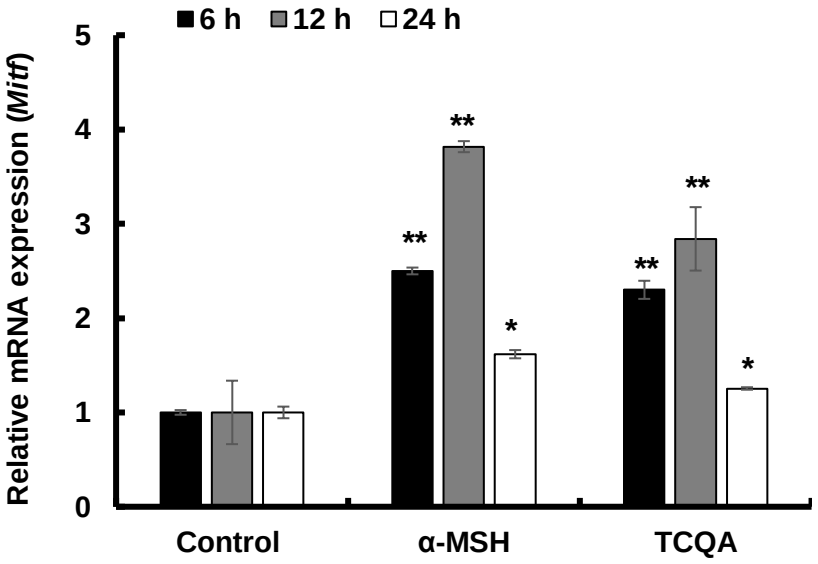

Figure 4.10. Gene expression of *Mitf* after 6, 12, and 24 h treatment with 25 µM TCQA and 200 nM α-MSH in B16F10. The mRNA level was quantified using TaqMan real-time PCR. Results represent the mean ± SD of three independent experiments. *Statistically significant ($P \leq 0.05$) difference between control and treated cells. **Statistically significant ($P \leq 0.01$) difference between control and treated cells.

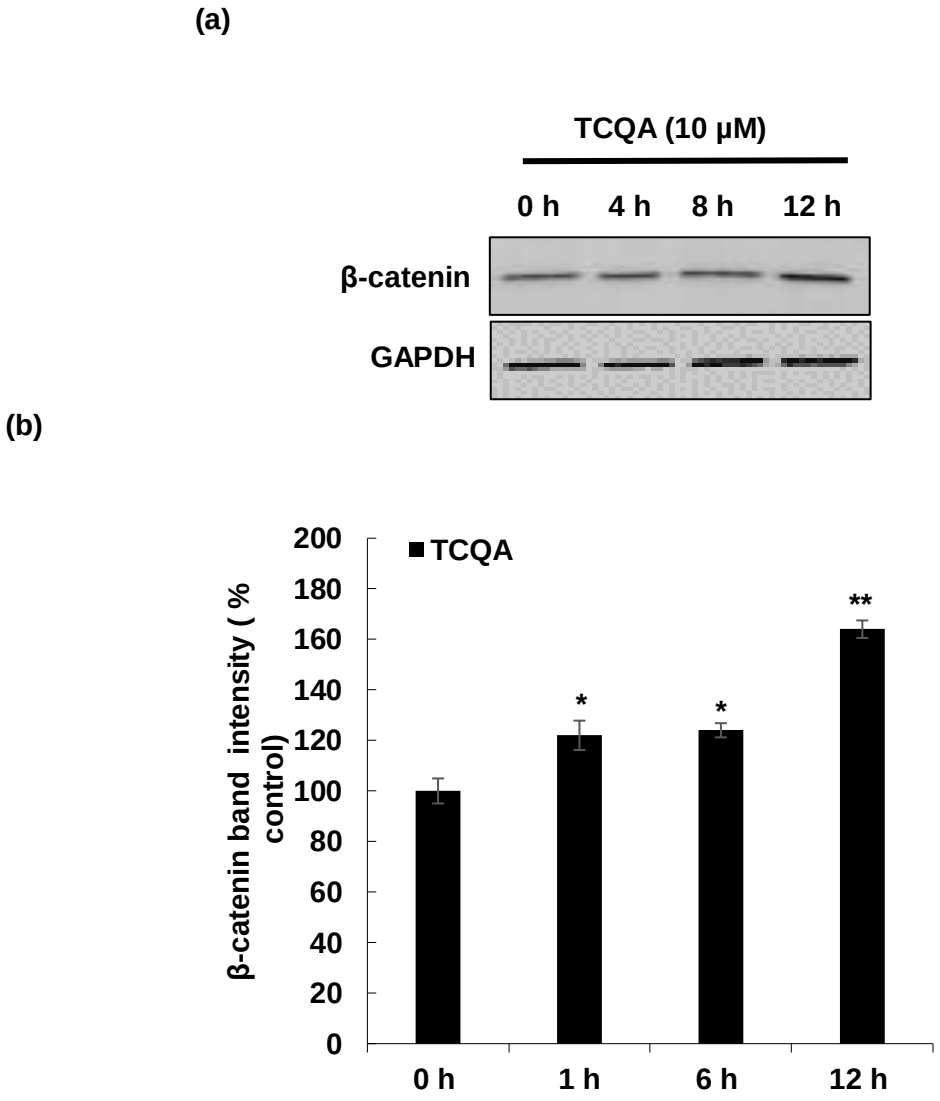

Figure 4.11. **β-catenin expression investigation after TCQA treatment in HEM** (a) β-catenin protein expression after 0, 4, 8, and 12 h treatment with 10 µM TCQA in HEM. (b) The band intensities was done comparing to GAPDH using LI-COR system. Results represent the mean ± SD of three independent experiments. *Statistically significant ($P \leq 0.05$) difference between control and treated cells. **Statistically significant ($P \leq 0.01$) difference between control and treated cells.

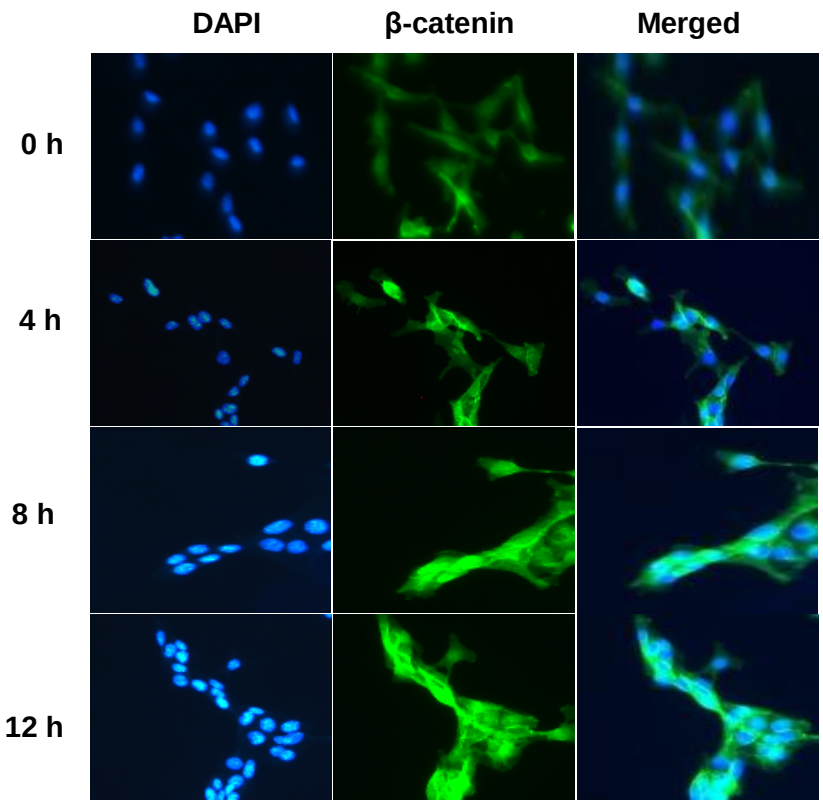

Figure 4.12. **Immunocytochemistry of β-catenin expression after 0, 4, 8, and 12 h treatment with 10 µM TCQA in HEM.** Scale bar = 25 µm; magnificence 20 X. The figure is divided into three panels, the first is DAPI to stain the nucleus, the second is for β-catenin staining, and the last panel is a merge between β-catenin and the nucleus.

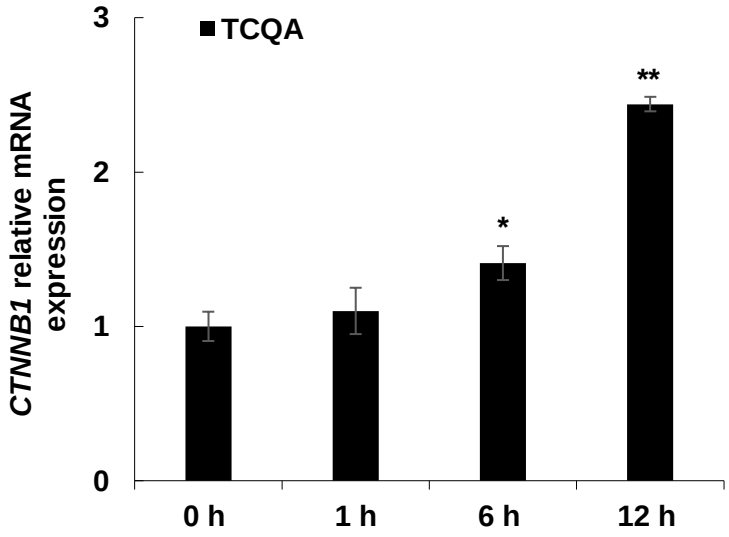

Figure 4.13. Gene expression of *CTNNB1* after 0, 1, 6, and 12 h treatment with 10 µM TCQA in HEM. The mRNA level was quantified using TaqMan real-time PCR. Results represent the mean ± SD of three independent experiments. *Statistically significant ($P \leq 0.05$) difference between control and treated cells. **Statistically significant ($P \leq 0.01$) difference between control and treated cells.

.

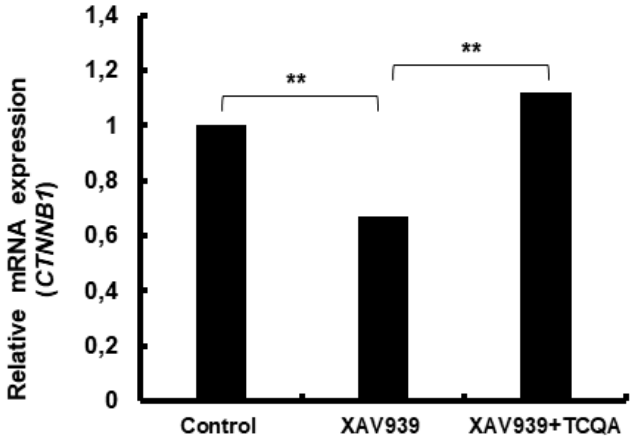

Figure 4.14. TCQA enhanced *CTNNB1* expression even after inhibition. Gene expression *CTNNB1* was determined after treatment with 10 µM XAV939 and with a co-treatment of 10 µM XAV939 and 10 µM TCQA for 24 h. The mRNA level was quantified using TaqMan real-time PCR. Results represent the mean ± SD of three independent experiments. *Statistically significant ($P \leq 0.05$) difference between control and treated cells. **Statistically significant ($P \leq 0.01$) difference between control and treated cells.

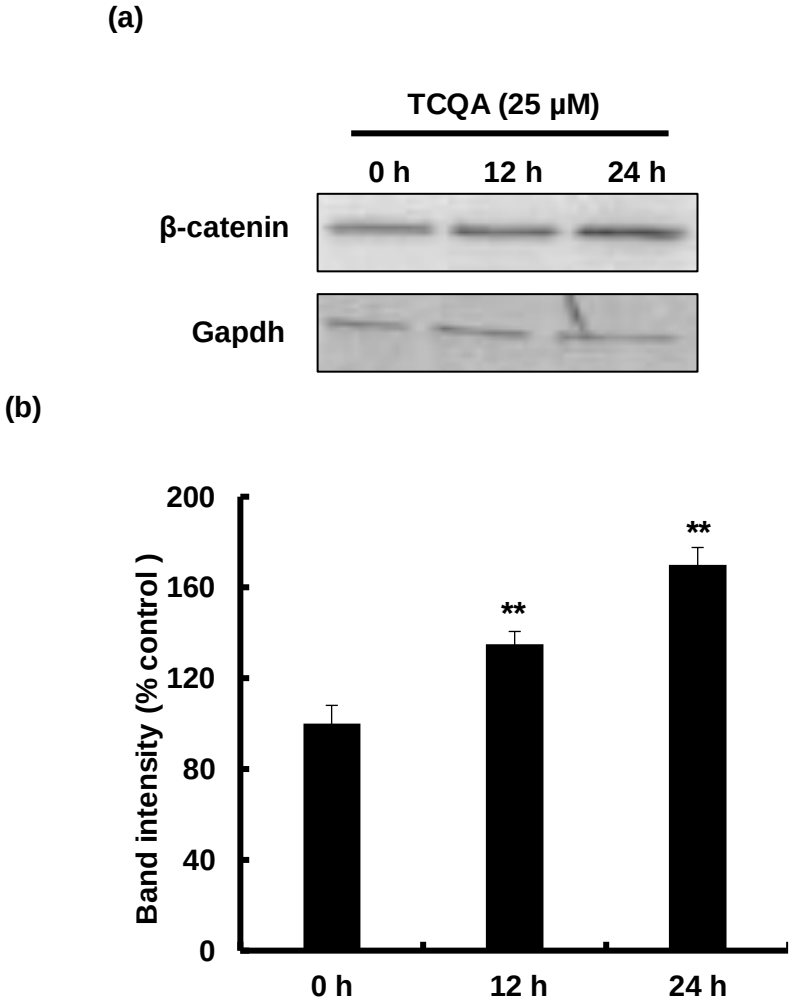

Figure 4.15. **TCQA enhanced β-catenin expression in B16F10.** (a) β-catenin protein expression after 0, 12, and 24 h treatment with 25 μM TCQA. (b) The band intensities was done comparing to GAPDH using LI-COR system. Results represent the mean ± SD of three independent experiments. *Statistically significant ($P \leq 0.05$) difference between control and treated cells. **Statistically significant ($P \leq 0.01$) difference between control and treated cells.

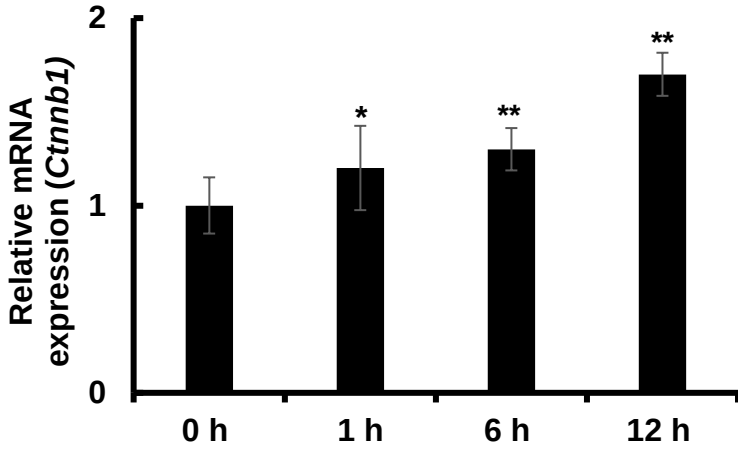

Figure 4.16. Gene expression of *Ctnnb1* after 0, 1, 6, and 12 h treatment with 25 µM TCQA in B16F10. The mRNA level was quantified using TaqMan real-time PCR. Results represent the mean ± SD of three independent experiments. *Statistically significant ($P \leq 0.05$) difference between control and treated cells. **Statistically significant ($P \leq 0.01$) difference between control and treated cells.

4. Discussion

In the adult hair follicle (HF), the growth and the pigmentation of the hair shaft are under cyclical control. The life of the follicular melanocyte (FM) located in the hair bulb, and the melanin biosynthesis are tightly coupled to the hair growth cycle [146,147].

In this chapter IV, TCQA was tested in pigment cell lines: human epidermal melanocytes (HEM), and B16 murine melanoma cells (B16F10) to further validate its effect on pigmentation as in chapter II, TCQA enhanced the pigmentation of C3H mice hair shaft. Melanin content in these cells was significantly upregulated upon TCQA treatment without affecting the cell viability (**Figure 4.1 and 4.2**). Melanin synthesis occurs in melanosomes, lysosome-related organelles where the melanogenic enzymes, tyrosinase (TYR), tyrosinase-related protein 1 (TYRP1), and dopachrome tautomerase (DCT) are located [149,154]. Melanin is synthesized through a series of interactions starting from L-tyrosine and catalyzed by these enzymes, generating brown/black eumelanin synthesized from l-dopachrome or red-yellow pheomelanin formed by the conjugation of cysteine or glutathione [155,156]. Here, TCQA upregulated the gene and the protein expression of the three melanogenesis enzymes in both human and mouse cell lines (**Figure 4.3, 4.4, 4.5, and 4.6**). The microphthalmia-associated transcription factor (MITF) regulates the transcription of TYR, TYRP1, and DCT and therefore the melanin synthesis. The gene and protein expression of Mitf were upregulated upon TCQA treatment in human melanocytes and B16F10 (**Figure 4.7, 4.8, 4.9 and 4.10**).

In chapter II, TCQA stimulated the pigmentation through Wnt/β-catenin signaling pathway. This signaling plays a critical role in melanocyte development and differentiation from the neural crest cells, and in the migration of the melanocytes precursors the melanoblasts to the HF and the epidermis [157,158]. The stability of β-catenin is elevated after binding of Wnt proteins to their receptors and leads to its transport into the nucleus, where it interacts and forms a complex with LEF/TCF transcription factors to positively regulate MITF transcription [159]. For this purpose, the effect of TCQA on β-catenin activation was investigated, and the protein and gene expression were upregulated upon TCQA treatment and the staining results in the melanocytes showed a transportation of β-catenin into the nucleus which explain the activation of MITF (**Figure 4.11, 4.12, 4.13, 4.15 and 4.16**).

On the other hand, the inhibition of β-catenin will lead to the non-activation of MITF in the melanocytes. Tankyrase are known to bind to AXIN to reduce its activity and this leads to the non-formation of β-catenin degradation complex and a further activation of canonical Wnt pathway [143]. XAV939 is a small molecule that inhibit tankyrase activity leading to β-catenin phosphorylation and non-translocation into the nucleus in lung adenocarcinoma A549 cell [144]. Whether XAV939 can inhibit or not β-catenin in human melanocytes has not yet been reported. Here, XAV939 decreased *CTNNB1* expression in HEM but after a co-treatment of with TCQA, *CTNNB1* expression was lifted. TCQA target specifically β-catenin and reduces its degradation in human melanocytes (**Figure 4.14**).

Taken together the finding of this chapter IV show that TCQA triggered the activation of Wnt/β-catenin pathway leading to the upregulation of pigmentation-associated genes and the enhancement of melanin content in human (melanocytes) and mouse (B16F10) pigment cell lines. Furthermore, β-catenin-mediated hair pigmentation induction effect of TCQA which caused the initiation of the anagen phase of the hair cycle and therefore the activation of MITF and the enhancement of melanin biosynthesis.

Chapter V: General discussion

Hair problems including hair loss (alopecia) and hair graying despite not being a dangerous disease, it can affect people's quality of life considering the importance of the hair in individual's general appearance. An alteration in the pathways controlling the hair growth/pigmentation cycle causes a dysregulation in the hair follicle (HF) function and the hair shaft development and color. The current available hair loss and graying remedies rely on synthetic chemicals ingredients and have shown many severe side effects and temporary results. Developing a safe drug with a lasting effect has become a necessity to treat hair disorders. Recently, the use of plant natural products that may affect the regulation of hair growth as well as the pigmentation at the molecular level has been approved in the mainstream of medicine. In this thesis, we aimed to investigate the role of a phenylpropanoids compound and a caffeoylquinic acid derivatives called 3,4,5-tri-*O*-caffeoylquinic acid or TCQA for the promotion of hair growth and the enhancement of hair pigmentation *in vivo* and *in vitro.*

In chapter II, TCQA was tested in eight-weeks-old C3H male mice and it successfully enhanced the growth and the pigmentation of the hair shaft of the treated mice. This effect was due to the fast induction and elongation of the anagen phase or the growth phase of the hair cycle caused by the activation of one key pathway, the Wnt/β-catenin. This famous pathway is known to interacts with other hair growth-associated pathways to promotes the HF cycle and morphogenesis [90,160]. In this chapter II, Rac/Ras-related genes such as *Rasgrp, Dock2, Rassf1, Dgki,* and *Plk2* were observed to be stimulated by TCQA. The expression of this pathway is detected in the ear and can mediates hair cells proliferation, and is involved in melanocytes development. Studies described that Rac/Ras signaling activation is initiated by β-catenin and this regulation is essential for vertebrate gastrulation [84,161–163]. In our study, we firstly reported that canonical Wnt can regulate Rac/Ras pathway via the activation of β-catenin by TCQA and this can affect hair growth/pigmentation cycle in mice model.

Interestingly, microarray results illustrated in chapter II, showed an upregulation in genes involved in stem cells differentiation and it has been reported that one cause of hair graying is the failure of differentiation of melanocytes stem cells (MCSs). Moreover, the immunohistochemistry results showed an upregulation in CD34 a bulge marker known to be upregulated when MSCs are differentiating. This can be an interesting point as we can test the effect of TCQA on the differentiation of MSC *in vivo* and *in vitro* in order to establish TCQA as anti-hair graying drug.

Moreover, we observed a downregulation in aging-associated genes upon TCQA treatment in mice skin and other study have showed that TCQA improved learning and memory in aged mice [74]. On the other hand, during melanin synthesis, reactive oxygen species (ROS) are produced leading to the depletion of MSCs pool, melanocytes damage, and skin and hair shaft aging [63,132,133]. In this study, TCQA downregulated genes involved in ROS emission. These finding suggest that TCQA can be a candidate to prevent hair and skin aging.

The hair growth/pigmentation promotion effect of TCQA observed *in vivo*, was further confirmed *in vitro*. In chapter III, human hair follicle dermal papilla cells (HFDPCs) were used and TCQA significantly increased the cell proliferation, the ATP content, and the gene expression of anagen phase marker alkaline phosphatase (*ALPL)*. These results were due to the activation of β-catenin strongly expressed in DP cells and its expression is associated with the anagen phase prolongation, and it directs the hair shaft morphogenesis while regulating the expression of secreted growth factors [105]. In chapter IV, this polyphenolic compound was applied to pigment cells lines: human epidermal melanocytes (HEM), and B16 murine melanoma cells (B16F10) to determine its effect on pigmentation. TCQA enhanced the melanin content, as well as the gene and the protein expression of the melanogenesis enzymes and their transcription factor Mitf in both cells lines. The activation of β-catenin by TCQA known to positively regulate MITF transcription, is responsible of the observed hair pigmentation promotion effect.

Additionally knowing the mode of action of TCQA is essential in order to established it as a commercial drug. In this thesis we want to propose a hypothesis about how TCQA acts inside the cells. In chapter III and IV, a commercial inhibitor XAV939 of Wnt/ β-catenin was used in human dermal papilla and human melanocytes. Upon application to the cells, the gene expression of β-catenin decreased but this inhibition was lifted after a co-treatment with TCQA. The mode of action of XAV939 is known, actually it acts on the inhibition of tankyrase. Tankyrase (TNK) are known to destabilize AXIN and that reduces β-catenin degradation and promotes its translocation into the nucleus and therefore its activation. XAV939 stabilizes AXIN levels leading to reduced β-catenin levels and activity. TCQA reduced the inhibition of XAV939 and on the other hand it upregulated *Fzd* and *Wnt* gene expression and reduced *Gsk3b* expression. In Figure 5.1, we proposed the mode of action TCQA but docking studies however should be necessary to further understand how TCQA bind and act inside the cell.

Another explanation about the mode of action of TCQA to promote pigmentation relies on its chemical structure. Actually, TCQA is composed of three catechol, and catechol moiety is thought to be responsible for the physiological or pharmacological action [164]. Moreover, this catechol structure of TCQA is similar to L-DOPA, the melanin precursors catalyzed by tyrosinase, and the melanin synthesis was found to be enhanced by TCQA. Additionally, TCQA promoted neural stem cell differentiation and dopamine (catechol moiety) content in brain and the melanocytes, and L-DOPA is found in the melanocytes melanosomes [74]. So TCQA acted on the biosynthesis of L-DOPA in the melanocytes and dopamine in the brain, for these reasons, we propose that the catechol moiety of TCQA appears to play an important role in its mechanism of action, although further chemical analysis are required.

Taken together, in this thesis TCQA caused firstly the initiation and elongation of anagen phase of the hair cycle in C3H mice. This induction of the anagen phase was followed by an enhancement of the hair shaft pigmentation of these mice. The molecular mechanism behind this effect was due to the upregulation of Wnt/β-catenin pathway and its target genes (**Figure 5.2**). The same effect was seen in human DP cells and human melanocytes. In this context, the potential effect of TCQA on the activation of melanocytes through a communication with dermal papilla cells via Wnt/β-catenin will be investigated. Clinical studies would be however necessary to introduce TCQA as a safer drug to initiate the hair growth cycle and to enhance melanogenesis.

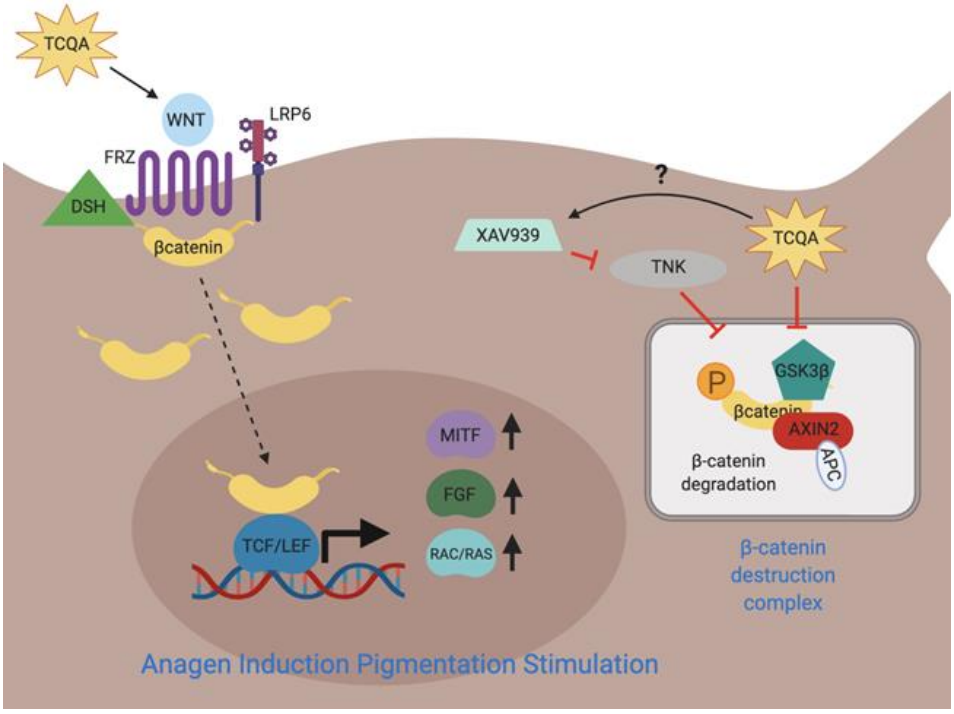

Figure 5.1. Proposed mechanism of action of TCQA in the HF.

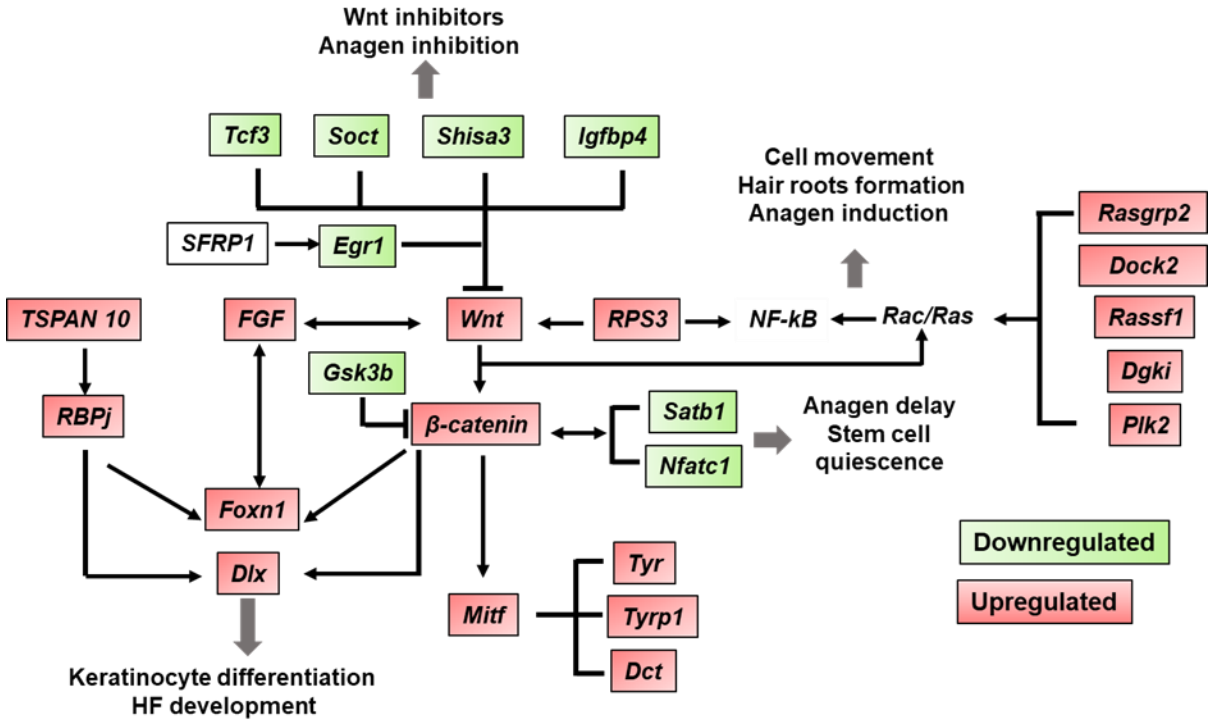

Figure 5.2.Molecular mechanism behind TCQA stimulating hair growth and pigmentation effect.

Acknowledgement

This thesis is dedicated to my beloved family and especially my parents for their endless love throughout my life and for their encouragement and for giving me strength not to give up and move forward. My two beloved brothers and my aunt who is like a parents to me, for their support and presence. A feeling of gratitude to my loving grandparents for always being there and for believing in me and, a special mention to Richard for his endless support and for sharing with me the joy and sorrow throughout this journey. I would like to thank all friends for their help and for being a second family to me.

Most of all my sincere appreciation and gratitude to my thesis supervisor, Professor Hiroko Isoda, Ph.D., for her assistance and guidance during the past three years. I would like to sincerely thank her for trusting in my work and providing all means to complete this research, also for her advices, scientific critics, and encouragements.

I would like also to extend my sincere acknowledgment to my co-supervisors, associate professor Myra O. Villareal, Ph.D for her valuable advices and for helping me during experiment and for her extensive experiences in the scientific publication procedure; associate professor Yusaku Miyamae, Ph.D for his guidance, his comments and questions that were very beneficial in the completion of the thesis.

Special thanks to Dr. Kazunori Sasaki Ph.D for helping through the animal experiment. I'm are also grateful for the help extended by Dr. Hiromi Yanagisawa and Dr. Aiko Sada i for their incredible support in mice experiments and all Isoda lab members for their daily assistance, interesting talks, and encouragement.

This study was partially supported by Japan Science and Technology Agency (JST), the Japan International Cooperation Agency's (JICA), Science and Technology Research Partnership for Sustainable Development (SATREPS), and the Ministry of Education, Culture, Sports, Science, and Technology (MEXT).

References

1. Jaks V, Kasper M, Toftgård R. The hair follicle-a stem cell zoo. Exp Cell Res. Elsevier Inc.; 2010; 316: 1422–8.

2. Schneider MR, Schmidt-Ullrich R, Paus R. The Hair Follicle as a Dynamic Miniorgan. Curr Biol. Elsevier Ltd; 2009; 19: R132–42.

3. Hardy MH. The secret life of the hair follicle. Trends Genet. 1992; 8: 55–61.

4. Yang CC, Cotsarelis G. Review of hair follicle dermal cells. J Dermatol Sci. 2010; 57: 2–11.

5. Lin MH, Leimeister C, Gessler M, Kopan R. Activation of the Notch pathway in the hair cortex leads to aberrant differentiation of the adjacent hair-shaft layers. Development. 2000; 127: 2421–32.

6. Millar SE. WNT signaling in the control of hair growth and structure. Dev Biol [Internet]. 1999; 207: 133–49. Available from: http://dx.doi.org/10.1006/dbio.1998.9140

7. Nishimura EK, Yoshida H, Kunisada T, Nishikawa SI. Regulation of E- and P-cadherin expression correlated with melanocyte migration and diversification. Dev Biol. 1999; 215: 155–66.

8. Tobin DJ, Slominski A, Botchkarev V, Paus R. The fate of hair follicle melanocytes during the hair growth cycle. J Investig Dermatology Symp Proc [Internet]. Elsevier Masson SAS; 1999; 4: 323–32. Available from: http://dx.doi.org/10.1038/sj.jidsp.5640239

9. Stenn KS, Paus R. Controls of hair follicle cycling. Physiol Rev. 2001; 81: 449–94.

10. Driskell RR, Clavel C, Rendl M, Watt FM. Hair follicle dermal papilla cells at a glance. J Cell Sci. 2011; 124: 1179–82.

11. Lavker RM, Sun T, Oshima H, Barrandon Y, Akiyama M, Ferraris C, Chevalier G, Favier B, Jahoda CAB, Dhouailly D, Panteleyev AA, Christiano AM. Hair Follicle Stem Cells. J Investig Dermatology Symp Proc. Elsevier Masson SAS; 2003; 8: 28–38.

12. Lin JY, Fisher DE. Melanocyte biology and skin pigmentation. Nature [Internet]. Nature Publishing Group; 2007; 445: 843. Available from: https://doi.org/10.1038/nature05660

13. Nishimura EK, Jordan SA, Oshima H, Yoshida H, Osawa M, Moriyama M, Jackson IJ, Barrandon Y, Miyachi Y, Nishikawa S-I. Dominant role of the niche in melanocyte stem-cell fate determination. Nature [Internet]. 2002; 416: 854–60. Available from: https://doi.org/10.1038/416854a

14. Elliott K, Stephenson TJ, Messenger AG. Differences in hair follicle dermal papilla volume are due to extracellular matrix volume and cell number: Implications for the control of hair follicle size and androgen responses. J Invest Dermatol [Internet]. Elsevier Masson SAS; 1999; 113: 873–7. Available from: http://dx.doi.org/10.1046/j.1523-1747.1999.00797.x

15. Müller-Röver S, Handjiski B, Van Der Veen C, Eichmüller S, Foitzik K, McKay IA, Stenn KS, Paus R. A comprehensive guide for the accurate classification of murine hair follicles in distinct hair cycle stages. J Invest Dermatol. 2001; 117: 3–15.

16. Lindner G, Botchkarev VA, Botchkareva N V., Ling G, Van Der Veen C, Paus R. Analysis of apoptosis during hair follicle regression (catagen). Am J Pathol. 1997; 151: 1601–17.

17. Ma L, Liu J, Wu T, Plikus M, Jiang TX, Bi Q, Liu YH, Müller-Röver S, Peters H, Sundberg JP, Maxson R, Maas RL, Chuong CM. “Cyclic alopecia” in Msx2 mutants: Defects in hair cycling and hair shaft differentiation. Development. 2003; 130: 379–89.

18. Messenger a G. The control of hair growth: an overview. J Invest Dermatol. 1993; 101: 4S-9S.

19. Blanpain C, Lowry WE, Geoghegan A, Polak L, Fuchs E. Self-renewal, multipotency, and the existence of two cell populations within an epithelial stem cell niche. Cell. 2004; 118: 635–48.

20. McNeill H, Woodgett JR. When pathways collide: Collaboration and connivance among signalling proteins in development. Nat Rev Mol Cell Biol [Internet]. Nature Publishing Group; 2010; 11: 404–13. Available from: http://dx.doi.org/10.1038/nrm2902

21. Guo L, Yu Q, Fuchs E. Targeting expression of keratinocyte growth factor to keratinocytes elicits striking changes in epithelial differentiation in transgenic mice. 1993; 12: 973–86.

22. Kuwahara A, Sakai H, Xu Y, Itoh Y, Hirabayashi Y, Gotoh Y. Tcf3 represses Wnt-β-catenin signaling and maintains neural stem cell population during neocortical development. PLoS One. 2014; 9: 1–12.

23. Andl T, Reddy ST, Gaddapara T, Millar SE. WNT signals are required for the initiation of hair follicle development. Dev Cell. 2002; 2: 643–53.

24. Merrill BJ, Gat U, DasGupta R, Fuchs E. Tcf3 and Lef1 regulate lineage differentiation of multipotent stem cells in skin. Genes Dev. 2001; 15: 1688–705.

25. Gat U, DasGupta R, Degenstein L, Fuchs E. De novo hair follicle morphogenesis and hair tumors in mice expressing a truncated β-catenin in skin. Cell. 1998; 95: 605–14.

26. Van Genderen C, Okamura RM, Farinas I, Quo RG, Parslow TG, Bruhn L, Grosschedl R. Development of several organs that require inductive epithelial- mesenchymal interactions is impaired in LEF-1-deficient mice. Genes Dev. 1994; 8: 2691–703.

27. Widlund HR, Horstmann MA, Roydon Price E, Cui J, Lessnick SL, Wu M, He X, Fisher DE. β-Catenin-induced melanoma growth requires the downstream target Microphthalmia-associated transcription factor. J Cell Biol. 2002; 158: 1079–87.

28. Huelsken J, Vogel R, Erdmann B, Cotsarelis G, Birchmeier W. β-Catenin controls hair follicle morphogenesis and stem cell differentiation in the skin. Cell. 2001; 105: 533–45.

29. Legrand JMD, Roy E, Ellis JJ, Francois M, Brooks AJ, Khosrotehrani K. STAT5 Activation in the Dermal Papilla Is Important for Hair Follicle Growth Phase Induction. J Invest Dermatol [Internet]. The Authors; 2016; 136: 1781–91. Available from: http://dx.doi.org/10.1016/j.jid.2016.04.014

30. St-Jacques B, Dassule HR, Karavanova I, Botchkarev VA, Li J, Danielian PS, McMahon JA, Lewis PM, Paus R, McMahon AP. Sonic hedgehog signaling is essential for hair development. Curr Biol. 1998; 8: 1058–69.

31. Wang LC, Liu ZY, Gambardella L, Delacour A, Shapiro R, Yang J, Sizing I, Rayhorn P, Garber EA, Benjamin CD, Williams KP, Taylor FR, Barrandon Y, et al. Conditional disruption of hedgehog signaling pathway defines its critical role in hair development and regeneration. J Invest Dermatol. Elsevier Masson SAS; 2000; 114: 901–8.

32. Jaks V, Barker N, Kasper M, van Es JH, Snippert HJ, Clevers H, Toftgård R. Lgr5 marks cycling, yet long-lived, hair follicle stem cells. Nat Genet. 2008; 40: 1291–9.

33. Huh SH, Närhi K, Lindfors PH, Häärä O, Yang L, Ornitz DM, Mikkola ML. Fgf20 governs formation of primary and secondary dermal condensations in developing hair follicles. Genes Dev. 2013; 27: 450–8.

34. Coutu DL, Galipeau J. Roles of FGF signaling in stem cell self-renewal, senescence and aging. Aging (Albany NY). 2011; 3: 920–33.

35. Lin WH, Xiang LJ, Shi HX, Zhang J, Jiang LP, Cai PT, Lin ZL, Lin BB, Huang Y, Zhang HL, Fu XB, Guo DJ, Li XK, et al. Fibroblast growth factors stimulate hair growth through β -Catenin and shh expression in C57BL/6 mice. Biomed Res Int. Hindawi Publishing Corporation; 2015; 2015.

36. Botchkarev VA, Kishimoto J. Molecular control of epithelial-mesenchymal interactions during hair follicle cycling. J Investig Dermatology Symp Proc. Elsevier Masson SAS; 2003; 8: 46–55.

37. Ten Dijke P, Hill CS. New insights into TGF-β-Smad signalling. Trends Biochem Sci. 2004; 29: 265–73.

38. Rishikaysh P, Dev K, Diaz D, Shaikh Qureshi WM, Filip S, Mokry J. Signaling involved in hair follicle morphogenesis and development. Int J Mol Sci. 2014; 15: 1647–70.

39. Kobielak K, Pasolli HA, Alonso L, Polak L, Fuchs E. Defining BMP functions in the hair follicle by conditional ablation of BMP receptor IA. J Cell Biol. 2003; 163: 609–23.

40. Kobayashi T, Urabe K, Winder A, Jiménez-Cervantes C, Imokawa G, Brewington T, Solano F, García-Borrón JC, Hearing VJ. Tyrosinase related protein 1 (TRP1) functions as a DHICA oxidase in melanin biosynthesis. EMBO J [Internet]. 1994; 13: 5818–25. Available from:

http://www.ncbi.nlm.nih.gov/pubmed/7813420%0Ahttp://www.pubmedcentral.nih.gov/articlerender.fcgi?artid=PMC395555

41. Hou L, Panthier JJ, Arnheiter H. Signaling and transcriptional regulation in the neural crest-derived melanocyte lineage: interactions between KIT and MITF. Development [Internet]. 2000; 127: 5379–89. Available from: http://www.ncbi.nlm.nih.gov/pubmed/11076759

42. D'Mello SAN, Finlay GJ, Baguley BC, Askarian-Amiri ME. Signaling pathways in melanogenesis. Int J Mol Sci. 2016; 17: 1–18.

43. Ngeow KC, Friedrichsen HJ, Li L, Zeng Z, Andrews S, Volpon L, Brunsdon H, Berridge G, Picaud S, Fischer R, Lisle R, Knapp S, Filippakopoulos P, et al. BRAF/MAPK and GSK3 signaling converges to control MITF nuclear export. Proc Natl Acad Sci. 2018; 115: E8668–77.

44. Passeron T, Valencia JC, Bertolotto C, Hoashi T, Le Pape E, Takahashi K, Ballotti R, Hearing VJ. SOX9 is a key player in ultraviolet B-induced melanocyte differentiation and pigmentation. Proc Natl Acad Sci. 2007; 104: 13984–9.

45. Levy C, Khaled M, Fisher DE. MITF: master regulator of melanocyte development and melanoma oncogene. Trends Mol Med. 2006; 12: 406–14.

46. Ouji Y, Yoshikawa M, Moriya K, Nishiofuku M, Matsuda R, Ishizaka S. Wnt-10b, uniquely among Wnts, promotes epithelial differentiation and shaft growth. Biochem Biophys Res Commun. 2008; 367: 299–304.

47. Zhou L, Xu M, Yang Y, Yang K, Wickett RR, Andl T, Millar SE, Zhang Y. Activation of β-Catenin Signaling in CD133-Positive Dermal Papilla Cells Drives Postnatal Hair Growth. PLoS One. 2016; 11: e0160425.

48. Almohanna HM, Ahmed AA, Tsatalis JP, Tosti A. The Role of Vitamins and Minerals in Hair Loss: A Review. Dermatol Ther (Heidelb) [Internet]. Springer Healthcare; 2019; 9: 51–70. Available from: https://doi.org/10.1007/s13555-018-0278-6

49. Tru RM. Molecular mechanisms of androgenetic alopecia. Exp Gerontol. 2002; 37: 981–90.

50. Hordinsky M, Junqueira AL. Alopecia areata update. Semin Cutan Med Surg. 2015; 34: 72–5.

51. Harrison S, Sinclair R. Telogen effluvium. 2002; : 389–95.

52. Schnohr P, Lange P, Nyboe J, Appleyard M, Jensen G. Gray hair, baldness, and wrinkles in relation to myocardial infarction: The Copenhagen City Heart Study. Am Heart J. 1995; 130: 1003–10.

53. ElFaramawy AAA, Hanna IS, Darweesh RM, Ismail AS, Kandil HI. The degree of hair graying as an independent risk marker for coronary artery disease, a CT coronary angiography study. Egypt Hear J [Internet]. Egyptian Society of Cardiology; 2018; 70: 15–9. Available from: https://doi.org/10.1016/j.ehj.2017.07.001

54. Shin H, Ryu HH, Yoon J, Jo S, Jang S, Choi M, Kwon O, Jo SJ. Association of premature hair graying with family history, smoking, and obesity: A cross-sectional study. J Am Acad Dermatol [Internet]. Elsevier Inc; 2015; 72: 321–7. Available from: http://dx.doi.org/10.1016/j.jaad.2014.11.008

55. Doubaj Y, De Sandre-Giovannoli A, Vera EV, Navarro CL, Elalaoui SC, Tajir M, Lévy N, Sefiani A. An inherited LMNA gene mutation in atypical Progeria syndrome. Am J Med Genet Part A. 2012; 158 A: 2881–7.

56. Seiberg M. Age-induced hair greying - The multiple effects of oxidative stress. Int J Cosmet Sci. 2013; 35: 532–8.

57. Tobin DJ, Paus R. Graying: Gerontobiology of the hair follicle pigmentary unit. Exp Gerontol. 2001; 36: 29–54.

58. Arck PC, Overall R, Spatz K, Liezman C, Handjiski B, Klapp BF, Birch-Machin MA, Peters EMJ. Towards a “free radical theory of graying”: Melanocyte apoptosis in the aging human hair follicle is an indicator of oxidative stress induced tissue damage. FASEB J. 2006; 20.

59. Commo S, Gaillard O, Bernard BA. Human hair greying is linked to a specific depletion of hair follicle melanocytes affecting both the bulb and the outer root sheath. Br J Dermatol. 2004; 150: 435–43.

60. Slominski A, Wortsman J, Plonka PM, Schallreuter KU, Paus R, Tobin DJ. Hair follicle pigmentation. J Invest Dermatol [Internet]. Elsevier Masson SAS; 2005; 124: 13–21. Available from: http://dx.doi.org/10.1111/j.0022-202X.2004.23528.x

61. Nishimura EK, Granter SR, Fisher DE. Mechanisms of hair graying: Incomplete melanocyte stem cell maintenance in the niche. Science (80-). 2005; 307: 720–4.

62. Nishimura EK, Suzuki M, Igras V, Du J, Lonning S, Miyachi Y, Roes J, Beermann F, Fisher DE. Key Roles for Transforming Growth Factor β in Melanocyte Stem Cell Maintenance. Cell Stem Cell. 2010; 6: 130–40.

63. Nishimura EK. Melanocyte stem cells: A melanocyte reservoir in hair follicles for hair and skin pigmentation. Pigment Cell Melanoma Res. 2011; 24: 401–10.

64. Li M, Marubayashi A, Nakaya Y, Fukui K, Arase S. Minoxidil-induced hair growth is mediated by adenosine in cultured dermal papilla cells: Possible involvement of sulfonylurea receptor 2B as a target of minoxidil. J Invest Dermatol [Internet]. Elsevier Masson SAS; 2001; 117: 1594–600. Available from: http://dx.doi.org/10.1046/j.0022-202x.2001.01570.x

65. Kaufman KD, Olsen EA, Whiting D, Savin R, DeVillez R, Bergfeld W, Price VH, Van Neste D, Roberts JL, Hordinsky M, Shapiro J, Binkowitz B, Gormley GJ, et al. Finasteride in the treatment of men with androgenetic alopecia. J Am Acad Dermatol. 1998; 39: 578–89.

66. Van Neste D, Fuh V, Sanchez-Pedreno P, Lopez-Bran E, Wolff H, Whiting D, Roberts J, Kopera D, Stene JJ, Calvieri S, Tosti A, Prens E, Guarrera M, et al. Finasteride increases anagen hair in men with androgenetic alopecia. Br J Dermatol. 2000; 143: 804–10.

67. Kwack MH, Kang BM, Kim MK, Kim JC, Sung YK. Minoxidil activates b -catenin pathway in human dermal papilla cells : A possible explanation for its anagen prolongation effect. J Dermatol Sci [Internet]. Japanese Society for Investigative Dermatology; 2011; 62: 154–9. Available from: http://dx.doi.org/10.1016/j.jdermsci.2011.01.013

68. Rathi V, Rathi JC, Tamizharasi S, Kumar A. Phcog Rev .: Short Review Plants used for hair growth promotion : A review. Rev Lit Arts Am. 2008; 2: 185–7.

69. Miyamae Y, Han J, Sasaki K, Terakawa M, Isoda H, Shigemori H. 3,4,5-tri-O-caffeoylquinic acid inhibits amyloid β-mediated cellular toxicity on SH-SY5Y cells through the upregulation of PGAM1 and G3PDH. Cytotechnology. 2011; 63: 191–200.

70. Han J, Miyamae Y, Shigemori H, Isoda H. Neuroprotective effect of 3,5-di-O-caffeoylquinic acid on SH-SY5Y cells and senescence-accelerated-prone mice 8 through the up-regulation of phosphoglycerate kinase-1. Neuroscience [Internet]. Elsevier Inc.; 2010; 169: 1039–45. Available from: http://dx.doi.org/10.1016/j.neuroscience.2010.05.049

71. KIMURA Y, OKUDA H, OKUDA T, HATANO T, AGATA I, ARICHI S. Studies on the activities of tannins and related compounds from medicinal plants and drugs. VI. Inhibitory effects of caffeoylquinic acids on histamine release from rat peritoneal mast cells. Chem Pharm Bull (Tokyo) [Internet]. 1985; 33: 690–6. Available from: http://joi.jlc.jst.go.jp/JST.Journalarchive/cpb1958/33.690?from=CrossRef

72. Kim HJ, Kim JS, Woo JT, Lee IS, Cha BY. Hyperpigmentation mechanism of methyl 3,5-di-caffeoylquinate through activation of p38 and MITF induction of tyrosinase. Acta Biochim Biophys Sin (Shanghai). 2015; 47: 548–56.

73. Tang B, Huang Y, Yang H, Tang P, Li H. Molecular mechanism of the binding of 3,4,5-tri-O-caffeoylquinic acid to human serum albumin: Saturation transfer difference NMR, multi-spectroscopy, and docking studies. J Photochem Photobiol B Biol [Internet]. Elsevier B.V.; 2016; 165: 24–33. Available from: http://dx.doi.org/10.1016/j.jphotobiol.2016.10.017

74. Sasaki K, Davies J, Doldán NG, Arao S, Ferdousi F, Szele FG, Isoda H. 3,4,5-Tricaffeoylquinic acid induces adult neurogenesis and improves deficit of learning and memory in aging model senescence-accelerated prone 8 mice. Aging (Albany NY) [Internet]. 2019; 11: 1–22. Available from: http://www.aging-us.com/article/101748/text

75. Plikus M V., Chuong CM. Complex hair cycle domain patterns and regenerative hair waves in living rodents. J Invest Dermatol. 2008; 128: 1071–80.

76. Alonso L, Fuchs E. The hair cycle. J Cell Sci. 2006; 119: 391–3.

77. Milner Y, Sudnik J, Filippi M, Kizoulis M, Kashgarian M, Stenn K. Exogen, shedding phase of the hair growth cycle: Characterization of a mouse model. J Invest Dermatol. Elsevier Masson SAS; 2002; 119: 639–44.

78. Kishimoto J, Burgeson RE, Morgan BA. Wnt signaling maintains the hair-inducing activity of the dermal papilla service Wnt signaling maintains the hair-inducing activity of the dermal papilla. Genes Dev. 2000; 14: 1181–5.

79. Paus R. Principles of hair cycle control. J Dermatol. 1998; 25: 793–802.

80. Visweswaran M, Pohl S, Arfuso F, Newsholme P, Dilley R, Pervaiz S, Dharmarajan A. Multi-lineage differentiation of mesenchymal stem cells - To Wnt, or not Wnt. Int J Biochem Cell Biol [Internet]. Elsevier Ltd; 2015; 68: 139–47. Available from: http://dx.doi.org/10.1016/j.biocel.2015.09.008

81. Choi YS, Zhang Y, Xu M, Yang Y, Ito M, Peng T, Cui Z, Nagy A, Hadjantonakis AK, Lang RA, Cotsarelis G, Andl T, Morrisey EE, et al. Distinct functions for Wnt/β-Catenin in hair follicle stem cell proliferation and survival and interfollicular epidermal homeostasis. Cell Stem Cell [Internet]. Elsevier Inc.; 2013; 13: 720–33. Available from: http://dx.doi.org/10.1016/j.stem.2013.10.003

82. Guo L, Yu Q-C, Fuchs1 E. Targeting expression of keratinocyte growth factor to keratinocytes elicits striking changes in epithelial differentiation in transgenic mice. EMBO J [Internet]. 1993; 12: 973–86. Available from: https://www.ncbi.nlm.nih.gov/pmc/articles/PMC413298/pdf/emboj00075-0168.pdf

83. Pan Y, Lin MH, Tian X, Cheng HT, Gridley T, Shen J, Kopan R. γ-Secretase functions through Notch signaling to maintain skin appendages but is not required for their patterning or initial morphogenesis. Dev Cell. 2004; 7: 731–43.

84. Habas R, Dawid IB, He X. Coactivation of Rac and Rho by Wnt/Frizzled signaling is required for vertebrate gastrulation. Genes Dev. 2003; 17: 295–309.

85. Bejaoui M, Villareal MO, Isoda H. β-catenin-mediated hair growth induction effect of 3,4,5-tri-*O*-caffeoylquinic acid. Aging (Albany NY) [Internet]. Impact Journals, LLC; 2019; 11: 4216–37. Available from: https://doi.org/10.18632/aging.102048

86. Le Pape E, Wakamatsu K, Ito S, Wolber R, Hearing VJ. Regulation of eumelanin/pheomelanin synthesis and visible pigmentation in melanocytes by ligands of the melanocortin 1 receptor. Pigment Cell Melanoma Res. 2008; 21: 477–86.

87. Huang DW, Sherman BT, Lempicki RA. Bioinformatics enrichment tools: Paths toward the comprehensive functional analysis of large gene lists. Nucleic Acids Res. 2009; 37: 1–13.

88. Zacariotti RL, do Valle R del R. Observation of mating in the Calico Snake Oxyrhopus petola Linnaeus, 1758. Herpetol Notes. 2010; 3: 139–40.

89. Millar SE. Molecular mechanisms regulating hair follicle development [Internet]. Journal of Investigative Dermatology. Elsevier Masson SAS; 2002. p. 216–25. Available from: http://dx.doi.org/10.1046/j.0022-202x.2001.01670.x

90. Lee S-H, Yoon J, Shin SH, Zahoor M, Kim HJ, Park PJ, Park W-S, Min DS, Kim H-Y, Choi K-Y. Valproic Acid Induces Hair Regeneration in Murine Model and Activates Alkaline Phosphatase Activity in Human Dermal Papilla Cells. PLoS One [Internet]. 2012; 7: e34152. Available from: http://dx.plos.org/10.1371/journal.pone.0034152

91. Sinclair R, Jolley D, Mallari R, Magee J, Tosti A, Piracinni BM, Vincenzi C, Happle R, Ferrando J, Grimalt R, Thérèse L, Van Neste D, Zlotogorski A, et al. Morphological approach to hair disorders. J Investig Dermatology Symp Proc. 2003; 8: 56–64.

92. Steingrímsson E, Copeland NG, Jenkins NA. Melanocyte stem cell maintenance and hair graying. Cell. 2005; 121: 9–12.

93. Driskell RR, Clavel C, Rendl M, Watt FM. Hair follicle dermal papilla cells at a glance. J Cell Sci [Internet]. 2011; 124: 1179–82. Available from: http://jcs.biologists.org/cgi/doi/10.1242/jcs.082446

94. Lin W, Xiang L-J, Shi H-X, Zhang J, Jiang L, Cai P, Lin Z-L, Lin B-B, Huang Y, Zhang H-L, Fu X-B, Guo D-J, Li X-K, et al. Fibroblast Growth Factors Stimulate Hair Growth throughβ-Catenin and Shh Expression in C57BL/6 Mice. Biomed Res Int. 2015; 2015: 1–9.

95. Lee J, Tumbar T. Hairy tale of signaling in hair follicle development and cycling. Semin Cell Dev Biol [Internet]. Elsevier Ltd; 2012; 23: 906–16. Available from: http://dx.doi.org/10.1016/j.semcdb.2012.08.003

96. Yamamoto N, Tanigaki K, Han H, Hiai H, Honjo T. Notch/RBP-J signaling regulates epidermis/hair fate determination of hair follicular stem cells. Curr Biol. 2003; 13: 333–8.

97. Blanpain C, Lowry WE, Pasolli HA, Fuchs E. Canonical notch signaling functions as a commitment switch in the epidermal lineage. Genes Dev. 2006; 20: 3022–35.

98. Honjo T. The shortest path from the surface to the nucleus: RBP-Jκ/Su(H) transcription factor. Genes to Cells. 1996; 1: 1–9.

99. Dornier E, Coumailleau F, Ottavi JF, Moretti J, Boucheix C, Mauduit P, Schweisguth F, Rubinstein E. Tspanc8 tetraspanins regulate ADAM10/Kuzbanian trafficking and promote Notch activation in flies and mammals. J Cell Biol. 2012; 199: 481–96.

100. Lowry WE, Blanpain C, Nowak JA, Guasch G, Lewis L, Fuchs E. Defining the impact of β-catenin/Tcf transactivation on epithelial stem cells. Genes Dev. 2005; 19: 1596–611.

101. Li J, Baxter RM, Weiner L, Goetinck PF, Calautti E, Brissette JL. Foxn1 promotes keratinocyte differentiation by regulating the activity of protein kinase C. Differentiation [Internet]. International Society of Differentiation; 2007; 75: 694–701. Available from: http://dx.doi.org/10.1111/j.1432-0436.2007.00176.x

102. Takabayashi Y, Nambu M, Ishihara M, Kuwabara M, Fukuda K, Nakamura S, Hattori H, Kiyosawa T. Enhanced effect of fibroblast growth factor-2-containing dalteparin/protamine nanoparticles on hair growth. Clin Cosmet Investig Dermatol. 2016; 9: 127–34.

103. Tsai SY, Sennett R, Rezza A, Clavel C, Grisanti L, Zemla R, Najam S, Rendl M. Wnt/β-catenin signaling in dermal condensates is required for hair follicle formation. Dev Biol [Internet]. Elsevier; 2014; 385: 179–88. Available from: http://dx.doi.org/10.1016/j.ydbio.2013.11.023

104. Maretto S, Cordenonsi M, Dupont S, Braghetta P, Broccoli V, Hassan AB, Volpin D, Bressan GM, Piccolo S. Mapping Wnt/ -catenin signaling during mouse development and

in colorectal tumors. Proc Natl Acad Sci [Internet]. 2003; 100: 3299–304. Available from: http://www.pnas.org/cgi/doi/10.1073/pnas.0434590100

105. Enshell-Seijffers D, Lindon C, Kashiwagi M, Morgan BA. β-catenin Activity in the Dermal Papilla Regulates Morphogenesis and Regeneration of Hair. Dev Cell [Internet]. Elsevier Ltd; 2010; 18: 633–42. Available from: http://dx.doi.org/10.1016/j.devcel.2010.01.016

106. Yamada T, Hasegawa S, Inoue Y, Date Y, Yamamoto N, Mizutani H, Nakata S, Matsunaga K, Akamatsu H. Wnt/β-Catenin and kit signaling sequentially regulate melanocyte stem cell differentiation in uvb-induced epidermal pigmentation. J Invest Dermatol. Elsevier Masson SAS; 2013; 133: 2753–62.

107. Dorsky RI, Raible DW, Moon RT. Direct regulation of nacre , a zebrafish MITF homolog required for pigment cell formation , by the Wnt pathway service Direct regulation of nacre , a zebrafish MITF homolog required for pigment cell formation , by the Wnt pathway. 2000; : 158–62.

108. Jouneau A, Yu YQ, Pasdar M, Larue L. Plasticity of cadherin-catenin expression in the melanocyte lineage. Pigment Cell Res. 2000; 13: 260–72.

109. Goding CR. Mitf from neural crest to melanoma: Signal transduction and transcription in the melanocyte lineage. Genes Dev. 2000; 14: 1712–28.

110. Villareal MO, Kume S, Neffati M, Isoda H. Upregulation of *Mitf* by Phenolic Compounds-Rich *Cymbopogon schoenanthus* Treatment Promotes Melanogenesis in B16 Melanoma Cells and Human Epidermal Melanocytes. Biomed Res Int [Internet]. 2017; 2017: 1–11. Available from: https://www.hindawi.com/journals/bmri/2017/8303671/

111. Moore KJ. Insight into the microphthalmia gene. Trends Genet. 1995; 11: 442–8.

112. Bonaventure J, Domingues MJ, Larue L. Cellular and molecular mechanisms controlling the migration of melanocytes and melanoma cells. Pigment Cell Melanoma Res. 2013; 26: 316–25.

113. Flaherty KT, Hodi FS, Fisher DE. From genes to drugs: targeted strategies for melanoma. Nat Rev Cancer [Internet]. Nature Publishing Group, a division of Macmillan Publishers

Limited. All Rights Reserved.; 2012; 12: 349. Available from: https://doi.org/10.1038/nrc3218

114. Kawakami A, Fisher DE. The master role of microphthalmia-associated transcription factor in melanocyte and melanoma biology. Lab Investig [Internet]. United States & Canadian Academy of Pathology USCAP, Inc; 2017; 97: 649. Available from: https://doi.org/10.1038/labinvest.2017.9

115. Gaggioli C, Buscà R, Abbe P, Ortonne JP, Ballotti R. Microphthalmia-associated transcription factor (MITF) is required but is not sufficient to induce the expression of melanogenic genes. Pigment Cell Res. 2003; 16: 374–82.

116. Shin SY, Choi JH, Jung E, Gil H-N, Lim Y, Lee YH. The EGR1–STAT3 Transcription Factor Axis Regulates α-Melanocyte–Stimulating Hormone–Induced Tyrosinase Gene Transcription in Melanocytes. J Invest Dermatol. 2019; 139: 1616–9.

117. Pingault V, Ente D, Dastot-Le Moal F, Goossens M, Marlin S, Bondurand N. Review and update of mutations causing Waardenburg syndrome. Hum Mutat. 2010; 31: 391–406.

118. Dong L, Li Y, Cao J, Liu F, Pier E, Chen J, Xu Z, Chen C, Wang RA, Cui R. FGF2 regulates melanocytes viability through the STAT3-transactivated PAX3 transcription. Cell Death Differ. 2012; 19: 616–22.

119. Riley PA. Melanin. Int J Biochem Cell Biol [Internet]. 1997; 29: 1235–9. Available from: http://www.sciencedirect.com/science/article/pii/S1357272597000137

120. Fuller BB, Drake MA, Spaulding DT, Chaudhry F. Downregulation of tyrosinase activity in human melanocyte cell cultures by yohimbine. J Invest Dermatol [Internet]. Elsevier Masson SAS; 2000; 114: 268–76. Available from: http://dx.doi.org/10.1046/j.1523-1747.2000.00860.x

121. Murtas D, Pilloni L, Diana A, Casula L, Tomei S, Piras F, Ferreli C, Maxia C, Perra MT. Tyrosinase and nestin immunohistochemical expression in melanocytic nevi as a histopathologic pattern to trace melanocyte differentiation and nevogenesis. Histochem Cell Biol [Internet]. 2019; 151: 175–85. Available from: https://doi.org/10.1007/s00418-018-1730-5

122. Trempus CS, Morris RJ, Ehinger M, Elmore A, Bortner CD, Ito M, Cotsarelis G, Nijhof JGW, Peckham J, Flagler N, Kissling G, Humble MM, King LC, et al. CD34 expression by hair follicle stem cells is required for skin tumor development in mice. Cancer Res. 2007; 67: 4173–81.

123. Joshi SS, Tandukar B, Pan L, Huang JM, Livak F, Smith BJ, Hodges T, Mahurkar AA, Hornyak TJ. CD34 defines melanocyte stem cell subpopulations with distinct regenerative properties. PLoS Genet. 2019; 15: e1008034.

124. Wu G, Huang H, Abreu JG, He X. Inhibition of GSK3 phosphorylation of β-catenin via phosphorylated PPPSPXS motifs of Wnt coreceptor LRP6. PLoS One. 2009; 4.

125. Zhu W, Shiojima I, Ito Y, Li Z, Ikeda H, Yoshida M, Naito AT, Nishi JI, Ueno H, Umezawa A, Minamino T, Nagai T, Kikuchi A, et al. IGFBP-4 is an inhibitor of canonical Wnt signalling required for cardiogenesis. Nature. 2008; 454: 345–9.

126. Geyfman M, Gordon W, Paus R, Andersen B. Identification of telogen markers underscores that telogen is far from a quiescent hair cycle phase. J Invest Dermatol. 2012; 132: 721–4.

127. Horsley V, Aliprantis AO, Polak L, Glimcher LH, Fuchs E. NFATc1 Balances Quiescence and Proliferation of Skin Stem Cells. Cell. 2008; 132: 299–310.

128. Keyes BE, Segal JP, Heller E, Lien W-H, Chang C-Y, Guo X, Oristian DS, Zheng D, Fuchs E. Nfatc1 orchestrates aging in hair follicle stem cells. Proc Natl Acad Sci [Internet]. 2013; 110: E4950–9. Available from: http://www.pnas.org/cgi/doi/10.1073/pnas.1320301110

129. Avigad Laron E, Aamar E, Enshell-Seijffers D. The Mesenchymal Niche of the Hair Follicle Induces Regeneration by Releasing Primed Progenitors from Inhibitory Effects of Quiescent Stem Cells. Cell Rep [Internet]. ElsevierCompany.; 2018; 24: 909-921.e3. Available from: https://doi.org/10.1016/j.celrep.2018.06.084

130. Chen H, Weng QY, Fisher DE. UV signaling pathways within the skin. J Invest Dermatol [Internet]. Elsevier Masson SAS; 2014; 134: 2080–5. Available from: http://dx.doi.org/10.1038/jid.2014.161

131. Yang Y, Jang G, Yang X, Wang Q, He S, Li S, Quach C, Zhao S, Li F, Yuan Z, Lee H-R, Zhong H, Liang C. Central role of autophagic UVRAG in melanogenesis and the suntan response. Proc Natl Acad Sci. 2018; 115: E7728–37.

132. Stout R, Birch-Machin M. Mitochondria's Role in Skin Ageing. Biology (Basel). 2019; 8: 29.

133. Tobin DJ. The cell biology of human hair follicle pigmentation. Pigment Cell Melanoma Res [Internet]. 2011; 24: 75–88. Available from: http://doi.wiley.com/10.1111/j.1755-148X.2010.00803.x

134. Paus R, Cotsarelis G. T He B Iology of H Air F Ollicles. New Engl Jouranal Med. 1999; 341: 491–7.

135. Rosenquist TA, Martin GR. Fibroblast growth factor signalling in the hair growth cycle: expression of the fibroblast growth factor receptor and ligand genes in the murine hair follicle. Dev Dyn [Internet]. 1996; 205: 379–86. Available from: http://www.ncbi.nlm.nih.gov/pubmed/8901049

136. Cotsarelis G, Sun TT, Lavker RM. Label-retaining cells reside in the bulge area of pilosebaceous unit: Implications for follicular stem cells, hair cycle, and skin carcinogenesis. Cell. 1990; 61: 1329–37.

137. Sano S, Kira M, Takagi S, Yoshikawa K, Takeda J, Itami S. Correction for Sano et al., Two distinct signaling pathways in hair cycle induction: Stat3-dependent and -independent pathways. Proc Natl Acad Sci [Internet]. 2015; 112: 201506638. Available from: http://www.pnas.org/lookup/doi/10.1073/pnas.1506638112

138. Jahoda CAB, Horne KA, Oliver RF. Induction of hair growth by implantation of cultured dermal papilla cells. Nature. 1984; 311: 560–2.

139. Kulak O, Chen H, Holohan B, Wu X, He H, Borek D, Otwinowski Z, Yamaguchi K, Garofalo LA, Ma Z, Wright W, Chen C, Shay JW, et al. Disruption of Wnt/β-Catenin Signaling and Telomeric Shortening Are Inextricable Consequences of Tankyrase Inhibition in Human Cells. Mol Cell Biol. 2015; 35: 2425–35.

140. Fuchs E, Merrill BJ, Jamora C, Dasgupta R. At the Roots of a Never-Ending Cycle. Dev Cell. 2001; 1: 13–25.

141. Adachi K, Watanabe Y, Inouye K. Activity of glucose-6-phosphate 1-dehydrogenase in hair follicles with male-pattern alopecia. Biosci Biotechnol Biochem. 1999; 63.

142. Zhang Y, Andl T, Yang SH, Teta M, Liu F, Seykora JT, Tobias JW, Piccolo S, Schmidt-Ullrich R, Nagy A, Taketo MM, Dlugosz AA, Millar SE. Activation of β-catenin signaling programs embryonic epidermis to hair follicle fate. Development. 2008; 135: 2161–72.

143. McGonigle S, Chen Z, Wu J, Chang P, Kolber-Simonds D, Ackermann K, Twine NC, Shie J, Miu JT, Huang K-C, Moniz GA, Nomoto K. E7449: A dual inhibitor of PARP1/2 and tankyrase1/2 inhibits growth of DNA repair deficient tumors and antagonizes Wnt signaling. Oncotarget. 2015; 6.

144. Li C, Zheng X, Han Y, Lv Y, Lan F, Zhao J. XAV939 inhibits the proliferation and migration of lung adenocarcinoma A549 cells through the WNT pathway. Oncol Lett. 2018; 15: 8973–82.

145. Slominski a, Paus R. Melanogenesis is coupled to murine anagen: toward new concepts for the role of melanocytes and the regulation of melanogenesis in hair growth. J Invest Dermatol. 1993; 101: 90S-97S.

146. Tobin DJ, Hordinsky M, Bernard BA. Hair pigmentation: a research update. J Investig Dermatol Symp Proc [Internet]. Elsevier Masson SAS; 2005; 10: 275–9. Available from: http://dx.doi.org/10.1111/j.1087-0024.2005.10117.x

147. Slominski A. Melanin Pigmentation in Mammalian Skin and Its Hormonal Regulation. Physiol Rev [Internet]. 2004; 84: 1155–228. Available from: http://physrev.physiology.org/cgi/doi/10.1152/physrev.00044.2003

148. Seiberg M, Marthinuss J, Stenn KS. Changes in expression of apoptosis-associated genes in skin mark early catagen. J Invest Dermatol [Internet]. Elsevier Masson SAS; 1995; 104: 78–82. Available from: http://dx.doi.org/10.1111/1523-1747.ep12613555

149. Park HY, Kosmadaki M, Yaar M, Gilchrest BA. Cellular mechanisms regulating human melanogenesis. Cell Mol Life Sci. 2009; 66: 1493–506.

150. Schiaffino MV. Signaling pathways in melanosome biogenesis and pathology. Int J Biochem Cell Biol [Internet]. Elsevier Ltd; 2010; 42: 1094–104. Available from: http://dx.doi.org/10.1016/j.biocel.2010.03.023

151. Rouzaud F, Kadekaro AL, Abdel-Malek ZA, Hearing VJ. MC1R and the response of melanocytes to ultraviolet radiation. Mutat Res - Fundam Mol Mech Mutagen. 2005; 571: 133–52.

152. Tsatmali M, Ancans J, Thody AJ. Melanocyte function and its control by melanocortin peptides. J Histochem Cytochem. 2002; 50: 125–33.

153. Hosoi J, Abe E, Suda T, Kuroki T. Regulation of Melanin Synthesis of B16 Mouse Melanoma Cells by 1α, 25-Dihydroxyvitamin D3 and Retinoic Acid. Cancer Res. 1985; 45: 1474–8.

154. Costin GE, Hearing VJ. Human skin pigmentation: Melanocytes modulate skin color in response to stress. FASEB J. 2007; 21: 976–94.

155. Slominski A, Zmijewski MA, Pawelek J. L-tyrosine and L-dihydroxyphenylalanine as hormone-like regulators of melanocyte functions. Pigment Cell Melanoma Res. 2012; 25: 14–27.

156. Slominski A, Moellmann G, Kuklinska E, Bomirski A, Pawelek J. Positive regulation of melanin pigmentation by two key substrates of the melanogenic pathway, L-tyrosine and L-dopa. J Cell Sci. 1988; 89: 287–96.

157. Dunn KJ, Brady M, Ochsenbauer-Jambor C, Snyder S, Incao A, Pavan WJ. WNT1 and WNT3a promote expansion of melanocytes through distinct modes of action. Pigment Cell Res. 2005; 18: 167–80.

158. Jin EJ, Erickson CA, Takada S, Burrus LW. Wnt and BMP signaling govern lineage segregation of melanocytes in the avian embryo. Dev Biol. 2001; 233: 22–37.

159. Takeda K, Yasumoto KI, Takada R, Takada S, Watanabe KI, Udono T, Saito H, Takahashi K, Shibahara S. Induction of melanocyte-specific microphthalmia-associated transcription factor by Wnt-3a. J Biol Chem. 2000; 275: 14013–6.

160. Kang J Il, Kim MK, Lee JH, Jeon YJ, Hwang EK, Koh YS, Hyun JW, Kwon SY, Yoo ES, Kang HK. Undariopsis peterseniana promotes hair growth by the activation of Wnt/β-catenin and ERK pathways. Mar Drugs. 2017; 15.

161. Habas R, He X. Activation of Rho and Rac by Wnt/Frizzled signaling. Methods Enzymol. 2006; 406: 500–11.

162. Kollmar R. Who does the hair cell's 'do? Rho GTPases and hair-bundle morphogenesis. Current Opinion in Neurobiology. 1999. p. 394–8.

163. Kalinec F, Zhang M, Urrutia R, Kalinec G. Rho GTPases mediate the regulation of cochlear outer hair cell motility by acetylcholine. J Biol Chem. 2000; 275: 28000–5.

164. Sutera M, De Caro V, Giannola L. Small endogenous molecules as moiety to improve targeting of CNS drugs motility. Exp. Op. Drug Delivery 2017; 14(1), 93-107